Fall 12-2017

Impacts of Oil Exposure During Early Life Development Stages In Sheepshead Minnows (*Cyprinodon variegatus*) Under Different Environmental Factors

Danielle Simning
University of Southern Mississippi

IMPACTS OF OIL EXPOSURE DURING EARLY LIFE DEVELOPMENT STAGES IN SHEEPSHEAD MINNOWS (*CYPRINODON VARIEGATUS*) UNDER DIFFERENT ENVIRONMENTAL FACTORS

by

Danielle Justine Simning

A Thesis
Submitted to the Graduate School,
the College of Science and Technology,
and the School of Ocean Science and Technology
at The University of Southern Mississippi
in Partial Fulfillment of the Requirements
for the Degree of Master of Science

December 2017

IMPACTS OF OIL EXPOSURE DURING EARLY LIFE DEVELOPMENT STAGES IN SHEEPSHEAD MINNOWS (*CYPRINODON VARIEGATUS*) UNDER DIFFERENT ENVIRONMENTAL FACTORS

by Danielle Justine Simning

December 2017

Approved by:

_____
Dr. Joe Griffitt, Committee Chair
Associate Professor, Ocean Science and Technology

_____
Dr. Frank Hernandez, Committee Member
Assistant Professor, Ocean Science and Technology

_____
Dr. Leila Hamdan, Committee Member
Associate Professor, Ocean Science and Technology

_____
Dr. Joe Griffitt
Chair, Department of Coastal Sciences, School of Ocean Science and Technology

_____
Dr. Karen S. Coats
Dean of the Graduate School

Published by the Graduate School

ABSTRACT

IMPACTS OF OIL EXPOSURE DURING EARLY LIFE DEVELOPMENT STAGES IN SHEEPSHEAD MINNOWS (*CYPRINODON VARIEGATUS*) UNDER DIFFERENT ENVIRONMENTAL FACTORS

by Danielle Justine Simning

December 2017

The release of approximately 5 million barrels of crude oil into the northern Gulf of Mexico during the 2010 Deepwater Horizon oil spill jeopardized estuarine ecosystem health from Texas to Florida. These estuarine habitats, which serve as nurseries for many important fisheries are also prone to rapid fluctuations in environmental stressors such as oxygen concentration, and salinity. The consequence of combined exposure to crude oil and suboptimal environmental factors during early life stage development of fish is still largely unknown. The objective of this project was to investigate the impacts of exposure to crude oil in combination with varying environmental stressors on *Cyprinodon variegatus* survival, gene expression, and genotoxicity.

The post-larval developmental stage was the most sensitive early life stage to oil and abiotic stress. Median lethal concentrations during the post-larval exposures followed a treatment dependent pattern with the greatest lethal effect seen under hypoxic-high salinity conditions (64.55 µg/L ± 12.81). Real-time PCR analysis identified down-regulation of *cyp1a1, epo*, and *arnt1*, target genes involved in the two common defense pathways, the aryl hydrocarbon receptor signaling pathway which modulates metabolism of polycyclic aromatic hydrocarbons (PAHs), and the hypoxia inducible 1-α signaling pathway which is responsible for resilience to hypoxic stress, this was only observed

under hypoxic-high salinity environmental conditions in treatments with PAH concentrations greater than 226 µg/L. Top toxicological functions impacted during post-larval development in all treatment comparisons included cholesterol biosynthesis, cardiotoxicity, and hepatoxicity. These findings indicate that the post-larval stage is the most sensitive to oil and environmental stress.

ACKNOWLEDGMENTS

I would like to thank my advisor Dr. Joe Griffitt at The University of Southern Mississippi. I would also like thank my committee members Dr. Hernandez and Dr. Hamdan. Dr. Griffitt and my committee members helped me successful complete my research and thesis be providing mentorship and guidance. I would also like to thank everyone in my lab for their help teaching me techniques to measure and analyze data. I would also like to acknowledge my funding source The Gulf of Mexico Research Initiative (GoMRI) without whom this research would not have been possible.

DEDICATION

I would like to dedicate this to my family.

TABLE OF CONTENTS

LIST OF TABLES

LIST OF ILLUSTRATIONS

LIST OF ABBREVIATIONS

cyp1a1	Cytochrome P450 1 alpha 1
epo	Erythropoietin
arnt1	Aryl Hydrocarbon Nuclear Translocator

Protein 1

qPCR	Real time Polymerase Chain Reaction
AhR	Aryl Hydrocarbon Receptor
HIF-α	Hypoxia Inducible Factor 1 alpha
PAHs	Polycyclic Aromatic Hydrocarbons
DWH	Deepwater Horizon
nGoM	northern Gulf of Mexico
SLCO	Sweet Louisiana Crude Oil
POPs	Persistent organic pollutants
cP450	Cytochrome P450
XREs	Xenobiotic Response Elements
HREs	Hypoxic Response Elements
AhRR	Aryl Hydrocarbon Receptor Repressor
Ub	Ubiquitin protein
pHVL	von Hippel-Lindau tumor-suppressor protein
bHLH	basic helix-loop-helix
NGS	Next Generation Sequencing
USM	The University of Southern Mississippi
GCRL	Gulf Coast Research Laboratory

GC-MS	Gas Chromatography-Mass Spectrometry
HEWAF	High Energy Water Accommodated Fraction
WAF	Water Accommodated Fraction
TPH	Total Petroleum Hydrocarbon
tPAH29	Total Polycyclic Aromatic Hydrocarbons 29
UV	Ultra Violet
BPM	Beats per minute
LC_{50}	Median Lethal Concentration
DO	Dissolved oxygen
ppb	Parts per billion
SHM	Sheepshead minnows
GoMRI	Gulf of Mexico Research Initiative
NRDA	National Resource Damage Assessment
bp	Base pair
DEGs	Differentially expressed genes
FDR	False Discovery Rate
RNAseq	RNA sequencing
ROS	Reactive Oxygen Species

CHAPTER I – GENERAL INTRODUCTION AND METHODS

Introduction

Deepwater Horizon Oil Spill

The 2010 Deepwater Horizon (DWH) oil spill threatened the ecosystem health of the many estuaries and coastal wetlands along the shores of the northern Gulf of Mexico (nGoM). The distribution of approximately 4.9 million barrels of crude oil released from the Macondo wellhead along greater than 2100 kilometers of coastline from Texas to Florida, was influenced by spill mitigation efforts including use of two million gallons of chemical dispersants, surface skimming, and *in situ* burning (Liu et al., 2012; Nixon et al., 2016). Oil distribution was also affected by sea surface processes such as currents and biochemical processes (Baker et al., 2016; Beyer et al., 2016; Liu et al., 2012). The DWH oil spill was unique because the release of oil occurred at 1522 m water depth, which led to the formation of both deep water and surface plumes (Beyer et al., 2016; Liu et al., 2012). Large deep sea plumes, up to 35 km long, were measures at depths from 500 to 1300 m (Spier et al., 2013; Valentine and Benfield, 2013). PAH concentrations in deep sea plumes reached 189 µg/L, where highly toxic benzene, toluene, ethylbenzene, and xylenes (BTEX), were measured in concentrations less than 78 µg/L (Beyer et al., 2016).

Oil released from the Macondo wellhead that reached the surface formed large surface slicks cumulatively covering 112,000 km^2 (Beyer et al., 2016). The thickness of the slick ranged from 0.1 to 1 mm (Beyer et al., 2016). Though efforts to minimize oil exposure to marine habitats were employed following the DWH oil spill, including the use of dispersants and sea surface slick burning, more than 2100 km of nGoM shoreline

was impacted (Beyer et al., 2016; Liu et al., 2012; Michel et al., 2013; Nixon et al., 2016). Exposure to crude oil during development in fish has been documented to increase mortality and developmental abnormalities, and decrease growth rates in sheepshead minnows, zebrafish , and haddock (Hendon et al., 2008; Incardona et al., 2004; Sørhus et al., 2016). The focus of much research investigating oil contamination lethality and developmental effects in marine and fresh water fish has been focused on phenotypic and morphological responses to oil, but still uncertain are the molecular processes responsible for the effects observed after exposure to oil (Pasparakis et al., 2016; Whitehead et al., 2012).

Polycyclic Aromatic Hydrocarbons (PAHs)

The oil released from the Macondo wellhead was a light crude oil called Sweet Louisiana Crude Oil (SLCO) (Kirman et al., 2016). SLCO has an average PAH composition of 10-45 % (Beyer et al., 2016; Jung et al., 2013; Liu et al., 2012; Ramachandran et al., 2006; Wang et al., 2014). PAHs are considered highly toxic components of crude oil and have been documented to cause an array of deleterious phenotypic responses such as acute mortality, reduced growth, liver and gill damage, cardiac edema, skeletal deformity, and immunosuppression which is dependent on the number of aromatic carbon structures (Bayha et al., 2017; Brown-Peterson et al., 2015; Hendon et al., 2008; Incardona et al., 2004; Jones et al., 2017; Ramachandran et al., 2006; Sammarco et al., 2013; Sørhus et al., 2016). These compounds are not only toxic but considered to be persistent organic pollutants (POPs), retaining their toxicity for many years, and are major contaminants in marine environments throughout the world (Jin et al., 2015; Ramachandran et al., 2006; Turner et al., 2014; Wang et al., 2014).

PAHs are chemicals that contain multiple six carbon double bonded ring structures and the number of aromatic carbon rings influences the compounds toxicity to exposed organisms (Incardona et al., 2004; Turner et al., 2014). Three and four aromatic carbon ring PAHs, including dibenzothiophene, phenanthrene, and pyrene, cause cardiac dysfunction including edema, and impair liver and skeletal developmental in zebrafish embryos (Incardona et al., 2004). A study investigating the induction of cytochrome P450 1 alpha (*cyp1a1*) activity of 61 parent PAHs concluded that 4-6 ring PAHs exhibited similar effects on *cyp1a1* activity as highly toxic dioxin chemicals in teleosts (Barron et al., 2004).

The main routes of PAH exposure in fish are passive diffusion at the gills and oral ingestion of contaminated food due to the lipophilic nature of the chemicals (Brauner et al., 1999; Evans et al., 2005; Turner et al., 2014). Most of the metabolism and detoxification of PAHs in exposed fish is completed by phase I detoxification enzymes in the cytochrome P450 (cP450) super family (Yang, 1988). The regulation of phase I and II detoxification enzymes including cP450 enzymes, is controlled by the aryl hydrocarbon receptor signaling pathway (AhR) which is activated in the presence of PAHs (Vorrink and Domann, 2014). Organisms exposed to PAHs often metabolize them by cytochrome P450 enzymatic activity through oxidation reactions (Turner et al., 2014) Though cytochrome P450 enzymes are the main xenobiotic metabolism process used by organisms to increase elimination of PAH, this oxidative process often results in the production of more toxic secondary metabolites which have carcinogenic effects (Turner et al., 2014)

AhR Signaling Pathway

Teleosts have highly conserved molecular signaling pathways that mitigate the deleterious effects associated with PAH stress (Kewley et al., 2004; Vorrink and Domann, 2014). The AhR signaling pathway is the dominant pathway to metabolize PAHs (Vorrink and Domann, 2014). The role of the AhR pathway in the elimination of halogenated hydrocarbons, and PAHs has been the focus of many studies to understand xenobiotic toxicity and metabolism (Denison and Nagy, 2003; Vorrink and Domann, 2014). AhR is ubiquitously expressed and located in the cytoplasm of tissue cells (Denison and Nagy, 2003). The conformational integrity of cytosolic AhR is maintained by chaperone proteins which include heat shock proteins (Hsp90), X-associated protein 2 (Xap2), and p23. Activation of AhR occurs when xenobiotic ligands such as PAHs bind to the receptor. The activation of AhR results in a conformational change that cleaves off chaperone proteins and exposes the nuclear location sequence, initiating translocation into the cell nucleus. Inside the nucleus, the activated AhR forms a heterodimer complex with the aryl hydrocarbon nuclear translocator protein (Arnt). The AhR:Arnt complex then binds to the xenobiotic response elements (XREs) in the promoter region of genes responsible for phase I and phase II xenobiotic metabolism, most notably cytochrome P450 1 alpha 1 (*cyp1a1*) enzyme (Denison and Nagy, 2003). The transcription of *cyp1a1* in all organisms leads to the accumulation of secondary reactive metabolites that produce DNA damage and disease (Di Giulio and Hinton, 2008; Nebert and Dalton, 2006). The production and accumulation of reactive oxygen species metabolites via biotransformation of PAHs by *cyp1a1* enzymatic metabolism results in the strict

regulation of the AhR pathway by the aryl hydrocarbon repressor receptor (AhRR) (Di Giulio and Hinton, 2008).

The induction of the AhR pathway by exogenous ligands has been speculated to cause deleterious effects on immune and cholesterol synthesis pathways (Bayha et al., 2017; Jones et al., 2017; Tanos et al., 2012). PAH exposure has been documented to decrease functions of the innate and adaptive immune response in fish and mammals, most notably suppressing an organism's ability to resist pathogenic infections (Bayha et al., 2017; Reynaud and Deschaux, 2006). Exposure to PAHs has resulted in the formation of skin lesions in juvenile southern flounder, hepatic lesions in mummichog, and gill hyperplasia in gulf killifish (Bayha et al., 2017; Reynaud and Deschaux, 2006).

Cholesterol synthesis is another pathway targeted by the activation of the AhR pathway (Regnault et al., 2014; Tanos et al., 2012; Xu et al., 2017). Cholesterol biosynthesis is essential in the maintenance of cell structure and growth (Tanos et al., 2012; Xu et al., 2017). Over activation of biosynthesis pathways and increased accumulation of cholesterol in the liver is correlated to liver cancer and necrosis, while inhibition of cholesterol synthesis causes cellular apoptosis (Regnault et al., 2014; Tanos et al., 2012; Xu et al., 2017).

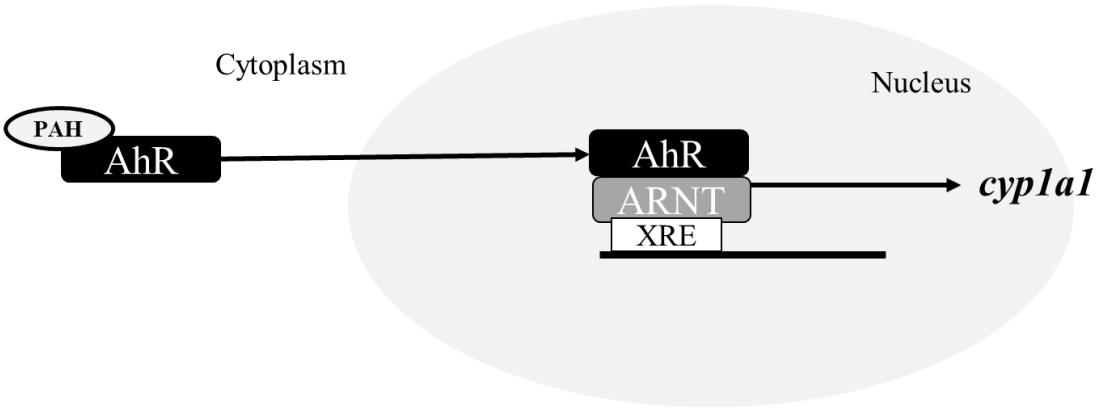

Figure 1. Diagram of the Aryl Hydrocarbon Receptor (AhR) Signaling Pathway activation and induction of cytochrome P450 1 alpha 1 (*cyp1a1).*

In the presence of polycyclic aromatic hydrocarbons (PAHs) the AhR moves into the nucleus and forms a heterodimer with the Aryl Hydrocarbon Nuclear Translocator protein (ARNT). This complex bind to the xenobiotic response elements (XRE) of DNA, acting as a transcription factor that induced transcription of cyp1a1, the main enzyme responsible for oxidative metabolism of PAHs and biomarker of oil exposure.

DWH impact on estuary ecosystem health

The three month duration during the spring of 2010 of the DWH oil spill has potential to negatively impact estuarine ecosystems along the nGoM. Estuaries of the nGoM are highly productive and variable environments, which serve as critical nursery habitats for many important fisheries, both recreational and commercial (Chesney et al., 2000; Sumaila et al., 2012). The commercial fishery in the nGoM is one of the most productive in the world which produces approximately 600 million dollars a year, and a third of the fishery species depend on coastal estuarine and wetland habitats (Fodrie et al., 2014; Mendelssohn et al., 2012). Daily and seasonal fluctuations in temperature, salinity, and dissolved oxygen can cause stress to organisms that inhabit these ecosystems (Whitehead, 2013). The potential for interaction effects to occur on both physiological and molecular levels in response to simultaneous exposure to crude oil and varying oxic

and salinity regimes is a concern when evaluating the impact of the 2010 DWH oil spill on the coastal estuaries of the nGoM. Multiple studies have documented oil exposure decreasing blood hemoglobin levels and gill chloride cells in developing fish (Goanvec et al., 2011; Whitehead, 2013). Morphological changes in gill structure result from oil exposure and produce organ-level responses that decreases gill permeability, ion regulation, and oxygen exchange (Evans et al., 2005; Goanvec et al., 2011; Whitehead, 2013). Synergistic effects on fish health have been documented to occur among many environmental contaminates, including oil, and sub-optimal salinity and oxic regimes (Adeyemi and Klerks, 2012). Most studies have focused on the effects of PAHs as a single stressor on fish health, but less is known about potential interaction effects between PAH exposure in combination with hypoxia and salinity, two common environmental stressors that impact larval fish health in nGoM estuaries which all rely on gill functions for homeostasis (Evans et al., 2005; Whitehead, 2013).

Osmoregulation

Salinity varies in coastal estuarine environments on a daily basis due to tidal fluctuations and differing degrees of freshwater discharge from rivers (Haney, 1999; Nordlie, 1987). Estuarine fishes have the ability to acclimate to rapid changes in salinity due to adapted ability to osmoregulate, which can be energetically costly (Nordlie et al., 1991; Whitehead, 2013). The gills are the main organs responsible for osmotic regulation in marine teleost (Evans et al., 2005; Sakamoto et al., 2001). Marine teleosts ingest water to maintain a consistent internal osmotic gradient hypo-osmotic to the marine environments, as they are constantly losing water and gaining ions by means of osmotic pressure (Sakamoto et al., 2001). Increased osmotic pressure during early life

stage development in fishes can lead to decreased growth and fitness, so in embryonic fish the chorion serves as a barrier to the external environment to reduce osmotic pressures on the embryo, allowing more energy to be allocated to development (Brown et al., 2011; Finn, 2007; Petereit et al., 2009; Sampaio and Bianchini, 2002). Studies have documented salinity disrupting and negatively affecting fish development and growth, even in euryhaline fish species. Patterson et al. (2012) investigated different salinity regimes on gulf killifish development and observed that low salinity resulted in decreased growth and survival due to increased osmotic pressure. Brown et al. (2012) investigated embryogenesis under different salinities in gulf killifish and found that percent hatch was affected by salinity although heart rate and total length was not. Brown et al. (2011) also investigated the combined effects of salinity and temperature on larval fish health. Increased time to hatch and total length was observed in high salinity (20 g/L) compared to low salinity (10 g/L). Early life stage developmental influences of salinity on Nile tilapia were investigated and results indicated increased mortality of larvae with increased salinity (Fridman et al., 2012).

Oxygen Tension

Low oxygen tension is an environmental stressor that can impact estuarine habitats in the nGoM. Hypoxia is defined as in situ dissolved oxygen concentration of 2.0 mg/L or less (Bianchi et al., 2010; Eldridge and Roelke, 2010; Rabalais et al., 2002). Following the 2010 DWH oil spill, the same habitats impacted by spill contaminants were potentially also exposed to seasonal hypoxic conditions (Fleming et al., 2009; Whitehead, 2013). The persistence and expansion of hypoxia in the nGoM is believed to be related to increased nutrient loading into riverine discharge which results in increased

algae blooms (Rabalais et al., 2002). Eutrophication is the main process involved in anthropogenic hypoxic zone formation in the nGoM due to release of nutrient rich waters from the Mississippi River associated with increased fertilizer use in the Mississippi watershed (Bianchi et al., 2010; Rabalais et al., 2002). Seasonal nutrient discharge with the Mississippi River freshet, in conjunction with seasonal (summer) water-column density stratification, driven by salinity and temperature gradients results in the formation of hypoxic zones below the depth of the pycnocline in the nGoM (Bianchi et al., 2010; Eldridge and Roelke, 2010; Rabalais et al., 2002). Hypoxic zones in nGoM estuaries are generally found in areas that have extended water residency time and temperature-salinity driven water stratification (Rabalais et al., 2002). Community level effects associated with hypoxic zones are habitat degradation, oxygen depletion and a decrease in biodiversity (Rabalais et al., 2002). Fish are highly adapted to the marine environment and have many mechanisms to combat the deleterious effects of hypoxia (Wu, 2002). For most fish, the gills serve as the primary organ responsible for respiration via a counter-current gas exchange system (Evans et al., 2005). Fish respond to hypoxia by increased ventilation rates across the gills and activation of the hypoxia inducible factor 1 alpha pathway (HIF-1α) which induces angiogenesis and erythropoiesis (Evans et al., 2005; Kulkarni et al., 2010; Lai et al., 2006; Landry et al., 2007; Vorrink and Domann, 2014).

HIF-1α Signaling Pathway

Hypoxia threatens ecosystem health and can cause mass mortality events, delayed organismal development, teratogenic effects, endocrine dysfunction, reduced hatching and reduced spawning rates (Dangre et al., 2010; Shang and Wu, 2004; Wu et al., 2003).

The hypoxia inducible 1 alpha signaling pathway is the primary pathway used to mitigate the negative effects of hypoxia (Vorrink and Domann, 2014). The HIF-1α pathway maintains cellular oxygen homeostasis by inducing the transcription of a suite of genes responsible for increased oxygen delivery, erythropoietin (*epo*), vascular endothelial growth factor (*vegf*), heme oxygenase-1, and glucose metabolism, glucose transporters (*glut-1* and *glut-4*) (Kewley et al., 2004; Kumar and Choi, 2015; Vorrink and Domann, 2014; Wu, 2002). Normoxia leads to proteasome degradation of the HIF-1α receptors, regulated by ubiquitin proteins (Ub) (Nikinmaa and Rees, 2005). Prolyl hydroxylation enzymes PHD-1, PHD-2, and PHD-3 catalyze the proline residual hydroxylation on the HIF-1α receptor (Semenza, 2001). The hydroxylation of the proline residuals is necessary to initiate binding of the von Hippel-Lindau tumor-suppressor protein (pVHL) (Kumar and Choi, 2015; Semenza, 2001). Once the pVHL protein binds the HIF-1α receptor, the ubiquitin proteins (elongins B and C, Cullin 2 (Cul2), and Rbx1) also bind to the receptor which is quickly destroyed by 26S proteasome digestion (Semenza, 2001). In the absence of oxygen, the prolyl hydroxylase activity is inhibited so the proline residuals are not hydroxylated, thus enabling the binding of the pVHL to HIF-1α and subsequent proteasome degradation (Nikinmaa and Rees, 2005; Semenza, 2001). The active HIF-1α receptor relocates to the nucleus where it forms a heterodimer protein complex with the Arnt protein (Vorrink and Domann, 2014). The HIF-1α:Arnt complex is a transcription factor that binds to the hypoxia response elements (HREs) in the promoter region of genes to allow increased oxygen delivery to hypoxic tissue by

erythropoiesis by induction of erythropoietin (*epo*) (Vorrink and Domann, 2014; Wu, 2002).

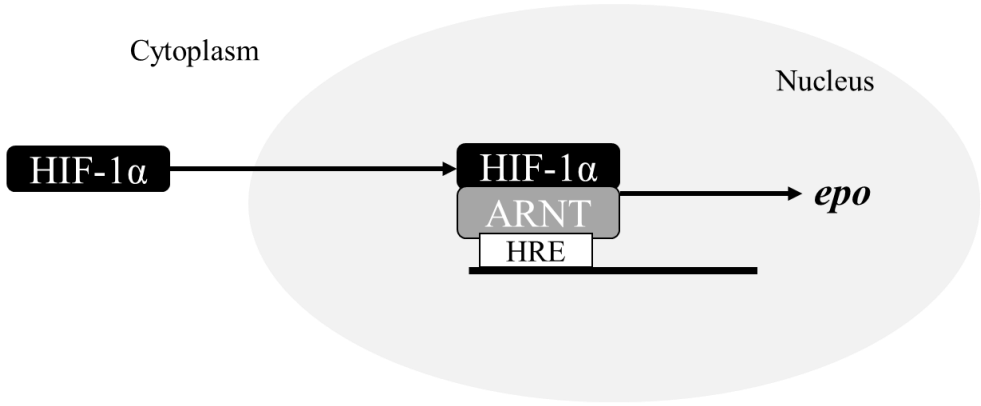

Figure 2. Diagram of the Hypoxia Inducible Factor 1 Alpha (HIF-1α) Signaling Pathway activation and induction of erythropoietin (*epo*).

In normoxic conditions, the HIF-1α is degraded. In hypoxic condition, the active HIF-1α receptor moves into the nucleus and forms a heterodimer with the Aryl Hydrocarbon Nuclear Translocator protein (ARNT). This complex bind to the hypoxic response elements (HRE) of DNA, acting as a transcription factor that induced transcription of *epo*, a gene responsible for production of red blood cells to increase oxygenated blood circulation to hypoxic tissues.

Cellular cross-talk between AhR and HIF-1α

Past research that investigated the effects of simultaneous exposure to PAH and hypoxic stress on aquatic organisms has indicated synergistic toxicity because of cellular cross-talk between the AhR and the HIF-1α signaling pathways (Fleming et al., 2009; Hendon et al., 2008; Schults et al., 2010; Vorrink and Domann, 2014; Yu et al., 2008). The AhR and HIF-1α receptors are both transcription factors that belong to the class I bHLH/PAS protein family, which must form heterodimer complexes with class II bHLH/PAS proteins to induce transcription of target genes (Kewley et al., 2004; Vorrink and Domann, 2014). Arnt is a class II bHLH/PAS protein that is the shared binding partner in both the AhR and HIF-1α signaling pathways (Gassmann et al., 1997; Vorrink

and Domann, 2014). The Arnt protein operates in both defense pathways, and is hypothesized to cause competitive inhibition of receptor binding resulting in activation of one pathway over the other. The outcome of this is the inability of an organism to cope with both oxygen and PAH stress simultaneously (Gassmann et al., 1997; Pollenz et al., 1999; Vorrink and Domann, 2014). Since the discovery of Arnt as the shared binding partner for the AhR and HIF-1α pathways, synergistic toxicity studies have focused on cross-talk at the Arnt node to explain the increased mortality and phenotypic response of fish. Many of these studies have proven inconclusive, and molecular processes involved in the synergistic toxicity of oil and hypoxic stress are largely still undetermined.

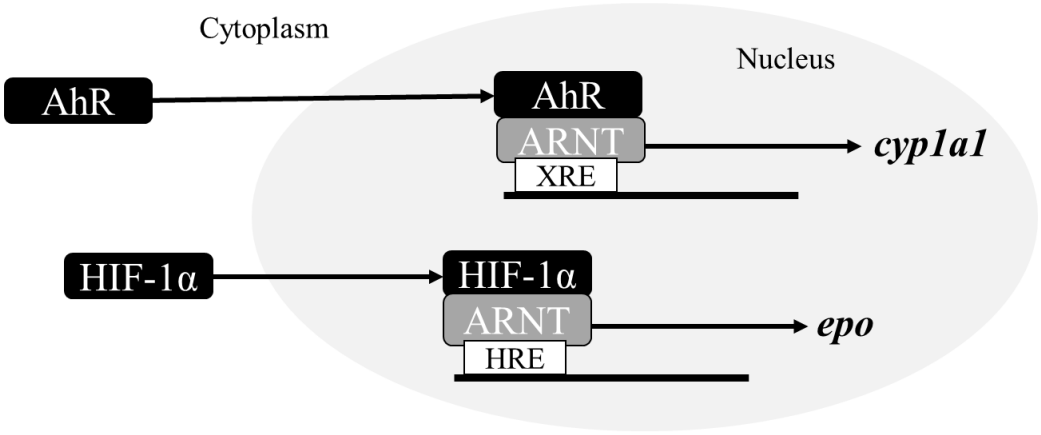

Figure 3. Diagram of cross-talk between the Aryl Hydrocarbon Receptor (AhR) Signaling Pathway and the Hypoxia Inducible Factor 1 Alpha (HIF-1α) Signaling Pathway.

The aryl hydrocarbon nuclear translocator protein (ARNT) is the shared transcription factor binding partner for both the AhR and the HIF-1α receptors. Simultaneous exposure to PAHs and hypoxia decreases an organisms ability to cope with both stressors due to saturation of available ARNT binding proteins.

Global Transcriptomics

Technological advancements have enabled researches to increase our understanding of transcriptomics by investigating gene expression profile variability

during developmental stages and in combination with environmental stressors (Qian et al., 2014; Wang et al., 2009). Hybridization-based techniques, microarrays and tag-based sequencing methods (e.g. SAGE, CAGE, and MPSS), were common methods used in early transcriptomics studies (Wang et al., 2009). Major limitations associated with these techniques are the lack of pre-existing genome information, cross-hybridization, an inability to map short tags, and the inability of whole transcriptomic sequencing (Qian et al., 2014). To overcome limitations associated with hybridization-based and tag-based sequencing methods, researchers developed next generation sequencing (NGS) techniques (Ekblom and Galindo, 2010; Wang et al., 2009).

RNA sequencing is a method used for mapping and quantifying an organism's transcriptome, and has been applied to fish species to better understand molecular responses to stressors (Qian et al., 2014; Schirmer et al., 2010). NGS requires a small amount of RNA to produce large quantities of data with high resolution and sensitivity, in a short amount of time when compared to hybridization-based and tag-based methods (Qian et al., 2014). Unlike microarray technology, RNA sequencing has multiple platforms, including 454 FLX pyrosequencing, SOLiD, Solexa GA (Illumina), and Heliscope (Ekblom and Galindo, 2010; Qian et al., 2014; Schirmer et al., 2010). Different sequencing methods are used by each platform which affects the number of reads and the length of the reads collected (Schirmer et al., 2010). NGS techniques are advancing our knowledge of genomic responses in model and non-model species. This information is enabling scientists to better understand the molecular processes involved in physiological changes and response to external stimuli and toxicants. Increased

understanding of toxicant modes of action and molecular pathway responses is necessary in understanding ecosystem health and resilience.

Overall this study was conducted to investigate how combined exposure to oil and environmental stress impacted *Cyprinodon variegatus* health. The first objective was to determine periods of increased PAH sensitivity in combination with hypoxic and osmotic stress during early life development of sheepshead minnow, *Cyprinodon variegatus.* The second objective was to investigate the occurrence of the cross-talk between the AhR and HIF-1α signaling pathways in early life development of *C. variegatus* under different environmental conditions. Finally, the last objective was to compare the global transcriptomic responses of C. variegatus to individual and combined exposure to oil, hypoxia, and oil + hypoxia.

The hypothesis used to test these objectives were:

H_1: Age will have an effect on Cyprinodon variegatus sensitivity and response to PAH toxicity.

H_0: There will be no difference in sensitivity and response to PAH toxicity between the three developmental stages in Cyprinodon variegatus.

H_2: Environmental factors will increase the toxicity of oil to Cyprinodon variegatus.

H_0: Environmental factors will have no effect on early life stage development of Cyprinodon variegatus.

CHAPTER II - DEVELOPMENTAL AND PHENOTYPIC RESPONSE OF CYPRINODON VARIEGATUS TO SOURCE OIL FROM THE 2010 DEEPWATER HORIZON SPILL UNDER ADVERSE ENVIRONMENTAL CONDITIONS.

Introduction

The amount of oil released, timing, and location of the 2010 Deepwater Horizon (DWH) oil spill presented unique challenges to exposed wildlife and ecosystems. The fisheries of the northern Gulf of Mexico (nGoM) were threatened following the release of 4.9 million barrels of crude oil 60 miles off the coast of Louisiana following the explosion of the DWH drilling platform (Beyer et al., 2016; Nixon et al., 2016; Turner et al., 2014). The release of oil into the nGoM occurred over an 87-day period, during spring and early summer months which coincident with both pelagic and coastal fish spawning periods (Chesney et al., 2000; Pasparakis et al., 2016; Whitehead, 2013). The Sweet Louisiana Crude Oil (SLCO) released into the nGoM is a complex mixture of chemicals comprised of *n*-alkanes, polycyclic aromatic hydrocarbons (PAHs), and trace metals(Kirman et al., 2016; Liu et al., 2012). Typically, 10 - 45% of SLCO is attributed to PAHs, which are known as persistent organic pollutes and are highly toxic to developing organisms (Incardona et al., 2004; Wang et al., 2014). Numerous studies have documented and identified developmental toxicities characteristic of PAH exposure in freshwater and marine fish species (Brown-Peterson et al., 2015; Incardona et al., 2005, 2004; Sørhus et al., 2016). PAH exposure during early life stages is primary linked to acute mortality, delayed hatching rates, and increased cardiac dysfunction (Hendon et al., 2008; Incardona et al., 2004; Sørhus et al., 2016). To better understand the extent of the 2010 DWH oil spill impacts on estuarine ecosystems in the nGoM, it is critical to

identify the early life stage of fish development most sensitive to PAH exposure effects. In addition, it is important to identify synergistic relationships associated with oil exposure under varying environmental parameters such as salinity and oxygen concentrations.

Crude oil, hypoxia, and variable salinity have been documented to cause deleterious effects in multiple fish species. Crude oil is known to cause cardiac dysfunction, abnormal craniofacial development, and impaired liver and kidney development in zebrafish, haddock, and gulf killifish (Incardona et al., 2006; Pasparakis et al., 2016; Sørhus et al., 2016). Zebrafish exposed to hypoxia during embryonic development experienced delayed development and increased teratogenic effects, while embryonic carp exposure to PAHs resulted in caused low hatch rates and increased larval mortality (Shang and Wu, 2004; Wu et al., 2003). Low salinity has also been documented to negatively affect fish development and growth, even in euryhaline fish species (Patterson et al., 2012). Patterson et al. (2012) investigated different salinity concentrations (0.5, 5.0, 8.0 and 12 ppt) on gulf killifish development and reported low salinities resulted in decreased growth and survival in juvenile killifish due to increased osmotic pressure. Brown et al. (2012) investigated embryogenesis in gulf killifish under different salinities, 0.4, 7, 15, and 30 g/L, results indicated that percent hatch success was affected by salinity, although heart rate and total length was not. Brown et al. (2011) also investigated the combined effects of salinity and temperature on gulf killifish, the study reported delayed time to hatch in the high salinity (20 g/L) compared to the low salinity (10 g/L). Early life stage developmental influences of salinity on Nile tilapia were investigated and results indicated increased mortality of larvae with increased salinity and

found delayed hatching rates were observed in high salinities greater than 15 ppt (Brown et al., 2011; Fridman et al., 2012).

Most studies have focused on the effects of PAHs as a single stressor on fish health, but less is known about potential interaction effects between PAH exposure in combination with hypoxia and salinity (Whitehead, 2013). The objective of this study was to identify periods of increased PAH sensitivity in sheepshead minnow, *Cyprinodon variegates.* The synergistic effects of oxygen and salinity stress during early life development stages of sheepshead minnow were also addressed. Sheepshead minnows are a widely distributed estuarine fish that inhabit the temperate coastal waters along the east coast of the United States to the tropical coastal waters of Mexico (Haney and Nordlie, 1997). This species displays continuous breeding events throughout the year that deposit fertilized embryos on the benthic surface of shallow estuarine and wetland habits (Kuntz, 1916). Sheepshead minnows are considered a resilient fish species because they can physiologically acclimate to rapid and extreme fluctuations in temperature, salinity, and dissolved oxygen levels (Haney and Nordlie, 1997). For these reasons, the sheepshead minnow was selected for study. The hypotheses of this research were: 1) post-hatch developmental stage of *C. variegatus* is the most sensitive to PAH toxicity; 2) increased mortality and developmental abnormalities will be positively correlated with increasing salinity, in conjunction with PAH exposure; 3) the maximum mortality will be attributable to combined exposure to hypoxic conditions and PAHs during early life stage development of *C. variegatus*.

Methods

Experimental animals

All embryos and larvae used in this study were collected from a *C. variegatus* adult brood stock maintained at The University of Southern Mississippi's (USM) Gulf Coast Research Laboratory (GCRL). For each experiment, embryos were collected during natural spawning events. Adult *C. variegatus* were acclimated to breeding water parameters (27 - 30°C) and placed on breeding diets one week before the breeding event. Breeding events were 12 -24 h periods which began with the placement of two breeding mats into each of the 12 *C. variegatus* raceways. Breeding mats were removed from adult *C. variegatus* enclosures, and embryos were collected. Collected embryos were combined into a single stock collection and rinsed with fresh water to remove any external saltwater parasites or pathogens. Rinsed embryos were rolled on fine nylon mesh to remove the embryonic microvilli to prevent embryos from clumping together. Unfertilized embryos were removed, fertilized embryos were transferred to experimental chambers or holding tanks. Embryos transferred to holding tanks were kept in 4 L glass containers and incubated at 30°C. The water parameters of the holding tanks were normoxic and the salinity was either 10 or 30 ppt depending on the experimental regime. Once embryos hatched (96 hpf) the newly hatched larvae were either directly transferred to experimental chambers for the post-hatch assays, or to a second 4 L holding tank with same water parameters until used for the post-larval experiments. The second holding tank had a 50% water renewal at 48 hph and began feeding. At 96 hph the larvae were transferred to experimental chambers used for the post-larval assays.

Experimental Design

To examine the individual and combined effects of PAH and environmental effects on the early life stage development in *C. variegatus*, 12 experiments were conducted. The experiments were divided into three developmental stages: embryonic, post-hatch, and post-larval (Figure 4), which were each subjected to four different exposure regimes. Experimental initiation began with a 48 h exposure period, followed by a depuration period (up to 8 dpf) (Figure 5). The 48 h exposure period subjected embryos or larvae to four different HEWAF treatment concentrations (6.25%, 12.5%, 50%, 100%) in combination with varying oxic (> 5.0 mg/L or 2.0 mg/L dissolved oxygen) and salinity (10 ppt or 30 ppt) regimes. All exposure treatments were executed in quadruplicate, yielding a total of 20 test chambers for normoxic and hypoxic exposures. During the depuration period, embryos or larvae were transferred to clean, normoxic conditions until experimental termination (12 dpf). Feeding began after the absorption of the yolk-sac, 2 days post hatching. Larvae were fed twice a day and the diet consisted of live rotifers for two days after the absorption of the yolk-sac, and then fed live brine shrimp nauplii until the experiment termination. The experiments were static 48h, 100% water renewal conditions at 30°C and a 16 hour-light and 8 hour-dark photoperiods.

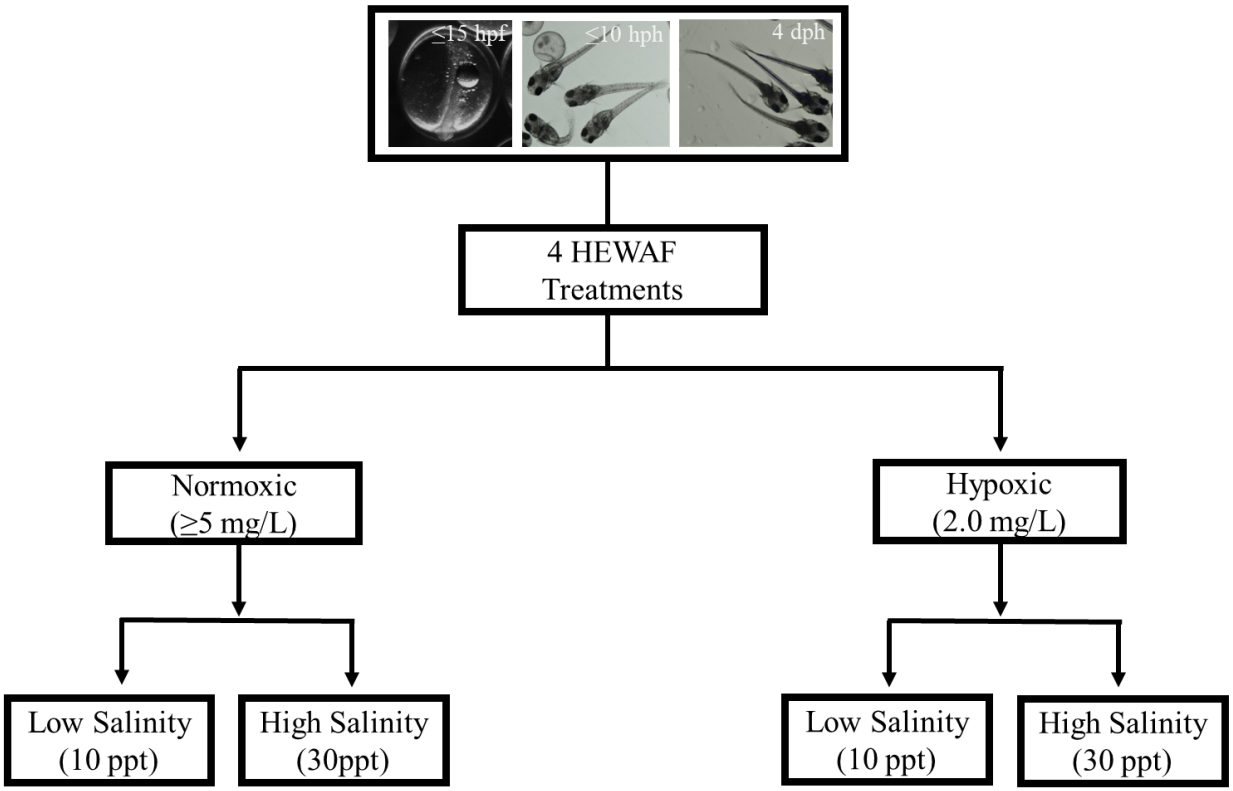

Figure 4. Experimental design.

This experimental design was used for all twelve, early life stage *Cyprinodon variegatus* experiments. Early life stage development was divided into three life stages: embryonic (~ 15 hpf), post-hatch (10 hph), and post-larval (96 hph). All three life stages were exposed to series of HEWAF concentrations, a control (0%), 6.25%, 12.5%, 50%, and 100% for 48 hours. HEWAF exposures were ran under normoxic (≥5 mg/L) and hypoxic (2.0 mg/L) conditions. Both normoxic and hypoxic HEWAF exposures were also conducted under low (10 ppt) and high salinity (30 ppt) conditions. HEWAF concentrations were ran in quadruplicates with a varying number of test organisms dependent on life stage, embryonic (n=40), post-hatch (n=30), and post-larval (n=20).

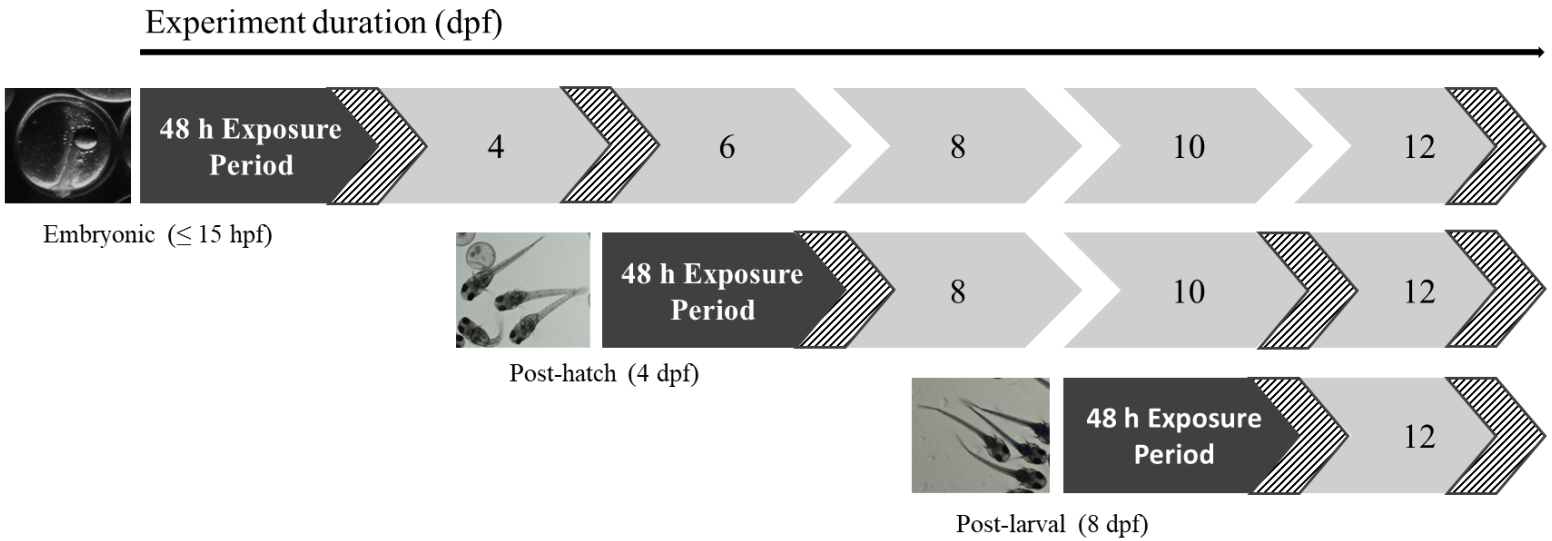

Figure 5. Exposure windows.

All early life stage development experiments begin with a 48 h exposure period to HEWAF treatments + oxic and salinity regime. Following the 48 h exposure period organism are transferred to clean normoxic water and monitored until 12 dpf. Three whole-body tissue samples were collected, 1) immediately after the 48 h exposure period, 2) after a short depuration period (48 – 96 h), and 3) at termination. All whole-body tissue sampling events are indicated by hashed lines.

Hypoxic Exposures

Hypoxic exposures were conducted in a Biospherix I-Glove incubator glovebox equipped with a PROOX model 360 oxygen control module. The dissolved oxygen concentration in the test chambers was maintained at 2.0 mg/L, using nitrogen gas to manipulate atmospheric oxygen in the glovebox. Water baths or heaters were added to maintain chamber at 30°C. Test chambers with test solutions were placed in the gloves box 24 h prior to exposure initiation to allow for dissolved oxygen to decrease to 2.0 mg/L and temperature to reach 30°C. After desired water parameters were observed, test organisms were added to test chambers and the exposure began. Following the 48 h exposure period, nitrogen gas flow to the chamber was turned off and ambient oxygen levels (≥ 5.0 mg/L) were maintained in the chamber for the duration of the experiment.

Normoxic Exposures

Normoxic exposures were conducted in a Precision Incubator set at 30°C. Test chambers with test solutions were placed in the incubator 4 h prior to exposure initiation to allow for test solution temperatures to reach 30°C. After the test solution reached target 30°C, test organisms will be added and the exposure will begin. The incubator temperature remained at 30°C for the duration of the exposure.

Experimental monitoring

Temperature, pH, dissolved oxygen, salinity, and ammonia, were monitored daily in all test chambers. Observations of mortality and developmental abnormalities were recorded daily for all experimental test chambers. Dead embryos or larvae were removed from the test chambers.

Artificial seawater

Artificial seawater was used for all experiments and for maintenance of adult *C. variegatus* brood stock. Artificial seawater used for this study was Fritz super concentrate two-part salt. Experimental water was ultra-violet sterilized and filtered through 0.22µm nitrocellulose membrane filters to remove solid particles (ThermoScientific, Waltham, MA). Treated experimental water was stored in 10 L Pyrex carboys and aerated until used.

Preparation of High Energy Water Accommodated Factions (HEWAF)

HEWAF stock solution was prepared using the method for large volume HEWAF production described by Forth et al. (2016), with modifications. Un-weathered, source oil collected from the DWH riser was used in the preparation of the stock HEWAF solution with a nominal concentration of 1 g/L. HEWAF was prepared using a heavy-duty blender (Waring Commercial). Three liters of artificial seawater were combined with 3.6 mL of source oil in a 3.8 L stainless steel blender container. The water-oil mixture was mixed on the low setting for 30 seconds and transferred to a 4 L separatory funnel. The separatory funnel containing the HEWAF solution was covered with aluminum foil, and allowed to settle for 1 hour. Following the 1 h settling period, the HEWAF stock solution was used to prepare experiment treatment concentrations by dilution (Table 1).

Table 1 *Treatment dilution calculations.*

Treatment	Artificial Seawater (mL)	Stock HEWAF (mL)
Control	500	0
6.25%	468.75	31.25
12.50%	437.5	62.5
25%	375	125
50%	250	250
100%	0	500

Table 1 Nominal HEWAF solutions (control, 6.25%, 12.5%, 50% and 100%) were prepared in 500 mL batches and then distributed into test chambers. All treatment dilutions were made from 1 g/L stock.

Analysis of stock HEWAF

One liter of each stock HEWAF solution (1 g/L) was sampled directly after HEWAF preparation, before test solutions were diluted. Stock HEWAF samples were collected in 1 L amber bottles, preserved with 10 mL of stabilized HPLC grade Methylene Chloride (DCM) and stored at 4°C (Fisher Scientific, Hampton, NH). Samples were shipped overnight on ice for PAH analysis by gas chromatography coupled with tandem mass spectrometry (GC/MS/MS) at The Center for Environmental Sciences and Engineering (Storrs, Connecticut). The total of PAH concentrations were quantified from all twelves HEWAF stock solutions by measuring 29 parent PAHs, alkyl PAHs, and alkyl PAH homologs (Table 2).

Table 2 *Total Polycyclic aromatic (PAHs) measured in stock HEWAF solutions.*

Parent PAHs	Alkyl PAHs	Alkyl PAH Homologs
Naphthalene	2-methyl naphthalene	methyl naphthalene
Acenaphthylene	2,6-dimethyl naphthalene	dimethyl naphthalene
Acenaphthene	1,3-dimethylnaphthalene	trimethyl naphthalene
Fluorene	1,5-dimethylnaphthalene	methyl fluorene
Phenanthrene	2,3,5-trimethylnaphthalene	methyl phenanthrene
Anthracene	1-methylfluorene	
Fluoranthene	3-methylphenanthrene	
Pyrene	9-methylphenanthrene	
Benzo(a)anthracene		
Chrysene		
benzo(b)fluoranthene		
Benzo(k)fluoranthene		
benzo(a)pyrene		
Indeno(1,2,3-cd)pyrene		
Dibenzo(ash)anthracene		
benzo(g,h,i)perylene		

List of the 29 PAHs measured by Gas Chromatography-Mass Spectrometry (GC-MS) in all twelve stock HEWAF solutions.

Fluorescence analysis

Total petroleum hydrocarbons (TPH) were measured using the SpectraMax M2 spectrometer. A sample of 3.5 mL of exposure water was collected from each test chamber during water quality monitoring at 0 h, 24 h, 48 h, and 72 h. The water samples were mixed with 3.5 mL of ethanol and stored in 7 mL scintillation vials at 4°C. TPH was quantified by the amount of fluorescence absorbed between 270 and 380 nm wavelengths. Fluorescence sample preparation and analysis followed methods described by Greer et al., (2012).

HEWAF PAH calculations

To quantify the amount of tPAH29 concentrations for the exposure test solutions, a linear regression model was used to obtain the relationship between the fluorescence values for each treatment and dilution concentrations. The equation was modified to determine the dilution factor for each treatment using the corresponding fluorescence values. Once the dilution factors were determined, they were multiplied by the tPAH29 concentration to estimate the tPAH29 concentration for each experimental treatment.

Embryonic Assays

The effects of PAH exposure on embryonic development in *C. variegatus* were examined under four combinations of parameters: normoxic + low salinity, normoxic + high salinity, hypoxic + low salinity, and hypoxic + high salinity. For all experiments, 50 embryos (≤ 15 hours post fertilization (hpf)) were randomly transferred into PYREX 150 ml crystalizing dishes containing 100 ml of UV sterilized and filtered artificial seawater controls (n=4) and four HEWAF treatments (6.25%, 12.5%, 50%, 100% (n=4 for each concentration)). Embryonic experiments consisted of an initial 48 h exposure followed by a 10 day depuration period. There were three whole body tissue sampling events at 48 h, 96 h, and 288 h. Each sampling event consisted of ten embryo/larvae randomly sampled and pooled from each test chamber. Images were taken of sampled organisms for growth analysis. Heart rates were recorded for a subsample (n=10) of embryos at 24 and 48h. Hatch rates and embryonic abnormalities were also monitored during the embryonic assays.

Post-Hatch Assays

The effects of PAH exposure on recently hatched *C. variegatus* larvae was examined under the four combinations of environmental parameters described above. For all experiments, 30 larvae (< 10 hours post hatch (hph)) were randomly transferred into PYREX 150 ml crystalizing dish containing 100 ml of UV sterilized and filtered artificial seawater controls (n=4) and four HEWAF treatments (6.25%, 12.5%, 50%, 100% (n=4 for each concentration)). Post-hatch experiments consisted of an initial 48 h exposure period followed by a 6 day depuration period. There were whole body tissue sampling events at 48 h, 144 h, and 192 h. Each sampling event consisted of ten larvae randomly sampled and pooled from each test chamber. Images were taken of sampled organisms for total growth and developmental abnormality analysis.

Post-larval Assays

The effects of PAH exposure on actively feeding *C. variegatus* larvae were examined under the four combinations of environmental parameters described above. For all experiments, 20 larvae (< 10 hph) were randomly transferred into PYREX 150 mL crystalizing dish containing 100 ml of UV sterilized and filtered artificial seawater controls (n=4) and four HEWAF treatments (6.25%, 12.5%, 50%, 100% (n=4 for each concentration)). Post-larval experiments consisted of an initial 48h exposure period followed by a 2 day depuration period. There were two whole body tissue sampling events at 48 h and 96 h. Each sampling event consisted of ten larvae randomly sampled and pooled from each test chamber. Images were taken of sampled organisms for total growth and developmental abnormality analysis.

Survivability Monitoring

Survivorship and development observations were recorded daily for all experimental test chambers. Dead embryos or larvae were recorded and removed from the test chambers. Cumulative mortality was calculated daily for each treatment condition for all developmental stages using the % mortality formula [(# of larvae alive/ # of larvae or embryos at test initiation) *100]. Cumulative embryo mortality was also recorded during the embryonic assays using the % embryo mortality formula [(# of viable embryos + dead embryos / the initial # of embryos) *100].

Heart Rate Analysis

Heart rates were measured at 24 hpf and 48 hpf in a subsample of 10 embryos from each experimental chamber (n=10). The heart rates were manually counted in test chambers using a Nikon SMZ1500 Stereoscope. For each embryo, heart rates were counted for 10 seconds and then converted to beats per minute (BPM).

Hatching

Hatch success was measured by calculating the percent of hatch and time to hatch across the HEWAF treatments and four exposure regimes. Percent hatch was calculated using the formula [(#hatched larvae / # embryos)].

Water Quality Monitoring

Daily water quality was performed and recorded. Water quality parameters measured were: temperature, pH, dissolved oxygen, salinity, and ammonia. Test parameters were measured in every test chamber during daily observations. Temperature and dissolved oxygen were measured using an optic YSI, pH was measured using a pH meter, salinity was measured with a refractometer, and ammonia was measured with test strips.

Image collection and analysis

Photo documentation was used to assess growth and developmental abnormalities of *C. variegatus*. Photos were taken at the initiation of exposures and during sampling events (48h, 96h, and termination). Ten randomly selected larvae were collected for sampling and imaging. Larvae and 5 ml of test chamber water were individually transferred to depression microscope slides for imaging. A Nikon SMZ1500 Stereoscope with a Nikon digital camera DXM 1200C was used for capturing images which were stored on an external hard drive (Nikon Instruments Inc., Melville, NY). iSolution lite imaging software was used for calibrating and measuring growth of larvae (IMT i-Solution INC., Easlley, SC).

Final length in millimeters was measured at the termination of all experiments and recorded for later comparisons between treatments and across developmental stages. Images were also used to document abnormal embryonic development in the embryonic assays. Embryonic abnormalities recorded included eye pigmentation, spinal curvature, and cardiac edema.

Statistics

The means of the treatment replicates and the standard deviation are presented in this chapter. Multiple linear regressions were used for each developmental stage to determine significance of stressors on mortality, growth, heart rate, and hatching using SigmaPlot 11.0 (Systat Software, Inc., San Jose, CA). Significance was considered at $p < 0.05$. Lethal concentrations of PAHs were calculated (LC_{50}) for all developmental stages in R and RStudio (R Foundation for Statistical Computing, Vienna, Austria; RStudio, Inc., Boston, MA). The LC_{50} values were calculated using the Dose Response

Curve (dcr) R package, which used a linear model to determine the concentration at which 50% of the experimental population resulted in mortality (Ritz et al., 2015). A one-way analysis of variance (ANOVA) was used to examine significance between heart rates between treatment groups using SigmaPlot 11.0 (Systat Software, Inc., San Jose, CA). Raw heart beat data was used to perform one-way ANOVA with a significance level of 0.001. All tests but one (embryonic normoxic-low salinity 24 h heart rate) failed a Shapiro-Wilk normality test and one test (embryonic normoxic-low salinity 24 h heart rate) failed the equality of variance test. The Holm-Sidak method was used as the multiple test correction for all ANOVAs.

Results

Water chemistry analysis

The concentration and abundance of the 29 PAH and PAH homologs measured from all 12 HEWAF solutions are represented in Figure 6. The most prominent PAH constitutes in all HEWAF solutions included naphthalene, methyl naphthalene, dimethyl naphthalene, and 2-methyl naphthalene. The PAH constituents between HEWAF samples remained constant, but test solution concentrations varied within and between developmental stages. To determine how salinity influences PAH concentration in the treatments, the tPAH29 concentrations of treatments were used in a linear regression to examine differences in PAH concentrations dependent on salinity (Figure 7). The PAH concentrations from the embryonic assays resulted in increased PAH concentrations observed in the 30 ppt treatments when compared to the 10 ppt treatments under both oxic regimes (Figure 7A & B). The treatment PAH concentrations for the post-hatch developmental stage resulted increased PAH concentration observed in normoxic-low

salinity (10 ppt) exposures, while the opposite was observed in hypoxic assays were high salinity conditions resulted in greater PAH concentrations (Figure 7C & D). In the post-larval assays, the PAH treatment concentrations in the normoxic – high salinity (30 ppt) exposures resulted in higher PAH concentrations observed in the higher HEWAF treatments (Figure 7E). Similar slopes were obtained from the PAH concentration linear regressions for the post-larval hypoxic assays, indicating that salinity had no effect on PAH concentration in the post-larval hypoxic assays (Figure 7F). The linear regression analysis of the HEWAF treatment concentrations resulted in a pattern of increased PAH concentrations with increased salinity. Another important result was that higher overall PAH concentrations were measured in hypoxic assays both within and across developmental stage exposures. The 100% HEWAF treatment concentrations for the normoxic assays were 268.38 ± 4.57 (10 ppt) and 368.55 ± 11.15 (30 ppt) for the embryonic exposures, 368.55 ± 4.23 (10 ppt) and 242.15 ± 9.07 (30 ppt) for the post-hatch exposures, and 198.56 ± 11.21 (10 ppt) and 274.00 ± 4.93 (30 ppt) for the post-larval exposures. The 100% HEWAF treatment concentrations for the hypoxic assays were 364.51 ± 70.16 (10 ppt) and 501.12 ± 30.63 (30 ppt) for the embryonic exposures, 319.58 ± 12.92 (10 ppt) and 511.75 ± 30.88 (30 ppt) for the post-hatch exposures, and 223.68 ± 18.98 (10 ppt) and 293.20 ± 111.66 (30 ppt) for the post-larval exposures (Table 3).

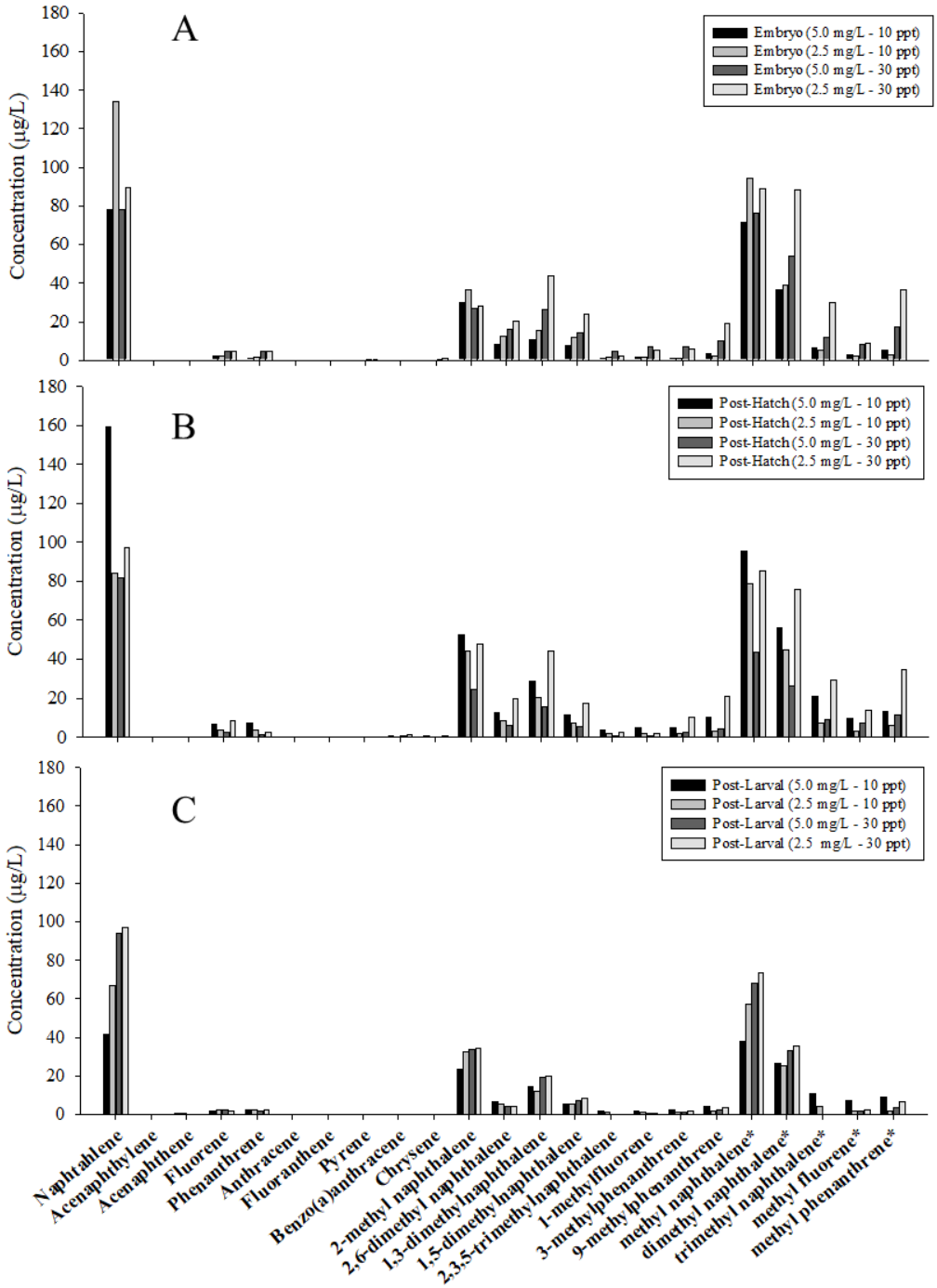

Figure 6. Stock HEWAF PAH Composite measured by Gas Chromatography-Mass Spectrometry (GC-MS) analysis.

The measured PAH concentrations (µg/L) from the 100% HEWAF from all 12 exposures was quantified by measuring 29 PAHs constituents. PAH concentration (µg/L) of the 4 embryonic assays (A), PAH concentration (µg/L) from the post-hatch assays (B), and the bottom graph is the PAH concentration (µg/L) from the post-larval assays (C).

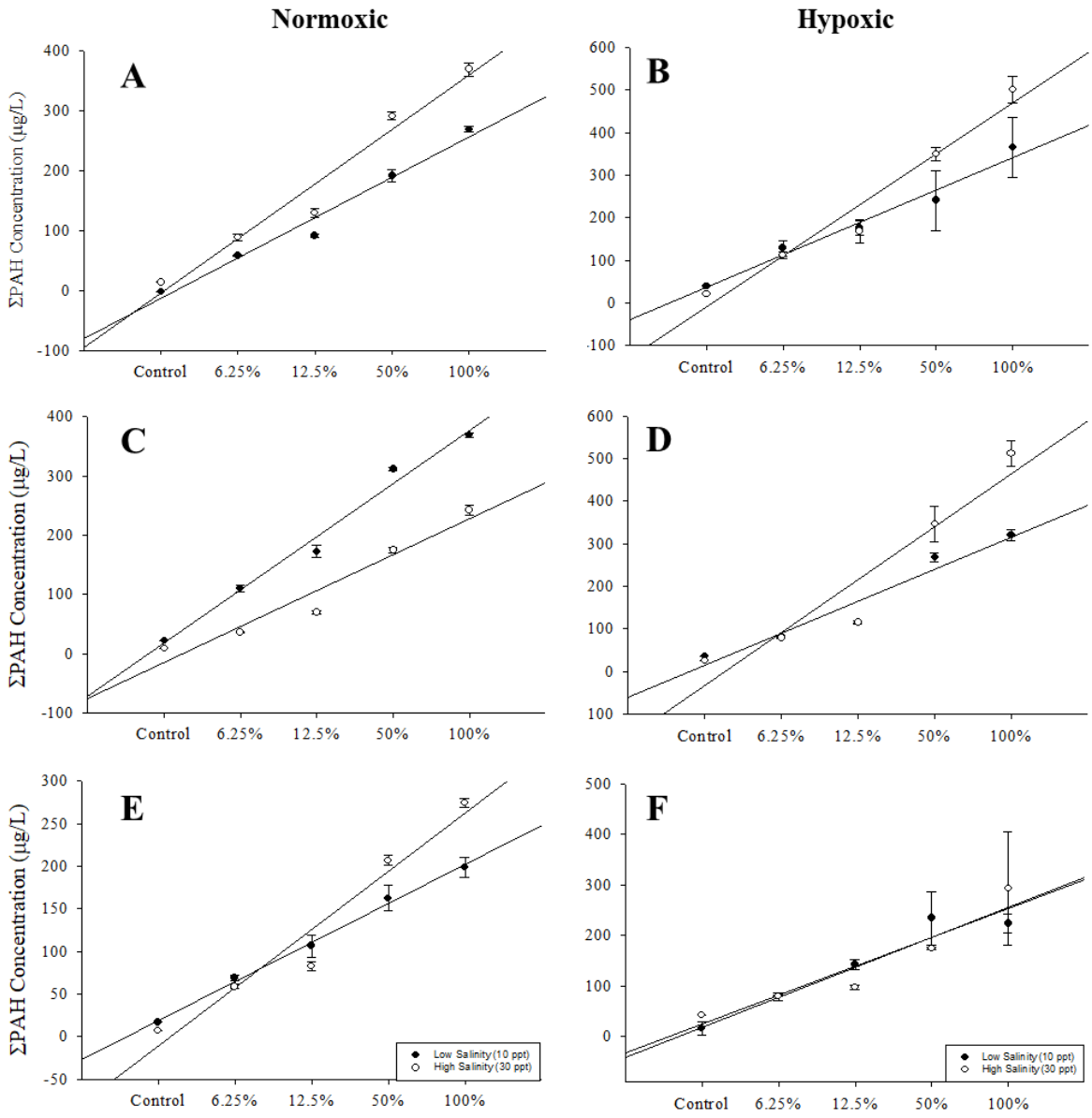

Figure 7. Relationship between PAH dilution and salinity concentration.

Linear regressions show the differences between the slopes of the HEWAF nominal treatment concentrations (µg/L) dependent on salinity. HEWAF dilution concentrations are represented by developmental stage, embryonic (A & B), Post-Hatch (C & D), and Post-Larval (E & F) and by oxic regime. The bars are the standard deviation between treatment replicates and the PAH concentrations are derived from the measured tPAH29.

Table 3 *tPAH29 HWEWAF concentration for nominal exposure dilutions.*

Normoxic Assays					
Exposure	Control	6.25%	12.5%	50%	100%
Embryonic (10 ppt)	0 ± 0.04	57.81 ± 0.56	90.94 ± 3.50	190.90 ± 9.64	268.38 ± 4.57
Embryonic (30 ppt)	13.38 ± 0.02	88.20 ± 5.92	128.61 ± 6.94	290.58 ± 6.66	368.55 ± 11.15
Post-hatch (10 ppt)	21.24 ± 0.02	110.22 ± 5.10	172.03 ± 10.43	311.17 ± 3.37	368.55 ± 4.23
Post-hatch (30 ppt)	8.82 ± 0.05	35.51 ± 0.87	69.79 ± 2.18	174.77 ± 4.73	242.15 ± 9.07
Post-larval (10 ppt)	17.09 ± 0.02	68.76 ± 3.63	106.35 ± 13.17	162.35 ± 15.18	198.56 ± 11.21
Post-larval (30 ppt)	7.10 ± 0.06	58.73 ± 2.57	82.64 ± 4.85	206.69 ± 6.12	274 ± 4.93
Hypoxic Assays					
Exposure	Control	6.25%	12.5%	50%	100%
Embryonic (10 ppt)	39.79 ± 0.04	128.78 ± 17.87	176.59 ± 17.60	240.69 ± 70.67	364.51 ± 70.16
Embryonic (30 ppt)	20.59 ± 0.08	112.67 ± 8.66	168.05 ± 27.80	349.74 ± 14.77	501.12 ± 30.63
Post-hatch (10 ppt)	35.96 ± 0.07	82.59 ± 2.75	116.44 ± 2.07	267.55 ± 10.97	319.58 ± 12.92
Post-hatch (30 ppt)	25.71 ± 0.49	79.01 ± 0.89	115.39 ± 4.40	345.82 ± 42.07	511.75 ± 30.88
Post-larval (10 ppt)	15.97 ± 13.68	79.59 ± 7.99	142.51 ± 9.14	234.95 ± 52.73	223.68 ± 18.98
Post-larval (30 ppt)	42.96 ± 0.16	80.15 ± 1.08	97.48 ± 4.31	174.62 ± 2.06	293.20 ± 111.66

Calculated treatment dilutions (µg/L) ± standard deviation.

Lethal Concentration Analysis (LC_{50})

The LC_{50} values for the embryonic and post-hatch assays were not able to be calculated due to the low or no mortality that occurred during the 48-h exposure period. LC_{50} values for all four exposure regimes were calculated for the post-larval developmental stage (Table 4). The results showed a shift in the sigmodal curve for the LC_{50} values toward the left with the addition of stressor combinations (Figure 8). The normoxic-low salinity exposure had the highest LC_{50} value 207. 13 ± 15.50 µg/L, which correlates to the lowest toxicity to free feeding SHM larvae. The combination of oil, hypoxia, and high salinity resulted in similar LC_{50} values (103.93 ± 15.63 µg/L and 103.16 ± 14.65 µg/L, respectively). The exposure regime with the lowest LC_{50},

indicating the highest toxicity to the larval SHM, was the simultaneous exposure of all three stressors, HEWAF, hypoxia, and high salinity (hypoxic + high salinity) with a value of 64.55 ± 12.81 µg/L (Table 4).

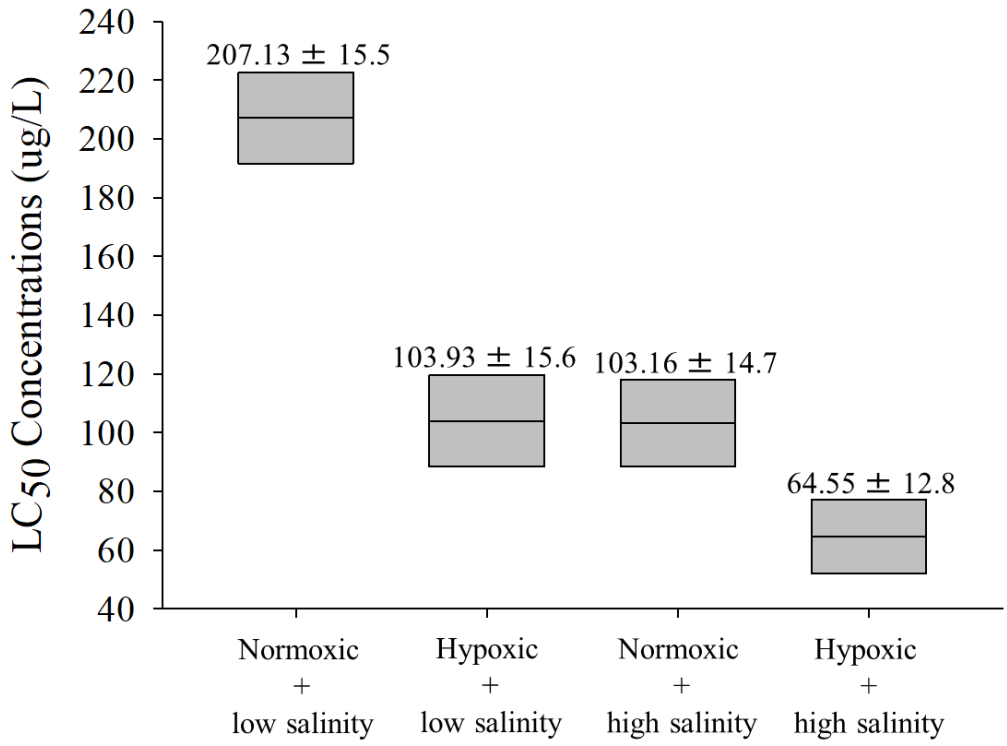

Figure 8. Modified Post-larval median lethal concentrations (LC_{50}) Box and whisker plot.

Lethal concentrations at which mortality occurred in half the treatment population is represented by the middle bar in the box plot and the top and bottom bar represent the standard error.

Table 4 *Post-Larval Median Lethal concentrations (LC_{50}) for each exposure regime with standard error.*

Developmental Stage	Exposure Regime	LC_{50} (µg/L)	Standard Error
Post-Larval	Normoxic - Low Salinity	207.13	± 15.50
	Hypoxic - Low Salinity	103.93	± 15.63
	Normoxic - High Salinity	103.16	± 14.65
	Hypoxic - High Salinity	64.55	± 12.81

Embryonic assays

Low percent mortality under all four exposures regimes regardless of PAH concentration was observed during the embryonic assays with mortality never exceeding 50% (Figure 9A). A multiple linear regression revealed that PAHs ($p = 0.004$) and dissolved oxygen ($p < 0.001$) had significant effects on the observed mortality during embryonic assays, while salinity had no significant effect (Table 5). Final growth was a sub-lethal endpoint also assessed using a multiple linear regression. The analysis indicated that two stressors significantly impacted the final lengths of the larvae: dissolved oxygen ($p = 0.001$) and salinity ($p < 0.001$), while PAH concentration showed no significant effect on larval growth (Figure 12A and Table 6).

Sub-lethal developmental toxicity endpoints included final growth, heart rate measurements, and hatch success embryos. Heart rate measurements were recorded as beats per minute (BPM) at 24 and 48 hpf (Figure 10 and 11 respectively). Heart rates at 24 hpf were significantly affected by both PAHs ($p = 0.039$) and dissolved oxygen concentrations ($p < 0.001$), whereas the heart rates at 48 hpf were only significantly impacted by PAH concentrations ($p = 0.032$) (Table 10). The effects of salinity, DO, and PAHs on embryonic hatch was measured at 96 hpf. The statistical analysis on percent hatched embryos at 96 hpf indicated that PAH ($p < 0.001$) and DO concentrations ($p < 0.001$) had significant effects on hatching success of exposed embryos (Table 11).

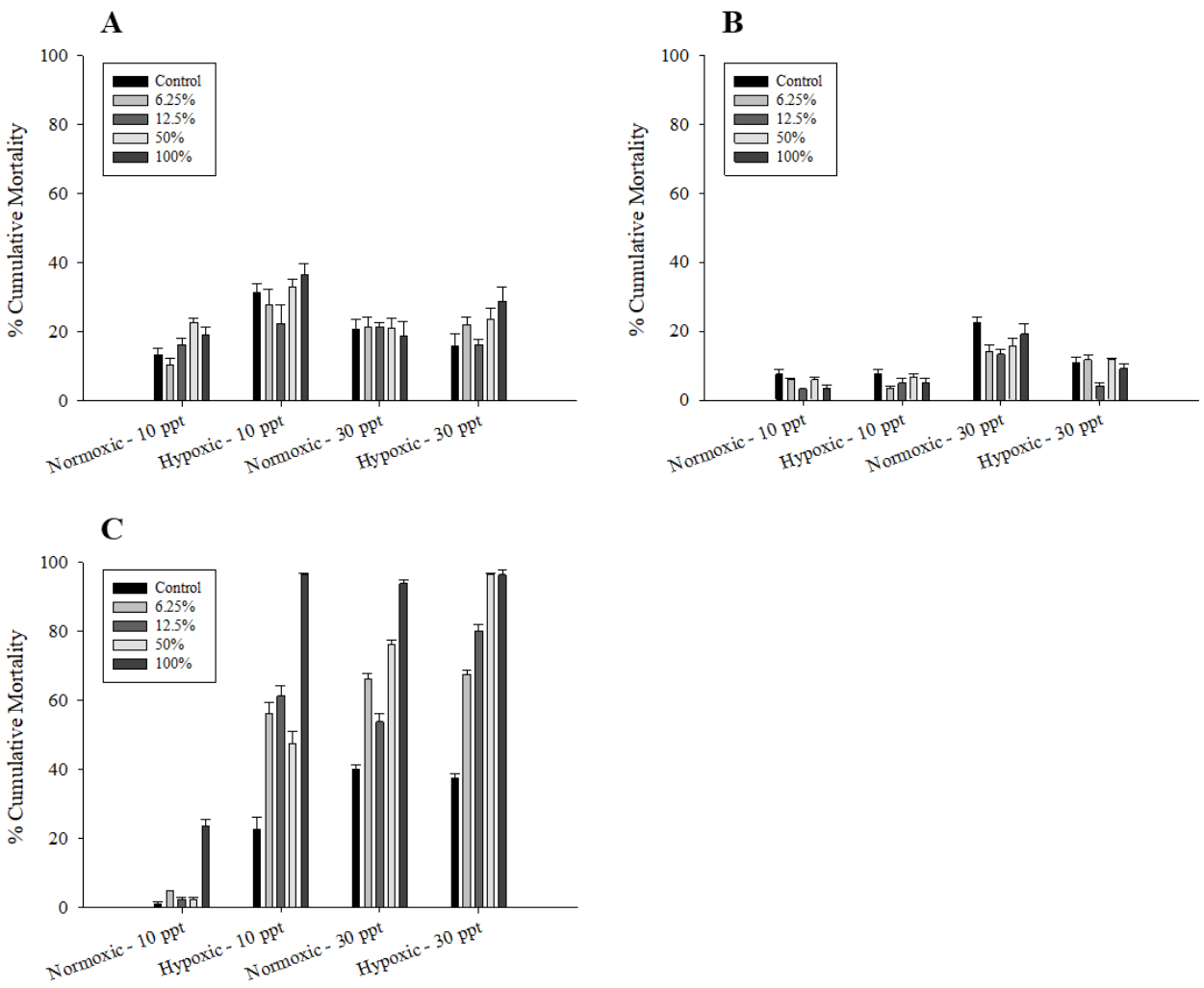

Figure 9. Percent cumulative mortality.

Cumulative mortality for all three developmental stages, embryonic (A), post-hatch (B), and post-larval (C), under all four exposure regimes.

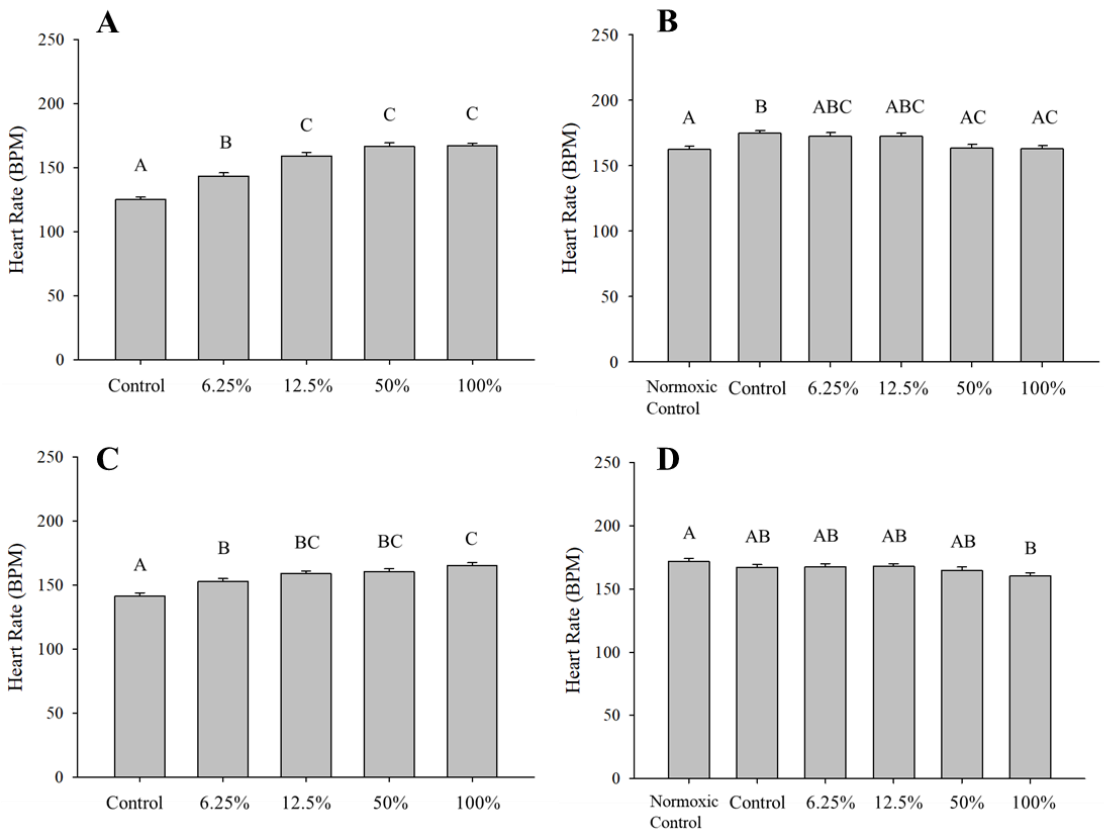

Figure 10. Embryonic heart rate response to HEWAF exposure under different environmental conditions at 24 h.

All graphs represent heart rate in beats per minute (BPM) response to HEWAF treatments in the presence of A) normoxic – low salinity conditions, B) hypoxic – low salinity conditions, C) normoxic – high salinity conditions, and D) hypoxic – high salinity condtions. Letters indicate significance with a p-value >0.05.

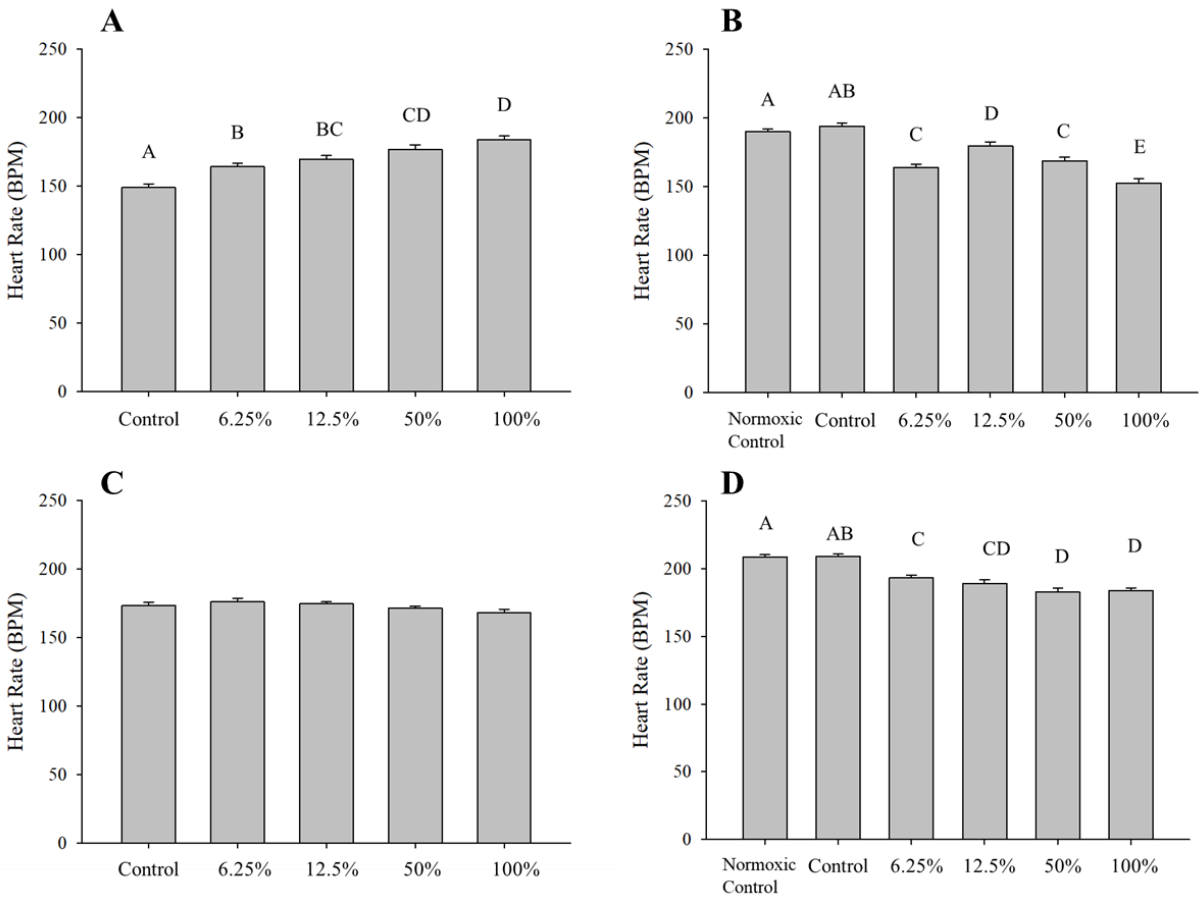

Figure 11. Embryonic heart rate response to HEWAF exposure under different environmental conditions at 48 h.

All graphs represent heart rate in beats per minute (BPM) response to HEWAF treatments in the presence of A) normoxic – low salinity conditions, B) hypoxic – low salinity conditions, C) normoxic – high salinity conditions, and D) hypoxic – high salinity conditions. Letters indicate significance with a p-value >0.05.

Post-hatch assay results

The post-hatch developmental stage resulted in the lowest cumulative mortality observed between all three developmental stages after exposure to the four experimental regimes and HEWAF treatments (Figure 6B). Less than 50% mortality occurred in all four exposure regimes regardless of HEWAF concentration, similar to the embryonic results. The percent mortality observed during the post-hatch developmental stage assays

were most significantly affected by the environmental stressors salinity ($p < 0.001$) and DO ($p = 0.005$), and that PAH concentration had no significant effect on cumulative mortality, according to the multiple linear regression analysis (Table 5). Final growth was the non-lethal developmental endpoint used to investigate the effects of PAH and environmental stressors on larval health. The multiple linear regression analysis indicated that the final growth during the post-hatch developmental stage assays was most significantly affected by PAH concentration ($p < 0.001$) and salinity ($p < 0.001$) (Figure 12B and Table 6).

Post-larval assay results

The results from the cumulative percent mortality and final length analysis during the post-larval assays indicated that the post-larval developmental stage is most sensitive to the individual and combined effects of salinity, hypoxia, and PAH exposure (Figure 6C). Cumulative percent mortality observed during the post-larval assays was significantly affected by all three stressors: salinity ($p < 0.001$), DO ($p < 0.001$), and PAH concentrations ($p < 0.001$) according the multiple linear regression analysis (Table 3). The final length measurements from the post-larval assays were also significantly affected by all stressors salinity ($p < 0.001$), DO ($p = 0.041$), and PAH ($p < 0.001$) (Figure 12C and Table 4).

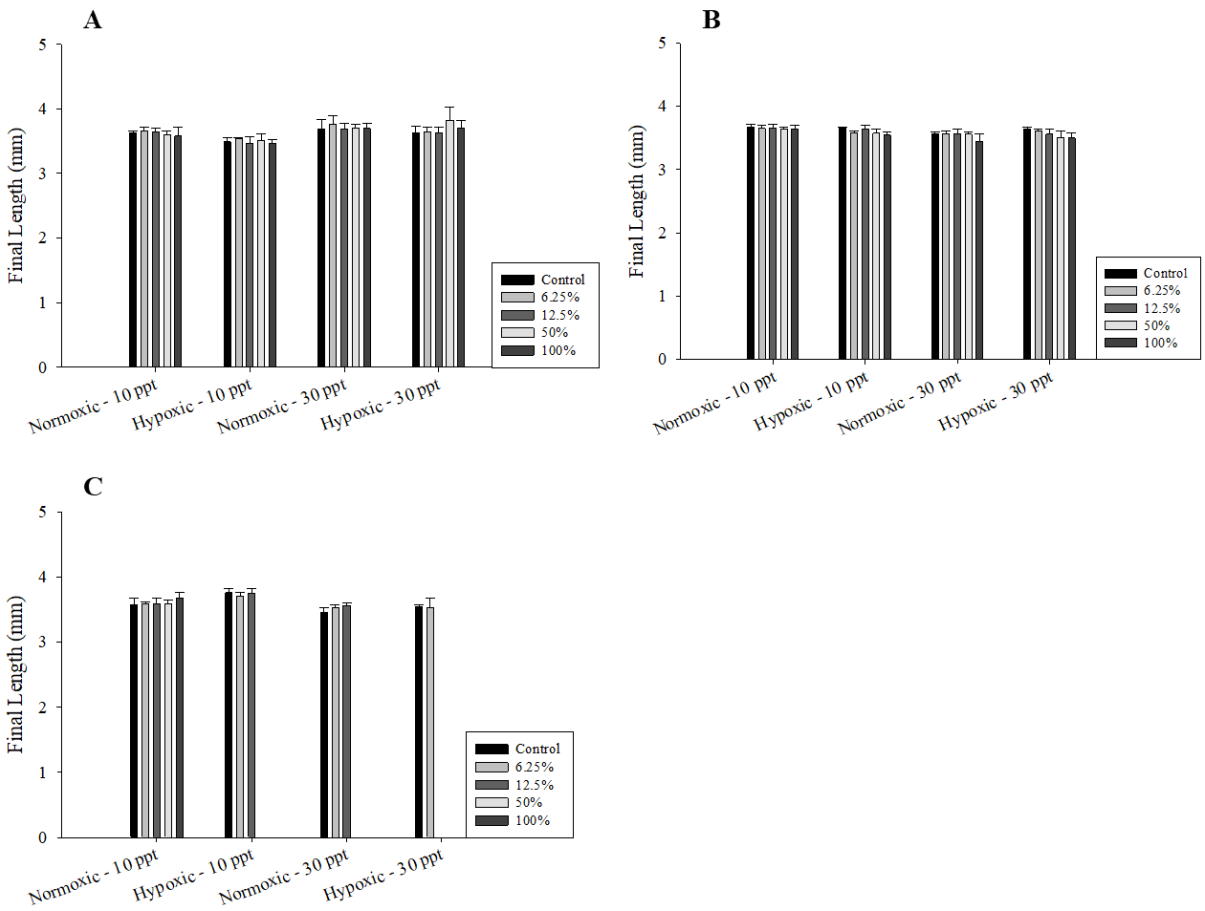

Figure 12. Final Length (mm) of larval Cyprinodon variegatus at termination (12 dpf) in response to HEWAF treatments and exposure conditions.

Embryonic final length for all four exposure conditions (A), post-hatch final length for all four exposure conditions (B), and post-larval final length for all four exposure conditions (C).

Table 5 *Multiple linear regression (MLR) for cumulative mortality across all developmental stages.*

	Embryonic	Post-hatch	Post-larval
Stressor	p-value	p-value	p-value
PAH	0.004	0.276	<0.001
Dissolved Oxygen	<0.001	0.005	<0.001
Salinity	0.062	<0.001	<0.001

Significance defined as $p < 0.05$.

Table 6 *Multiple linear regression (MLR) for final growth across all developmental stages.*

	Embryonic	Post-hatch	Post-larval
Stressor	p-value	p-value	p-value
PAH	0.404	<0.001	<0.001
Dissolved Oxygen	0.001	<0.001	0.041
Salinity	<0.001	0.611	<0.001

Significance defined as $p < 0.05$.

Table 7 *Multiple linear regression (MLR) for embryonic heart rates impacted during embryonic exposures.*

	24 h	48 h
Stressor	p-value	p-value
PAH	0.039	0.032
Dissolved Oxygen	<0.001	0.130
Salinity	0.683	0.105

Significance defined as $p < 0.05$.

Table 8 *Multiple linear regression (MLR) for embryonic mortality and hatch success.*

	Embryo Mortality	% Hatch
Stressor	p-value	p-value
PAH	0.039	<0.001
Dissolved Oxygen	<0.001	<0.001
Salinity	0.683	0.458

Significance defined as $p < 0.05$.

Comparative results

The combined cumulative mortality results from all 12 experiments suggested that the post-larval developmental stage in C. *variegatus* is the most sensitive to the individual and combined exposure of PAHs and adverse environmental conditions. The highest cumulative mortality occurred during the post-larval assays, with over 50% mortality observed for all tested HEWAF treatments in three out of the four exposure regimes. The second highest cumulative mortality was observed during the embryonic assays and was only significantly affected by PAH contamination and DO concentrations. Finally, the embryonic stage showed the least effects on cumulative mortality rates. These data suggest that yolk-sac larvae are the most resilient to acute lethal effects of PAH exposure under adverse environmental conditions.

Discussion

The decreased survival observed in the post-larval developmental stage seen here in provides further evidence to support the post-larval developmental stage in *C. variegatus* as the most sensitive to PAH exposure. Increased lethal effects of PAH exposure during larval fish development has been observed in sheepshead minnows

exposed to a single PAH treatment, pyrene, at concentrations of 60 and 120 ppb (Hendon et al., 2008). Larval enhanced toxicity to PAHs has also been observed in mahi-mahi and zebrafish species when compared to embryonic mortality (Incardona et al., 2004; Mager et al., 2016).

The minimal effects of PAH exposure on growth of *C. variegatus* during all three developmental stages maybe be explained by the timing and duration of the PAH exposure. All oil exposures occurred at the transition point into the next developmental stage which only lasted for 48 hours, after which the surviving embryos/larvae were transferred to clean, normoxic water and monitored until 12 dpf. The acute exposure to oil under varying environment conditions was not enough to cause significant differences in growth rates within and between developmental stages.

The post-larval developmental stage exhibited the highest cumulative mortality from HEWAF exposure among all four exposure conditions, but salinity and hypoxia significantly affected the toxicity of oil during the embryonic and post-hatch assays as well. High salinity conditions (30 ppt) correlated to increased cumulative mortality in the post-hatch and post-larval assays, but had no significant effects on embryonic mortality. The MS-GC and fluorescence analysis of the stock and treatment HEWAF solutions from the current set of experiments show similar concentrations of PAHs between the low and high salinity regimes, contradicting previous research suggesting that the bioavailability of oil decreases with increased salinity conditions (Ramachandran et al., 2006). Due to similar levels of PAHs being found in both salinity regimes, the differential effects of salinity on the mortality and growth of the exposed organisms may be a result of

increased osmotic pressure and metabolic cost, rather than differences in PAH concentrations (Ramachandran et al., 2006; Whitehead, 2013).

Salinity changes not only elicit responses in living organisms, but can also influence the presence and persistence of other adverse environmental conditions such as hypoxia. Hypoxia is a common marine stressor which is the result of both natural and anthropogenic sources, with increased hypoxia during the summer months in the estuaries along the nGoM (Bianchi et al., 2010; Rabalais et al., 2002). In this experiment, hypoxia also had a significant effect on mortality across all early life stages of *C. variegatus*, but only significantly impacted total growth in embryonic and post-larval assays. The increased HEWAF toxicity in the presence of hypoxia is most likely related to the gills and increased metabolic demands.

The synergistic potential of all treatments on both mortality and growth was most severe during the post-larval assays. The LC_{50} values decreased as the number of stressors increased. The increase in HEWAF toxicity with the combination of stressors can possibly be explained by increased metabolic demands and the gill morphology and function.

Embryonic fish are enclosed by the chorion, which provides a barrier between the embryo and the external environmental, therefore limiting the direct contact with oil. The post-hatch developmental stage was hypothesized to be the most sensitive PAH exposure, but displayed the highest resilience to PAHs. The oil exposure during the post-hatch developmental stage occurred while the larvae had yolk-sacs and were not feeding freely which may have limited the ingestion of PAHs. The increased sensitivity of the post-larval SHM to PAH exposure may be explained by increased exposure to PAHs and

increased metabolic demand. The larvae used for the post-larval assays were 96 hph and freely feeding on brine shrimp nauplii, which could have been due to increased exposure of oil via ingestion as well as exposure at the gills.

A common factor linking all three of the stressors is their dependence on the gills. Fish gills have direct contact with the external environment, and serve a critical role ion and gas exchange (Evans et al., 2005). The morphology of the gills is comprised of counter current vascular systems and lipid rich tissues to aid in transport of oxygen and ions with the environment, but these morphological characteristics make the gills the primary route of oil exposure in fish (Evans et al., 2005; Ramachandran et al., 2006). The lipid rich tissues of the gills PAHs to passively diffuse across the gill membranes, inducing local and systemic metabolic responses (Ramachandran et al., 2006). Changes to gill structure and ability as a result of oil contamination can cause confounding effects on routine metabolic functions to maintenance internal ion and oxygen homeostasis.

The increased toxicity of HEWAF observed during the post-larval assays could be a result of impaired osmoregulation, inhibiting the larvae's responses to increased osmotic pressure. These data provide similar results to oil exposures under different salinity conditions in intraperitoneal injected rainbow trout, which also resulted in inhibited osmoregulation functions, independent of gill morphology (Engelhardt et al., 1981). Oil contamination has also been documented to change to the gill tissue and cell structures, decreasing the exposed fish's osmoregulatory ability (Goanvec et al., 2011; Whitehead, 2013). Research investigating oil exposure on gulf killifish documented altered gene regulation of multiple ion transporters in the gills of exposed fish after oil exposure (Whitehead et al., 2012). Oil exposure to juvenile turbot decreased the number

of mucocytes and chloride cells in gill epithelium and oil exposure to juvenile flounder resulted in lamellar telangiectasia and epithelial proliferation which decreased osmotic regulatory ability in juvenile fish (Brown-Peterson et al., 2015; Goanvec et al., 2011). Fish embryos are protected from the external environmental conditions by the chorion which prevents direct contact of oil to the developing embryo, further indicating that the synergist effects of salinity on the oil toxicity may be a result of physical damage of oil at the gills and loss of osmoregulatory ability.

The additive effect of hypoxia on the toxicity of HEWAF may also be a result of inhibited oxygen exchange at the gills. Oil exposure under normoxic environmental conditions has been documented to decrease the vascular oxygen levels as a result of decreased hematocrit levels in catfish (Brauner et al., 1999). Morphological changes to the gill structures, such as epithelium necrosis and inflammation, has been documented in juvenile brown spot grouper, flounder, and zebrafish (Brown-Peterson et al., 2015; Sørhus et al., 2016) The changes in gill morphology can limit the surface area of the gill lamellae and decrease oxygen exchange.

The current research identified that in sheepshead minnows, post-larval developmental stage is the most sensitive early life stage to oil exposure. The research also determined that HEWAF exposure under hypoxic - high salinity conditions resulted in a synergistic toxicity effects of oil to larvae SHM. The findings from this experiment provide critical evidence to further understanding of the impact of oil on developing organisms in estuarine habitats in the presence of environmental stressors

CHAPTER III - CROSS-TALK BETWEEN THE ARYL HYDROCARBON RECEPTOR SIGNALING PATHWAYS (AHR) AND THE HYPOXIA INDUCIBLE FACTOR 1-ALPHA SIGNALING PATHWAY (HIF-1A)

Introduction

On April 20, 2010, the largest marine oil spill in U.S. history occurred when the Deepwater Horizon (DWH) oil rig exploded (Allan et al., 2012; Sumaila et al., 2012). An estimated 4.9 million barrels of crude oil were released into the northern Gulf of Mexico (nGoM), impacting more than 2100 km of coastline ecosystems, including estuarine habitats (Allan et al., 2012; Beyer et al., 2016; McNutt et al., 2012; Whitehead, 2013). Polycyclic aromatic hydrocarbons (PAHs) are highly toxic components of crude oil and known to cause cardiac edema, and abnormal liver, gill, and skeletal development (Brown-Peterson et al., 2015; Hendon et al., 2008; Incardona et al., 2004; Jones et al., 2017; Ramachandran et al., 2006; Sørhus et al., 2016). The impacts of the mass release of crude oil into the nGoM are further compounded due to the extent of hypoxic conditions these same coastal habitats. Hypoxia threatens the ecosystem health of habitats and has been known to cause mass mortality events, delayed development, teratogenic effects, endocrine dysfunction, reduced hatching success and spawning rates (Dangre et al., 2010; Shang and Wu, 2004; Wu et al., 2003). Simultaneous exposures to PAH and hypoxic stress on aquatic organisms have indicated a potential synergistic toxicity to occur because of cellar cross-talk between the Aryl Hydrocarbon Receptor Signaling (AhR) and the Hypoxia Inducible Factor 1 alpha signaling (HIF-1α) pathways (Fleming et al., 2009; Hendon et al., 2008; Schults et al., 2010; Vorrink and Domann, 2014; Yu et al., 2008). Cross talk between the AhR and HIF-1α pathways inhibit an

organism's ability to simultaneously metabolize PAHs and increase oxygen delivery to hypoxic tissues which decreases individual fitness.

Since the discovery of aryl hydrocarbon nuclear translocator protein (Arnt) as the shared binding partner for the AhR and HIF-1α pathways, synergistic toxicity studies have focused on cross-talk between these two pathways at the Arnt node to explain the increased mortality and phenotypic response of fish in the presence of both stressors. Many of the results produced from these studies have proven to be inconclusive and molecular processes involved in the synergistic toxicity of oil and hypoxic stress are still undetermined. This research has provided vital information concerning the toxicity and modes of action of individual constituents of oil and oil mixtures, but has ignored interaction between oil and environmental factors. Therefore, the inclusion of abiotic factors in the examination of oil exposure on fish health is critical to understanding of how oil exerts toxicity to marine organism in natural environments (Adams, 2005; Whitehead, 2013).

The current research addresses gaps in knowledge regarding the effects of complex oil mixtures in combination with multiple environmental stressors. Sheepshead minnow (SHM) were used in this study because they are a common estuarine species distributed throughout the nGoM (Kuntz, 1916). The SHM also breeds year-around and is a benthic egg layer, which increases its exposure risk to both hypoxia and PAHs during early life stage development (Hendon et al., 2008; Kuntz, 1916). The objective of this research is to investigate the occurrence of the cross-talk between the AhR and HIF-1α signaling pathways in early life development of sheepshead minnow (*Cyprinodon variegatus*) under different environmental conditions. Specifically, the research wanted

to identify developmental windows of increases sensitivity to crude oil, synergistic relationships with abiotic factors, and molecular modes of toxicity. Real-time quantitative polymerase chain reactions (qPCR) to measure AhR and HIF-1α pathway activity. The results from this study provide evidence that synergistic toxicity of oil and environmental factors was influenced by exposure conditions, age, and *arnt1* expression.

Methods

Experimental Design

To investigate potential cross-talk between the AhR and the HIF-1α signaling pathways a series of twelve static 48 h HEWAF exposures were designed. The experiments were divided into three developmental stages: embryonic (≤15 hpf), post-hatch (≤10 hph), and post-larval (96 hph). All developmental stages were subjected to four different environmental condition combinations normoxic-low salinity (≥ 5.0 mg/L – 10 ppt), hypoxic-low salinity (2.0 mg/L – 10 ppt), normoxic-high salinity (≥ 5.0 mg/L – 30 ppt), and hypoxic-high salinity (2.0 mg/L – 30 ppt). Experiments began with a 48 h exposure period that subjected embryos or larvae to 4 different HEWAF treatment concentrations (6.25%, 12.5%, 50%, 100%) in combination with the four different exposure regimes. All exposure treatments were executed in quadruplicates, for a total of 20 test chambers. After the exposure period, a subset of embryos/larvae (n=10) were sampled for whole body tissue analysis.

Normoxic Assays.

Normoxic exposures were conducted in a Precision Incubator set at 30°C (VWR, Radnor, PA). Low and high salinity exposures were conducted under normoxic conditions for each developmental stage. Test chambers were placed in the incubator 4 h

prior to exposure initiation to allow for test solution temperatures to reach 30°C. After the test solution reached target 30°C, test organisms were added and initiated exposures. The incubator temperatures were maintained at 30°C for the duration of the experiments.

Hypoxic Assays

Hypoxic exposures were conducted in a BioSpherix I-Glove incubator glovebox equipped with a PROOX model 360 oxygen control module (BioSpherix, Ltd. Parish, NY). The dissolved oxygen levels in the test chambers were maintained at 2.0 mg/L, by using nitrogen gas to manipulate the atmospheric oxygen. Temperature was maintained at 30°C using heaters (for embryonic exposures) and water baths (post-hatch and post-larval exposures). Low and high salinity exposures were conducted under hypoxic conditions for each developmental stage. Test chambers were placed in the glovebox 12 h prior to exposure initiation to allow for dissolved oxygen levels to decrease to 2.0 mg/L and temperatures to reach 30°C. After desired water parameters were reached, test organisms were added to test chambers and the exposures began.

HEWAF Preparation

Source oil from the Gulf of Mexico Research Initiative (GoMRI) was used to make 1 g/L stock HEWAF solutions for all twelve exposures. HEWAF was made following Natural Resource Damage Assessment (NRDA) methods described by Forth et al. (2017) as described in chapter II (Forth et al., 2017).

Water chemistry analysis

The concentration of tPAH29 in all test chambers was calculated using Gas Chromatography- Mass spectrometry (GC-MS) stock for solutions and fluorescence readings from the individual test chambers as described in the methods section of chapter

II. The known oil concentrations values were used in a linear regression model described in more detail in the methods section of chapter II.

To quantify the amount of tPAH concentrations for the exposure test solutions, a linear regression model was made in Sigma Plot. The linear regression was used to obtain the relationship between the treatments fluorescence values and dilutions in the form of a line equation. The equation was modified to determine the dilution factor for each treatment using the corresponding fluorescence values. Once the dilution factors were determined they were multiplied by the tPAH29 concentration to estimate the tPAH29 concentration for each experimental treatment.

Tissue collection

To examine gene expression during the early life stages of SHM in response to oil and environmental stressors, pooled whole-body tissue samples were collected directly following the 48 h exposure period. For embryonic exposures, 10 embryos were randomly sampled, flash frozen with liquid nitrogen in a 1.0 mL cryofreeze tube and stored at -80°C until downstream analysis was performed. For the post-hatch and post-larval exposures, 10 larvae were randomly sampled and stored in 1.5 mL centrifuge tubes filled with 750 mL of RNA later at -80°C until downstream analysis was performed.

RNA Isolation and cDNA Synthesis

Total RNA was isolated from pooled whole-body tissue samples collected at 48 h. Qiagen's RNeasy Mini Kit was used for RNA isolation, following manufactures protocol with modifications (Qiagen, Valencia, CA). To increase RNA yield, all 1200 µL of homogenate sample was added to RNeasy spin columns. To increase the RNA purity, a second rinse with RW1 buffer was performed to minimize salt contamination. The

concentration and purity of the total RNA was measured using NanoDrop 2000 Spectrophotometer and RNA samples were stored in -80°C (ThermoScientific, Waltham, MA). Total RNA samples isolated from 48 h samples was reverse transcribed into cDNA using the RevertAid RT kit (ThermoScientific, Waltham, MA). cDNA synthesis followed manufacture's protocol for 20 μL reactions.

Real-time Polymerase Chain Reaction (qPCR)

To examine the activation of AhR and HIF-1α pathways, the expression of *cyp1a1, epo,* and *arnt1* were measured using qPCR from the 48 h total RNA samples (Table 9). Gene expression of *cyp1a1, epo, arnt1* and the endogenous control 18s rRNA, were measured using the quantitation-Comparative CT (ΔΔCT) methods with Fast SYBER™ Green Master Mix measured on an ABI 7500 Fast real time PCR machine (Applied Biosystems, Foster City, CA). Ct values were converted to fold change expression relative to control treatments using DataAssist™ software (ThermoScientific, Waltham, MA). The activity of the AhR and HIF-1α signaling pathways was predicted using the relative gene expression values of the target genes. The relative gene expression of the target genes was measured in all three developmental stages: embryonic, post-hatch and post-larval, under low (10 ppt) and high (30 ppt) salinity conditions. All HEWAF treatments were normalized to the experimental control samples, and the gene expression of *cyp1a1, epo,* and *arnt1* were normalized using the endogenous control gene, *18s* rRNA. Target genes primers sequence, size and melting points are listed in Table 9.

Table 9 *Cyprinodon variegatus specific primers used to measure relative gene expression of target genes.*

Gene Name	Direction	Sequence (5' to 3')	Size (bp)	T_m (°C)
18s	Forward	GCTGAACGCCACTTGTCC	18	56.9
	Reverse	ATTCCGATAACGAACGAGACTC	22	54.3
cyp1a1	Forward	GCAGATTAACCACGACCCAGAG	22	57.6
	Reverse	GCATCGCCTCCTTCCTAAGC	20	58.2
epo	Forward	GGCCAATCTGTGACCTGA	18	54.7
	Reverse	TGCTCCGTTGCGTCTTTC	18	55.9
arnt1	Forward	TCCCTCGTTCCCACCTGTAA	20	57.8
	Reverse	GGCTTGTAGTTGGCCTCAGT	20	57.4

Results

Embryonic Assays

The relative gene expressions of target genes *(cyp1a1, epo,* and *arnt1*) were measured by qPCR methods to elucidate the potential cross-talk between the AhR and HIF-1α signaling pathways. The relative gene expression of *cyp1a1* was up-regulated for both oxic regimes under low salinity conditions (Figure 13A and B). Fold change expression for *epo* and *arnt1* in the normoxic-low salinity exposure did not exceed 1-fold change, and no treatment patterns were observed. Similar expression patterns for *epo* and *arnt1* were observed under the hypoxic-low salinity conditions (Figure 13B). Up-

regulation of *epo* and *arnt1* was observed in all HEWAF treatments except 12.5% treatment which was down-regulated (Figure 13B).

Upregulation of *cyp1a1* was observed in both the normoxic and hypoxic- high salinity exposures in a treatment dependent manner (Figure 14A and B). The regulation pattern of *epo* and *arnt1* was similar under normoxic-high salinity condition, resulting in up-regulation of both genes in all treatments except the 12.5% HEWAF treatment (Figure 14A). Under hypoxic-high salinity conditions *epo* showed upregulation in all treatments except the highest HEWAF treatment. No clear expression pattern of *arnt1* under hypoxic-high salinity conditions were observed, but decreased expression of *arnt1* was observed in both the 50 and 100% HEWAF treatments (Figure 14B).

Post-Hatch Assays

The expression of *cyp1a1* was upregulated in the low salinity exposures under both oxic regimes (Figure 15A and B). Under hypoxic conditions, the expression of *cyp1a1* increased in a dose dependent pattern, while no clear treatment pattern was observed under normoxic conditions (Figure 15A). No discernible patterns of *epo* and *arnt1* expression were noted in the normoxic-low salinity exposures, but increased down-regulation of *arnt1* was observed in the 6.25 %, 12.5%, and the 100% HEWAF treatments (Figure 15A). The hypoxic-high salinity condition induced an up-regulation of both *epo* and *arnt1* in a dose dependent manner, though *epo* resulted in a stronger expression response (Figure 15B).

The expression pattern of *cyp1a1* under high salinity conditions was similar to the expression pattern observed in the low salinity exposures, up-regulation occurred under both normoxic and hypoxic conditions. Up-regulation of *epo* expression was observed in

both the normoxic-high salinity and hypoxic-high salinity exposures, while no clear pattern was noted under normoxic conditions, a dose-dependent increase of *epo* was observed in the hypoxic exposure. No apparent pattern of *arnt1* expression was observed in the high salinity exposures, except under normoxic conditions, down-regulation occurred in the 6.25%, 50%, and 100% HEWAF treatments while only up-regulation of *arnt1* was observed under hypoxic conditions (Figure 16A and B).

Post-Larval assays

Regulation of *cyp1a1* during post-larval development in the low salinity assays resulted in up-regulation in all treatments for both oxic regimes (Figure 17A and B). The normoxic-low salinity exposure resulted in a dose dependent down-regulation of both *epo* and *arnt1* while up-regulation was only seen in the control and the lowest HEWAF treatments for *epo*, and only in the control treatments for *arnt1* (Figure 17A). Hypoxic-low salinity conditions induced a dose-dependent increase of *epo* expression which was opposite of the expression patterns observed under normoxic conditions, while similar down-regulation patterns were obtained for expression of *arnt1* under both oxic regimes (Figure 17B).

A dose dependent increase in *cyp1a1* relative gene expression was observed under normoxic-high salinity conditions (Figure 18A). Conversely under hypoxic-high salinity conditions increased *cyp1a1* expression was only recorded in the lowest (6.25% and 12.5%) HEWAF treatments and a significant down-regulation of *cyp1a1* was observed in the highest (50 and 100%) HEWAF treatments (Figure 18B). The down regulation of *cyp1a1* is not only unique to the hypoxic-high salinity exposure, but also only occurred in the post-larval developmental stage. The expression of *epo* under both oxic regimes

resulted in a dose-dependent pattern. In normoxic conditions, up-regulation of *epo* was recorded in all treatments, while under hypoxic conditions up-regulation was only observed in the lowest HEWAF treatments and down-regulation of gene expression was observed in the two high HEWAF treatments (Figure 18A). Minor down-regulation of *arnt1* expression was recorded in the 3 highest HEWAF treatments under normoxic-high salinity conditions. Under hypoxic-high salinity conditions *arnt1* expression was slightly upregulated in the 6.25 and 12.5% treatments, while 4-fold decrease was observed in the 50 and 100% treatments (Figure 18B).

Across treatment analysis

The embryonic exposures resulted in the greatest observed expression of *cyp1a1* under both salinity regimes (Figure 10 and 11). Expression of *epo* in the post-larval, high salinity exposure results in the highest upregulation of *epo* across all developmental stages (Figure 15). No clear expression patterns of *arnt1* were observed within or across developmental stages. A general trend of decreased regulation was observed in the post-hatch and post-larval exposures in the HEWAF treatments relative to the controls with the strongest decreased expression occurred under low salinity conditions (Figure 12 and 14). A similar dose-dependent response of *cyp1a1* was observed in the both salinity conditions for the post-hatch exposures and the low salinity post-larval exposure. A complete down-regulation of *cyp1a1* expression was observed only in the post-larval developmental stage, only under hypoxic and high salinity environmental conditions in the two highest HEWAF treatments (Figure 15). No clear pattern of *epo* expression was observed in all the embryonic and post-hatch exposures. The expression of *epo* from the high salinity, post larval exposure resulted in a similar pattern to the *cyp1a1* expression,

complete down-regulation of *epo* mRNA was observed in the two highest HEWAF treatments (Figure 15).

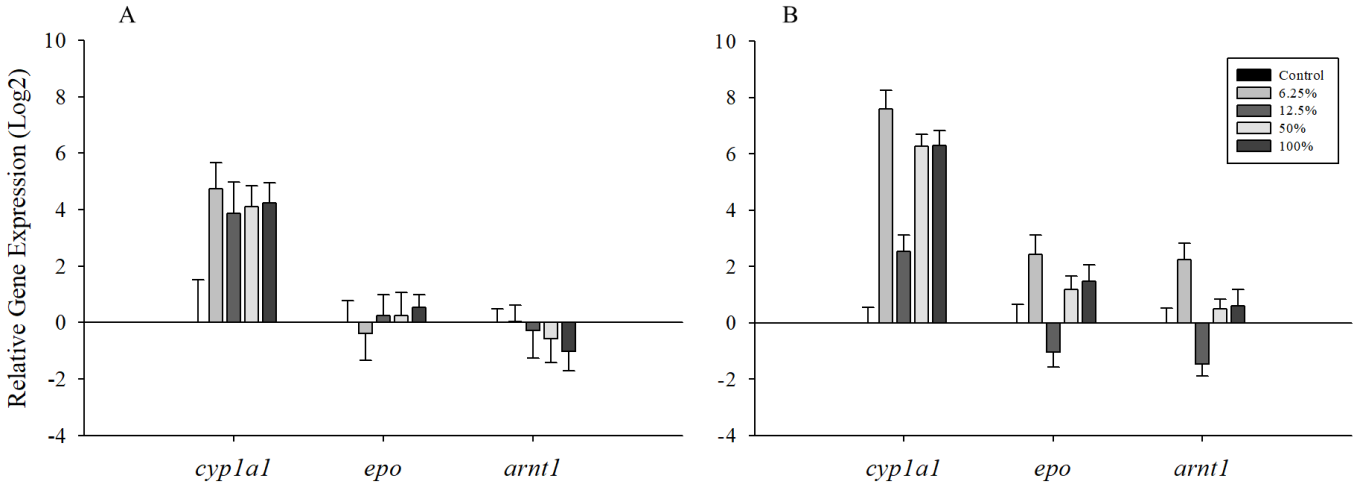

Figure 13. *Cyprinodon variegatus* embryonic relative gene expression of *cyp1a1*, *epo*, and *arnt1* in response to HEWAF exposure under low salinity (10 ppt) conditions in combination with different oxic regimes.

Target gene response under normoxic conditions (≥ 5.0 mg/L) (A) and target gene expression under hypoxic conditions (2.0 mg/L) (B). Gene expression data was normalized to 18s rRNA.

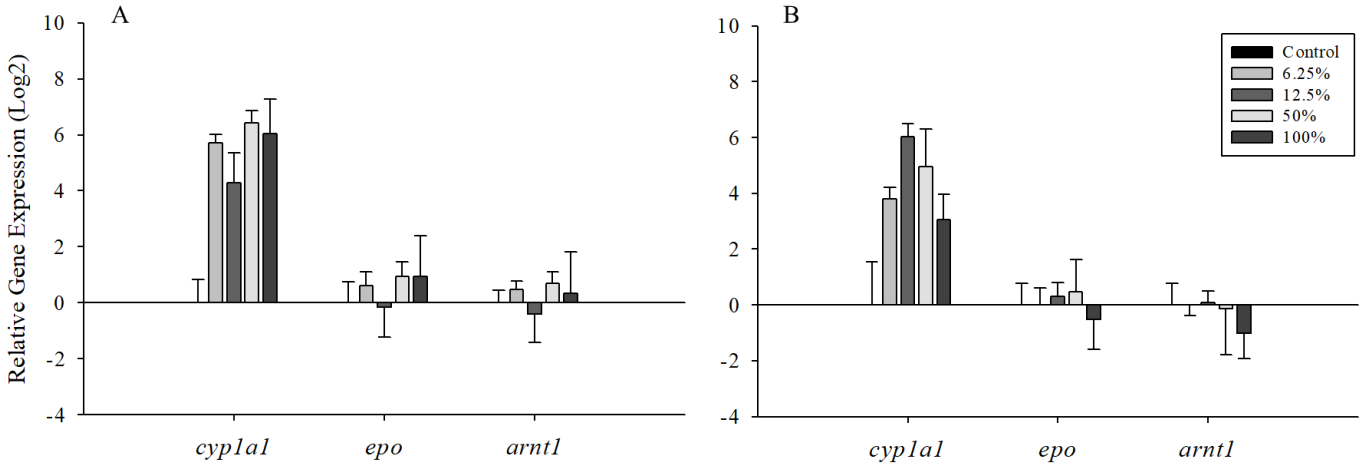

Figure 14. *Cyprinodon variegatus* embryonic relative gene expression of *cyp1a1*, *epo*, and *arnt1* in response to HEWAF exposure under high salinity (30 ppt) conditions in combination with different oxic regimes.

Target gene response under normoxic conditions (≥ 5.0 mg/L) (A) and target gene expression under hypoxic conditions (2.0 mg/L) (B). Gene expression data was normalized to 18s rRNA.

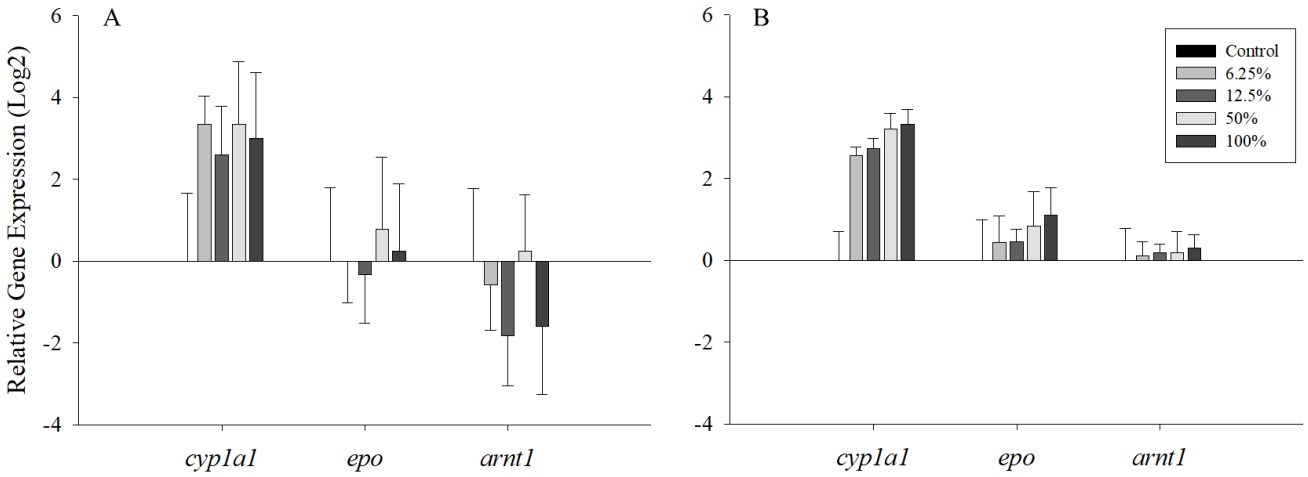

Figure 15. *Cyprinodon variegatus* post-hatch relative gene expression of *cyp1a1*, *epo*, and *arnt1* in response to HEWAF exposure under low salinity (10 ppt) conditions in combination with different oxic regimes.

Target gene response under normoxic conditions (≥ 5.0 mg/L) (A) and target gene expression under hypoxic conditions (2.0 mg/L) (B). Gene expression data was normalized to 18s rRNA.

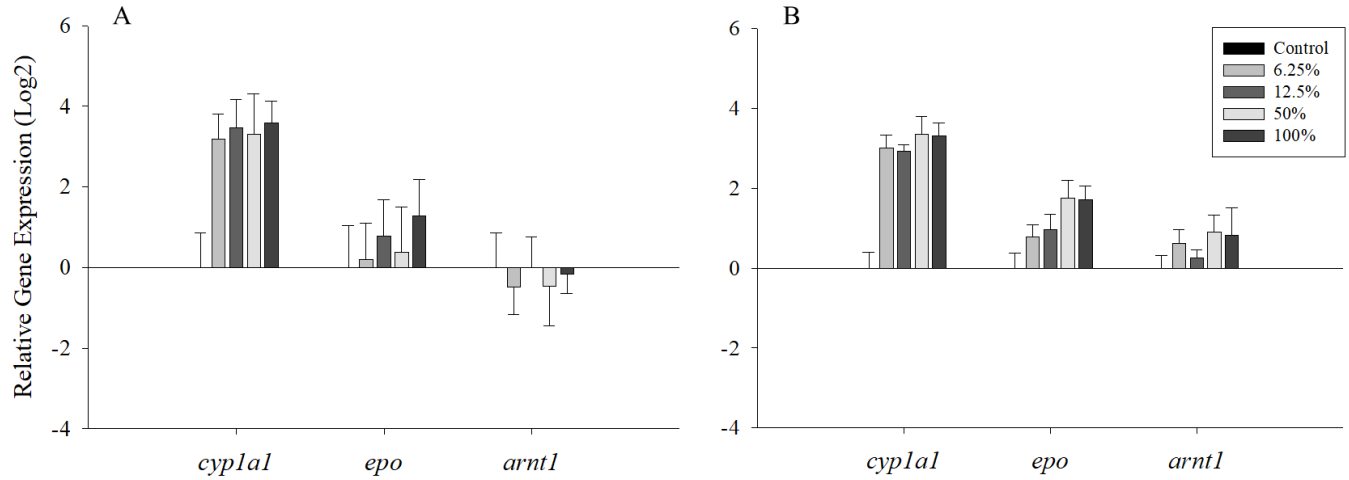

Figure 16. *Cyprinodon variegatus* post-hatch relative gene expression of *cyp1a1*, *epo*, and *arnt1* in response to HEWAF exposure under high salinity (30 ppt) conditions in combination with different oxic regimes.

Target gene response under normoxic conditions (≥ 5.0 mg/L) (A) and target gene expression under hypoxic conditions (2.0 mg/L) (B). Gene expression data was normalized to 18s rRNA.

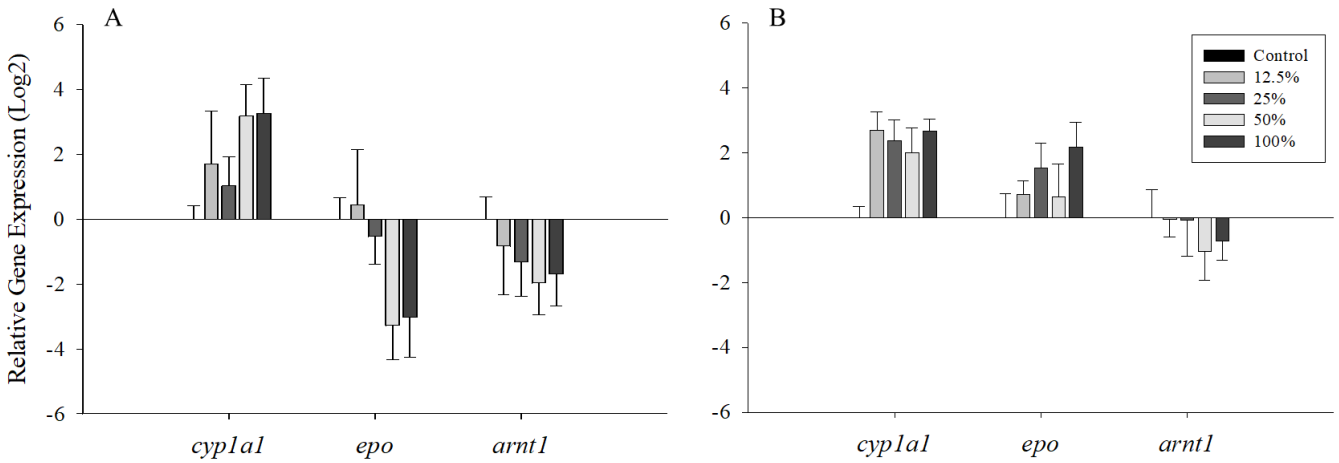

Figure 17. *Cyprinodon variegatus* post-larval relative gene expression of *cyp1a1*, *epo*, and *arnt1* in response to HEWAF exposure under low salinity (10 ppt) conditions in combination with different oxic regimes.

Target gene response under normoxic conditions (≥ 5.0 mg/L) (A) and target gene expression under hypoxic conditions (2.0 mg/L) (B). Gene expression data was normalized to 18s rRNA.

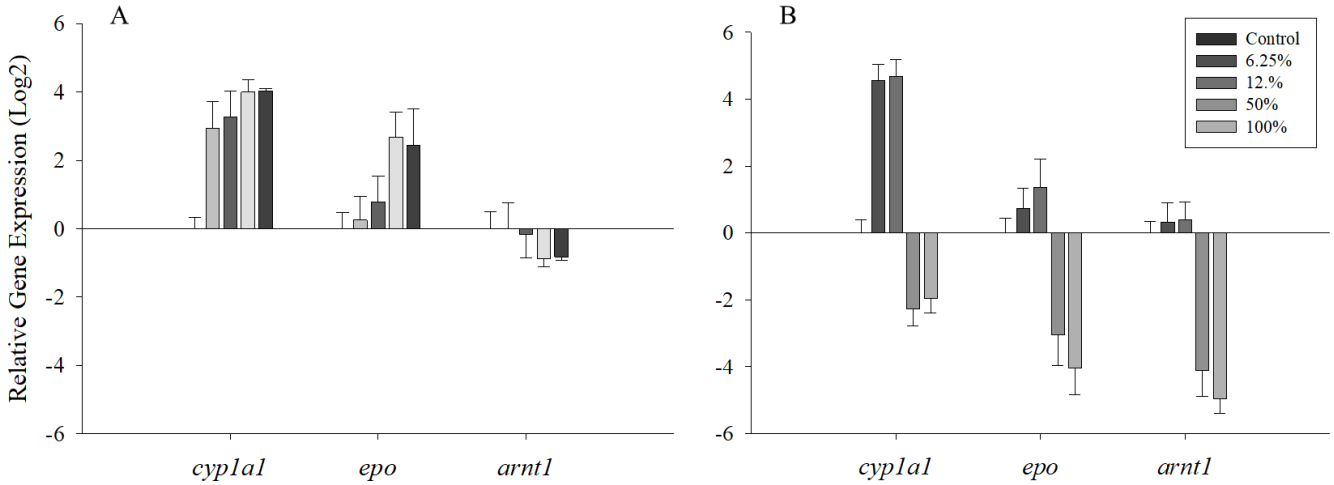

Figure 18. *Cyprinodon variegatus* post-larval relative gene expression of *cyp1a1*, *epo*, and *arnt1* in response to HEWAF exposure under high salinity (30 ppt) conditions in combination with different oxic regimes.

Target gene response under normoxic conditions (≥ 5.0 mg/L) (A) and target gene expression under hypoxic conditions (2.0 mg/L) (B). Gene expression data was normalized to 18s rRNA.

Discussion

No combination of exposure conditions resulted in the cross-talk due to competitive inhibition between the AhR and HIF-1α signaling pathways in early life development of sheepshead minnow based on the observed relative gene expression of *cyp1a1* and *epo*. These finding contrast the previous research that suggest that the cross-talk is due to receptor affinity to the Arnt protein and competitive inhibition (Gassmann et al., 1997; Gradin et al., 1996; Prasch et al., 2004; Vorrink and Domann, 2014). Dasgupta et al. (2016) reported that hypoxic stress paired with oil exposure inhibited *cyp1a1* expression and increased observed DNA damage. The study used ethoxy resorufin O-deethylase assay (EROD) to measure the *in vivo cyp1a1* activity in larval sheepshead minnows. The decreased *cyp1a1* activity was suggested to be a result of competitive binding at the AhR to Arnt (Dasgupta et al., 2016).

The down-regulation of both *cyp1a1* and *epo* expression was only observed in the experimental regime which included oil, hypoxia, and high salinity exposure conditions. The observed decreased mRNA expression of both genes indicates synergistic effects occurring between variable environmental conditions and PAH exposure. This synergism resulted in suppression of both the AhR and HIF-1α signaling pathways. Similar observation of decreased expression of AhR and HIF-1α target genes have been documented in mammals and fish in the presence of PAH and hypoxia (Chan et al., 1999; Fleming et al., 2009; Schults et al., 2010). Fleming et al. (2009) investigated benzo[a]pyrene (BaP) combined with hypoxic stress in *Fundulus heteroclitus* fish cells: cells exposed to both stressors resulted in a decrease in HIF-1α receptors and a decrease in AhR pathway activity (Fleming et al., 2009). Mutual repression of the AhR and HIF-

1a pathways was observed in human liver cells exposed to the AhR antagonist TCDD with chemically induced hypoxia (Nie et al., 2001). TCDD reduced reporter gene activity while hypoxia reduced *cyp1a1* activity in liver cells: this mutual repression was hypothesized to be related to DNA binding changes (Nie et al., 2001). Vorrink et al (2014) also concluded that the observed attenuated response of AhR to PCB 126 following exposure to hypoxic conditions may also be a result of conformational changes in receptor binding ability to the Arnt protein (Vorrink et al., 2014). The depression of *cyp1a1* and *epo* mRNA expression in the current study provides further evidence to support the occurrence of reciprocal cross-talk between the AhR and HIF-1α signaling pathways in *C. variegatus*.

No pathway inhibition was observed in the embryonic and post-hatch developmental stages under any experimental condition. The *cyp1a1* and *epo* relative gene expression for those developmental stages was up-regulation, indicating that both pathways were active simultaneously. Target gene expression analysis from the post-larval developmental stage resulted in similar up-regulation in the embryonic and post-hatch exposures under normoxic-low salinity conditions, indicating no pathway inhibition. However, under hypoxic-high salinity conditions post-larval specimens revealed *cyp1a1* and *epo* expression down-regulation relative to controls. These data suggest that post-larval SHM are most sensitive to synergistic effects of PAHs and environmental conditions. These conclusions are supported by data from previous studies of embryonic SHM exposure to pyrene and hypoxia (Hendon et al., 2008). The results from Hendon et al. 2008 provided no evidence for cross-talk to occur between the AhR and HIF-1α pathway by inhibition of *vegf* expression during embryonic

development. Brewton et al. (2013) also showed evidence of an age-dependent response to PAH exposure by measuring *cyp1a1* expression in early life stages of spotted seatrout. The study indicated that the greatest decrease in *cyp1a1* activity and total length was observed in the juvenile life stage (Brewton et al., 2013).

Expression patterns of *arnt1* in response to oil exposure under hypoxic-high salinity conditions indicated that *arnt1* is the driving mechanism behind the suppression of *cyp1a1* and *epo* expression during post-larval development in *C. variegatus*. The shared binding partner, *arnt1*, is required for activation of both AhR and HIF-1α pathways (Gassmann et al., 1997; Tomita et al., 2000). Gassmann et al. (2009) and Tomita et al. (2000) used *arnt1* deficient cells in mice to determine the importance of *Arnt1* in xenobiotic and hypoxic stress response. The *arnt1* deficient cells were unable to induce expression of HIF-1α target genes. Likewise, *arnt1* deficient mice were unable to induce expression of AhR target genes (Gassmann et al., 1997; Tomita et al., 2000). The role of *arnt1* in the AhR and HIF-1α pathways has led researchers to hypothesize that cross-talk between the two pathways is limited by *arnt1* expression and receptor affinity (Gradin et al., 1996; Pollenz et al., 1999; Prasch et al., 2004). Under hypoxic-high salinity conditions, the mRNA expression of *arnt1* was down-regulated in the highest HEWAF treatments. Since *arnt1* is a required binding partner for both AhR and HIF-1α receptors, decreased gene expression directly impacts the expression of *cyp1a1* and *epo*. Fleming et al. (2009) concluded that the observed suppression of AhR mediated enzymatic activity in topminnow hepatocarinoma cells in the presence of hypoxia was reversed by the over-expression of *arnt* (Fleming et al., 2009). The results from this research support the finding that *arnt* regulation results in cross-talk between the AhR

and HIF-1α pathways. The data presented here also indicates that the expression of *arnt* is not constitutively expressed as previously thought, but is influenced by external abiotic factors (Pollenz et al., 1999).

CHAPTER IV COMPARATIVE GENOMIC RESPONSE OF CYPRINODON VARIEGATUS TO OIL AND HYPOXIA.

Introduction

The Deepwater Horizon (DWH) oil spill is largest marine oil spill in U.S. history which released approximately 5 million barrels of crude oil over the course of 3 months into the northern Gulf of Mexico (nGoM) during the late spring of 2010 (Beyer et al., 2016). The oil spill occurred after the DWH oil platform exploded about 60 km off the coast of Louisiana (Beyer et al., 2016). The mass release of oil into the nGoM impacted more than 2100 km of estuary and nursery habitat for many important commercial and recreational fisheries during their peak spawning seasons (Pasparakis et al., 2016). The amount of oil released, the duration of the spill, and habitats impacted has potential to cause serious lethal and sublethal effects on exposed species related to reproduction impairment and abnormal development in contaminated waters. The majority of past adult and developmental oil toxicity experiments have investigated mortality rates, developmental toxicity, and molecular oil detoxification pathways. The focus of much ecotoxicological research investigating oil contamination lethality and developmental effects has been focused on phenotypic and morphological responses to oil, but still uncertain are the molecular processes responsible for the effects observed after exposure to oil (Pasparakis et al., 2016; Whitehead et al., 2012).

Global transcriptomics allows researchers to evaluate whole organismal responses to toxicants and environmental stressors. Classical ways to assess the effects of oil on marine organisms relied on morphological evaluations and gene targeting. There are a large number of papers have documented the developmental effects associated with oil

exposure, salinity, and hypoxia, but little is known about the molecular processes responsible for the observed effects (Pasparakis et al., 2016). Molecular studies targeting specific genes involved in key developmental processes and defense pathways have been the primary way to link molecular and phenotypic response to oil and environmental conditions, but is limited in scope (Schirmer et al., 2010; Xu et al., 2017). The use of next generation tools such as RNA sequencing allows researchers to identify chemical expression profiles and molecular modes of action to link them to physiological functions and responses (Schirmer et al., 2010). RNA sequencing technology is mostly used for transcriptome characterization and differential gene expression analysis, but it has also been used to improving genome annotation, discover novel transcripts and single nucleotide polymorphisms, and to investigate post-transcription modification (Ekblom and Galindo, 2010).

Whitehead et al. (2012) investigated differences in genome expression profiles of *F. grandis* in response to oil contamination from the 2010 DWH oil spill. The study concluded that the differences observed in the genome profiles after oil contamination resulted in decreased physiological functions involving osmoregulation, respiration, and excretion, which persisted for 2 months post oiling (Whitehead et al., 2012). Another study used RNA sequencing to investigate molecular pathways negatively impacted by oil exposure in the early life stages of mahi-mahi (Xu et al., 2016). That study revealed that oil toxicity not only resulted in the activation of the cytochrome P450 signaling pathway, but also impacted the E1E2 signaling, steroid biosynthesis, and ribosome biogenesis pathways (Xu et al., 2016). Other studies have used NGS technology to investigate pathways involved in physiological stress response to adverse environmental

conditions. A study by Xia et al. (2013) investigated high salinity and starvation in combination with pathogen infection in *Lates calcarifer*, the Asian seabass. The results indicated that 200 pathways were affected under all treatment conditions, resulting in decreased activity of multiple metabolic, hormone, and growth pathways (Xia et al., 2013). Atlantic salmon were used to investigate transcriptional responses to temperature and low oxygen stress which reported that cholesterol and protein ubiquitination were among the most significantly affected pathways (Olsvik et al., 2013). Data collected using NGS technology is enabling scientists to better understand the molecular processes involved in physiological changes and response to external stimuli and toxicants which is necessary in understanding ecosystem health and resilience.

The first objective of this study was to investigate age-specific differences in *Cyprinodon variegatus* transcriptome response to exposure to oil, hypoxia, and the combination of both during early life stages in *C. variegatus*. The second objective was to compare the transcriptional response of *C. variegatus* larvae (96 hph) to oil and hypoxic stress. Combined, these aims compare different toxicological pathways involved in response to individual and combined conditions, to provide a better understanding of molecular processes involved in oil metabolism and hypoxic defense.

Methods

Animals and DHW oil exposure.

Post-larval *C. variegatus* were hatched from embryos collected from the adult *C. variegatus* brood stock at The University of Southern Mississippi's Gulf Coast Research Laboratory. Embryos were collected using benthic mesh and PVC breeding nets during a 12 h breeding period. Collected embryos were rolled to remove external cilia to prevent

clumping and subjected to a fresh water rinse to prevent spreading of marine pathogens. Processed embryos were transferred to a 4 L aerated holding tank. Hatched larval were removed and transferred to another 4-L aerated holding tank and grown out to 96 hph. GoMRI source oil collected from the head of the Macondo well head was used to prepare a 1 g/L HEWAF following the methods described in chapter II. Two 48 h HEWAF exposures were conducted using 96 hph *C. variegatus* larvae under normoxic conditions (≥ 5.0 mg/L) and hypoxic conditions (2.0 mg/L) exposed to four dilutions of HEWAFs (6.25%, 12.5%, 50%, 100%). Exposures were conducted in 150 mL Pyrex crystalizing dishes with four replicates per treatment conditions (n=20), with 20 larvae per test chamber. Larvae were randomly collected from each test chamber and pooled for the 48 h whole body tissue samples. Larvae samples were immediately placed in 750 mL of RNAlater and stored in an -80°C until RNA isolation.

Water chemistry analysis

The concentration of tPAH29 in all test chambers was calculated using MS/MS/GC from stock solution, and fluorescence readings were taken from the individual test chambers as described in the methods section of Chapter II. The known oil concentrations values were used in a linear regression model described in more detail in the methods section of Chapter II.

RNA-isolation, cDNA library construction, and sequencing.

Total RNA was isolated from 48 h whole body tissue samples using Qiagen's RNeasy Mini Kit following the same protocol described in Chapter II's RNA Isolation methods (Qiagen, Valencia, CA). Total RNA was diluted into 30 µL samples and concentrations per microliter were measured using a Nano Drop 2000 Spectrophotometer

(ThermoScientific, Waltham, MA). Two nanograms of total RNA per sample were sent to Purdue Genomic Core Facility in West Layfette, Indiana for cDNA library prep and sequencing. Triplicate total RNA samples from the control and 12.5% HEWAF treatment from the normoxic-high salinity and hypoxic- high salinity exposures were sent for sequencing. Total RNA samples were overnight express shipped from USM's Gulf Coast Research Laboratory to the Purdue Genomic Core Facility on dry ice. Multiple cDNA libraries were constructed at the PGCF from the total RNA samples using a Library Construction RNA polyA+ Kit. Illumina HiSeq 2500 was used to sequence paired-end 2 X 100 bp sequencing reads (Illumina, San Diego, CA) (Figure 19).

Reference guided assembly and annotation of sheepshead minnow transcriptome using CLC genomics.

Adaptor trimmed and quality clipped raw sequencing reads were used for reference guided transcriptome assembly using CLC Genomic Workbench software (Aarhus, Denmark). Paired-end reads for each sample were imported into CLC Genomics Workbench and failed reads and reads that had low quality scores were removed. The paired-end reads were merged together and quality control reports were generated for the merged read sequences. Merged reads were then mapped to the *Cyprinodon variegatus* reference genome (NCBI accession number GCF_000732505.1) to assemble the transcriptome for the samples. Gene expression calculations were generated from assembled sample transcripts using the gene tracks from the reference genome of *C. variegatus* for all 25,075 mapped genes. A combined quality control report was run on the assembled sample transcripts. A principle component analysis (PCA) plot was generated from the sample transcripts to determine correlations between samples.

Differentially expressed genes were calculated for four different exposure comparisons (Figure 19).

Gene ontology and Ingenuity Pathway Analysis.

Gene ontology analysis was performed on the four differential gene expression comparisons using *Homo sapiens* annotation tracks. *H. sapiens* annotation tracks were used to map the gene ontology of the *C. variegatus* differentially expressed genes (DEGs) to obtain gene symbols for the human gene orthologs, which is required to do further pathway analysis using Ingenuity Pathway Analysis (IPA) (Ingenuity Systems Inc., Redwood City, CA, USA). Human gene orthologs were used to evaluate pathway enrichment for two reasons, the first that the program used for the analysis only recognizes mammalian genes, and second, to get a more robust data analysis because human pathways are studied more than fish pathways and better annotated. The three *C. variegatus* treatment comparison DEG lists with the human ortholog gene symbols were uploaded to IPA and used for Core and Comparison analysis. The three treatment RNA-Seq comparisons that were used for pathway analysis were hypoxic control vs normoxic control, normoxic oil vs normoxic control, hypoxic oil vs hypoxic control, and hypoxic oil vs normoxic control. The three comparisons were used to investigate different modes of action that hypoxia and oil had individually on developing larvae, and to determine how the modes of actions changed with exposed to both toxicants simultaneously. IPA-Core analysis was used to investigate the individual effects associated with the different exposures on the developing *C. variegatus* larvae's canonical pathways and the toxicological functions and associated perturbations of affected pathways. IPA-Comparison analysis was used to compare differences in the *C. variegatus* larvae

molecular responses to hypoxic stress, PAH stress, and the combination of both stressors. IPA – Core analysis settings were ingenuity knowledge based reference set, both direct and indirect relationships were identified, and included significantly DEG with false discovery rate (FDR) < 0.1 (Benjamini-Hochberg correlation). IPA uses two statistics, the Fisher's exact test to represent statistically significant, non-random association with p-values ≤ 0.05, and z-scores to predict activity or inhibition of molecules and pathways based on data in the sample data sets and other peer-reviewed literature in the ingenuity based reference set (Figure 19).

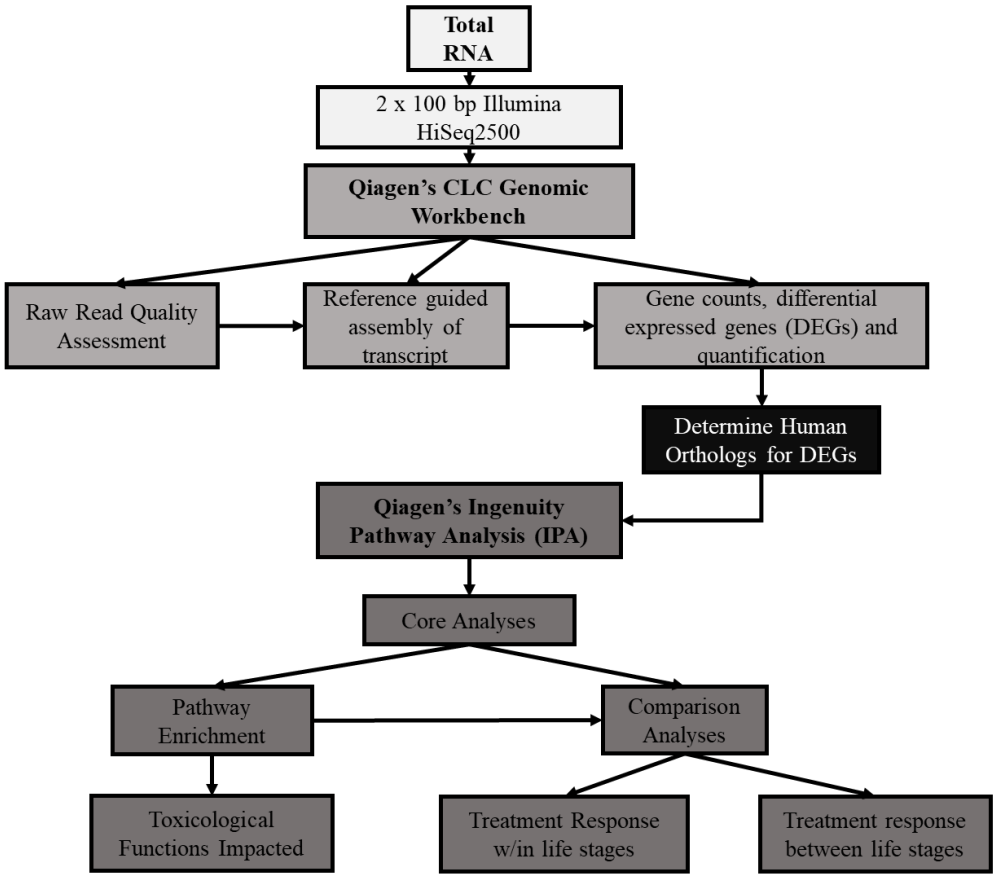

Figure 19. Bioinformatic Pipeline for RNA sequencing, transcriptome assembly, and Pathway analysis for *Cyprinodon variegatus.*

Results

Reference guided assembly of Cyprinodon variegatus transcriptome and annotation.

Three RNA sequencing libraries were constructed, one for each developmental stage. The libraries consisted of 12 samples, with three samples from the control and 12.5% HEWAF treatments under both normoxic and hypoxic conditions. The total Illumina HiSeq2500 reads generated from the embryonic RNA sequencing library for all 12 samples was 482,529,914, with an average read count of 40,210,826. The total number of Illumina HiSeq2500 reads generated from the post-hatch RNA sequencing library for all 12 samples was 807,350,208 with an average read count of 67,279,184 (Table 10). The total number of Illumina HiSeq2500 reads generated from the post-larval RNA sequencing library for all 12 samples was 491,533,802 with an average read count of 40,961,150 (Table 10). Since the post-larval developmental stage was the only stage used for pathway analysis, only the quality reports of this life stage are reported below. The reads from all three RNAseq libraries were mapped to the *C. variegatus* reference genome with high mapping success. The mean mapping success for the normoxic post-larval sample reads to the reference genome was 81.43% and the hypoxic samples has a mean mapping success of 82.35% using CLC genomics read mapping tools. More than 90% of the reads mapped to the reference genome mapped to genes in both the normoxic and hypoxic samples (Table 11).

Table 10 *Embryonic and post-hatch sequence reads and reference guided transcript mapping.*

Embryonic			
Sample Name	**Total Reads**	**% Mapped Pairs**	**% Fragments Mapped to Genes**
Normoxic Control 1	34,026,390	82.66	90.16
Normoxic Control 2	30,652,850	90.19	89.03
Normoxic Control 3	36,095,988	77.62	85.79
Normoxic Oil 1	33,318,320	83.08	86.97
Normoxic Oil 2	44,685,748	82.78	88.05
Normoxic Oil 3	46,299,680	84.67	88.21
Total	225,078,976		
Mean	37,513,163	83.50	88.04
Sample Name	**Total Reads**	**% Mapped Pairs**	**% Fragments Mapped to Genes**
Hypoxic Control 1	42,518,736	81.72	89.72
Hypoxic Control 2	39,966,096	83.32	87.97
Hypoxic Control 3	40,339,930	78.02	84.00
Hypoxic Oil 1	59,496,366	84.21	91.99
Hypoxic Oil 2	35,672,640	80.16	87.44
Hypoxic Oil 3	39,457,170	82.22	87.19
Total	257,450,938		
Mean	42,908,490	81.61	88.05
Post-Hatch			
Sample Name	**Total Reads**	**% Mapped Pairs**	**% Fragments Mapped to Genes**
Normoxic Control 1	63,871,334	82.77	93.74
Normoxic Control 2	71,692,724	83.79	94.31
Normoxic Control 3	63,798,454	86.37	94.12
Normoxic Oil 1	72,254,180	81.70	94.13
Normoxic Oil 2	71,688,870	81.41	94.57
Normoxic Oil 3	55,227,366	83.97	93.76
Total	398,532,928		
Mean	66,422,155	83.34	94.11
Sample Name	**Total Reads**	**% Mapped Pairs**	**% Fragments Mapped to Genes**
Hypoxic Control 1	72,226,508	83.36	94.82
Hypoxic Control 2	56,989,450	83.41	94.71
Hypoxic Control 3	73,134,368	84.21	94.39
Hypoxic Oil 1	62,219,982	84.30	93.80
Hypoxic Oil 2	69,410,912	83.53	93.99
Hypoxic Oil 3	74,836,060	85.61	93.90
Total	408,817,280		
Mean	68,136,213	84.07	94.27

Samples are separated by oxic regime, normoxic (top) and hypoxic (bottom). All samples were mapped to using Qiagen's CLC genomics workbench software following the refence genome guided approach. The reference genome was Cyprinodon variegatus.

Table 11 *Post-larval sequence reads and refence guided transcript mapping analysis. Samples are separated by oxic regime, normoxic (top) and hypoxic (bottom).*

Post-Larval			
Sample Name	**Total Reads**	**% Mapped Pairs**	**% Fragments Mapped to Genes**
Normoxic Control 1	41,945,866	79.80	92.21
Normoxic Control 2	40,826,118	80.37	92.98
Normoxic Control 3	47,660,068	80.14	93.01
Normoxic Oil 1	41,305,022	79.58	92.71
Normoxic Oil 2	37,879,912	84.05	92.82
Normoxic Oil 3	42,847,694	84.62	92.44
Total	252,464,680		
Mean	42,077,447	81.43	92.70
Sample Name	**Total Reads**	**% Mapped Pairs**	**% Fragments Mapped to Genes**
Hypoxic Control 1	38,937,810	82.17	91.85
Hypoxic Control 2	42,588,922	84.55	92.57
Hypoxic Control 3	42,458,806	80.95	92.71
Hypoxic Oil 1	40,123,578	81.33	91.99
Hypoxic Oil 2	39,927,128	83.19	92.47
Hypoxic Oil 3	35,032,878	81.90	92.45
Total	239,069,122		
Mean	39,844,854	82.35	92.34

Total reads refers to the total number of nucleotide sequences obtained from Illumina HiSeq. % mapped pairs refers to the percentage of paired end reads that were aligned to the reference genome and the % fragments mapped to genes indicates the percentage of reads mapped to genomic coding portions of the transcript. All samples were mapped to using Qiagen's CLC genomics workbench software following the refence genome guided approach. The reference genome was Cyprinodon variegatus.

Principle component analysis (PCA) was used to exam interrelations between oil, hypoxia, and life stage. Gene expression tracks from all three RNAseq libraries were used for the PCA (Figure 20). The first PCA plot included the gene expression tracks from all three life stages. This multivariance analysis revealed that age was the strongest component driving the genomic response to oil and hypoxic exposure, which is evident from the discrete clustering of gene tracks into three clusters, embryonic, post-hatch, and post larval (Figure 20). Oxygen regime also influenced gene track clustering across all developmental stages (Figure 21, 22, and 23). The embryonic gene track clustering

distinctly clustered into normoxic and hypoxic clusters, but showed no prevalent clustering patterns in response to oil exposure (Figure 21). The results indicated that the embryos are more sensitive to environmental conditions than PAHs, which may be a result of protection from the chorion. The post-hatch principle analysis reported the clearest cohort clustering patterns by oil and oxic treatment for all three life stages analyzed (Figure 22). The post-larval results from the PCA showed similar clustering patterns as observed in the post-hatch samples, but oxic regime had less of an effect on cluster organization than oil treatment (Figure 23). The post-larval normoxic gene track samples were all very similar and distinct from the other sample tracks while all three hypoxic samples were loosely bunched together.

Figure 20. Principal Component Analysis (PCA) of gene expression tracks across all life stages.

Gene expression tracks from all life stages were used to compare clustering patterns across all three life stages. Clustering patterns clearly indicate that age of exposed fish is the top driver of SHM response to oil and hypoxic exposures. The legend located in the bottom left corner of the figure. Figure generated using Qiagen' CLC Genomics Workbench software.

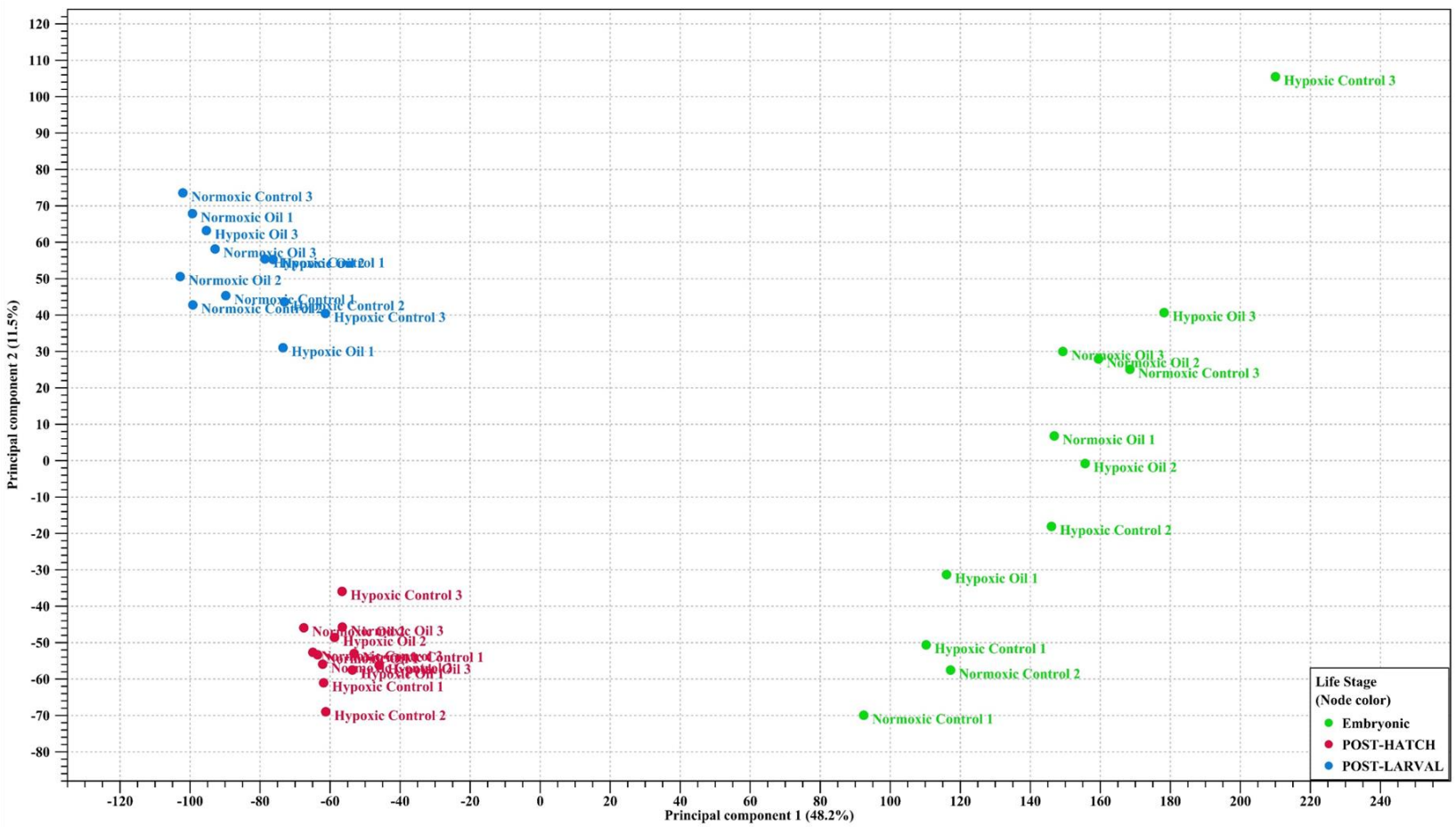

Figure 21. Embryonic Principal Component Analysis (PCA) using gene expression tracks.

The embryonic samples gene expression tracks significantly cluster together based on oil treatment and oxic regime. The legend located in the bottom left corner of the figure.

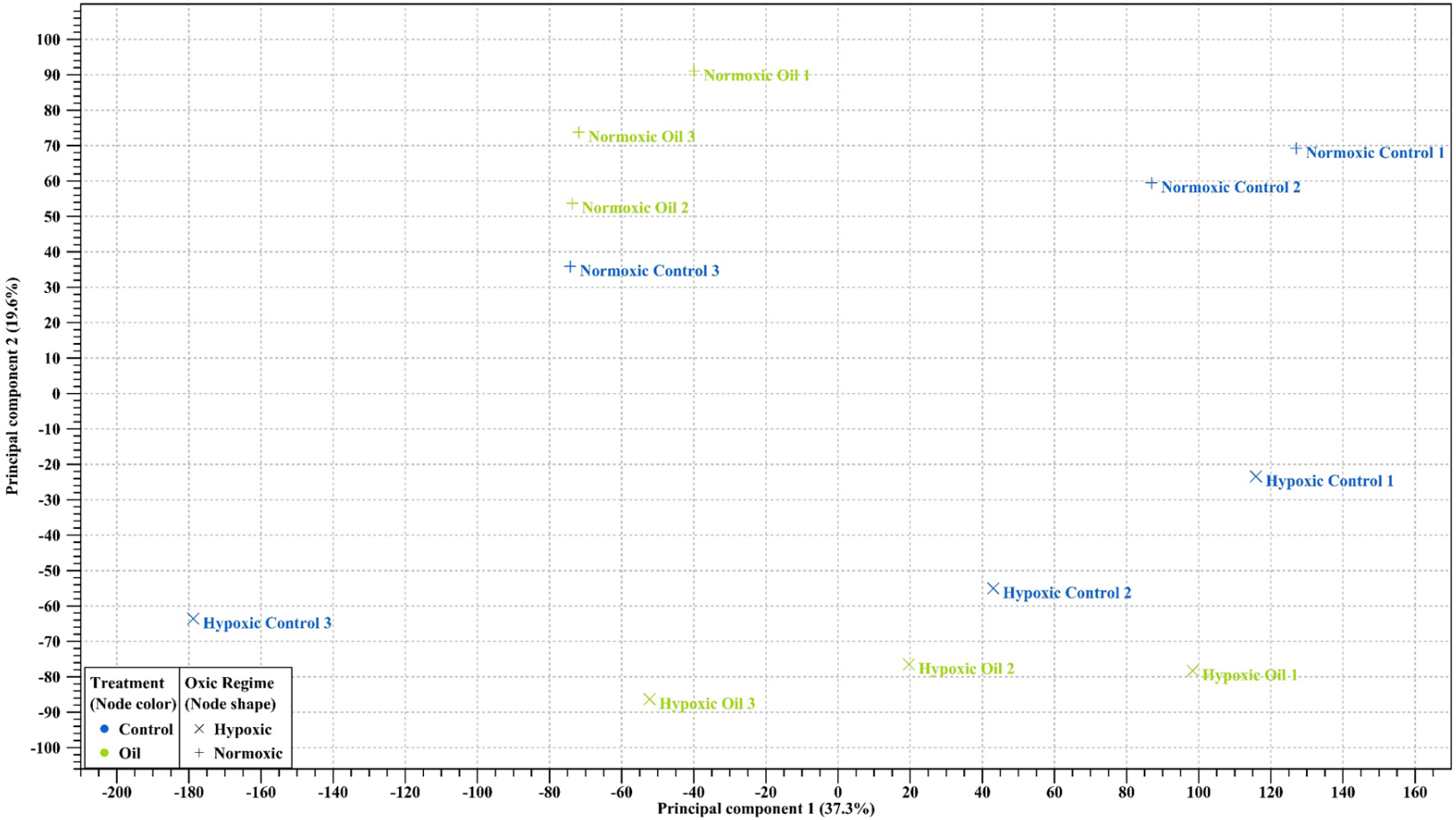

Figure 22. Post-hatch Principal Component Analysis (PCA) using gene expression tracks.

The post-hatch samples gene expression tracks significantly cluster together based on oil treatment and oxic regime. The legend located in the bottom left corner of the figure.

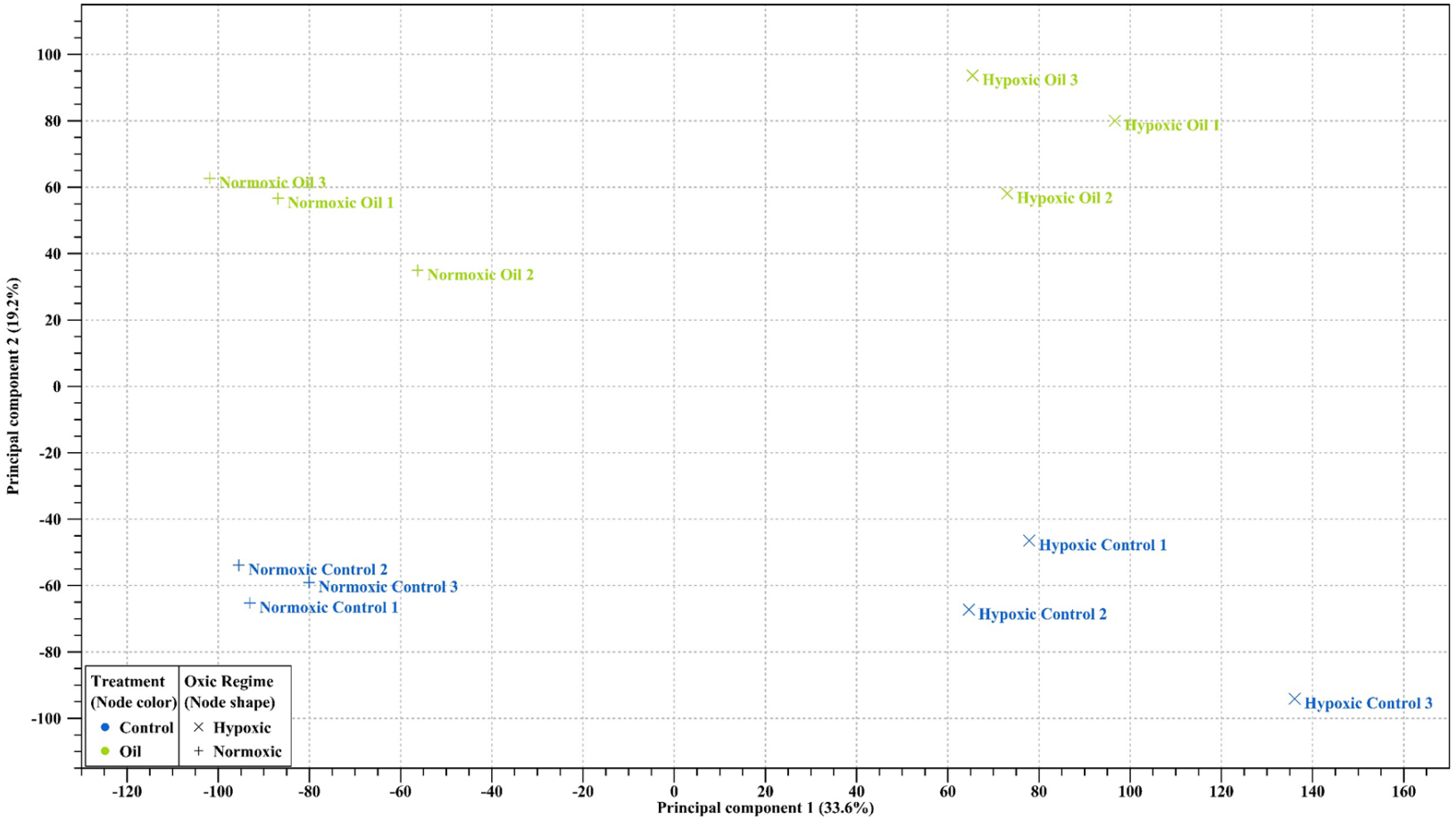

Figure 23. Post-larval Principal Component Analysis (PCA) using gene expression tracks.

The post-larval samples gene expression tracks significantly cluster together based on oil treatment and oxic regime. The legend located in the bottom left corner of the figure.

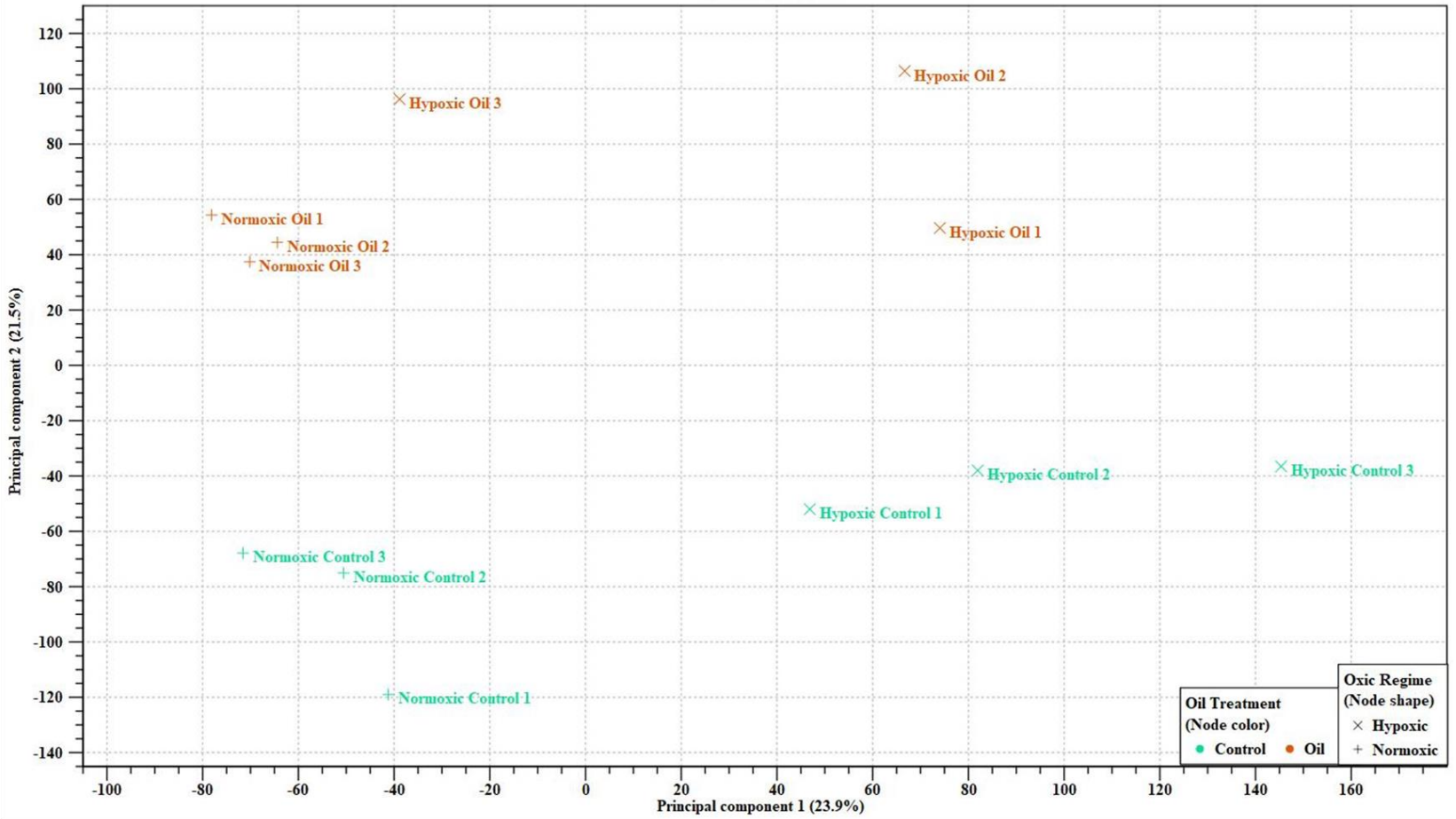

Differentially expressed genes analysis

Total counts were the expression values used to generate the differential expressed gene (DEG) list from the *C. variegatus* transcriptome. Differential gene expression and pathways analysis were performed on the sample transcriptomes generated from the assembled mapped reads that passed quality control cut-offs. Heatmaps were generated using CLC genomic RNA Seq tool to visualize DEGs between the oiled and control samples for all twelve sample transcripts with an absolute fold change > 1.5 and a FDR < 0.05. Sample clustering patterns were similar to the PCA patterns.

A heat map including all developmental stage DEGs resulted in clear clustering patterns by age (Figure 24). These data are consistent with patterns in the PCA analysis, the cluster patterns suggest different responses to oil and hypoxic expose are dependent on life stage. Individual heat maps were used to analyses significant DEG patterns in each life stage which had a minimum absolute fold change of 1.5 and a FDR $\leq$ 0.05. Differentially expressed genes in the embryonic RNAseq samples resulted in two distinct groups, normoxic and hypoxic samples and then two sub clusters, oil and control treatments (Figure 25). The heart map also indicated that normoxic samples had a greater gene expression induction than the hypoxic group, indicated by the number of red genes (genes with greater than 1.5 absolute fold change). The post-hatch and post-larval heatmaps also have the same clustering patterns as the embryonic samples, separated by oxic regime and then by oil treatment (Figure 26 and 27). The post-hatch RNAseq samples show a slightly higher induction of gene expression in response to hypoxic stress when compared to the normoxic samples (Figure 26). The post-larval samples appear to

have a similar response to both oxic regimes based on levels of gene expression induction (Figure 27).

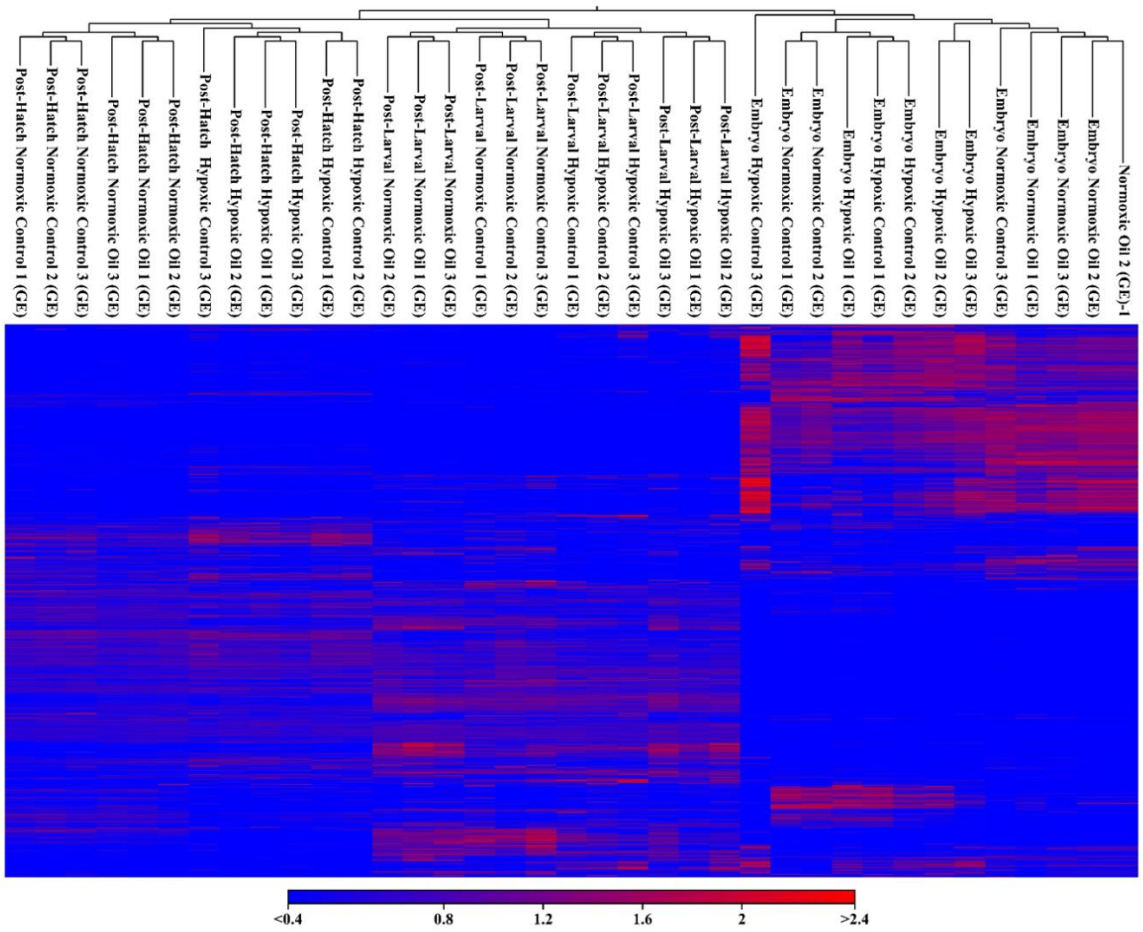

Figure 24. *Cyprinodon variegatus* gene expression heat map during embryonic, post-hatch, and post-larval exposures.

The total gene counts were generated from the embryonic, post-hatch, and post-larval gene expression tracks of the sample reads. Unique clustering of gene expression for each early life stage indicates an age specific molecular response to oil and hypoxic stress in C. variegatus. The columns represent individual sample expressions and the rows represent individual gene expression.

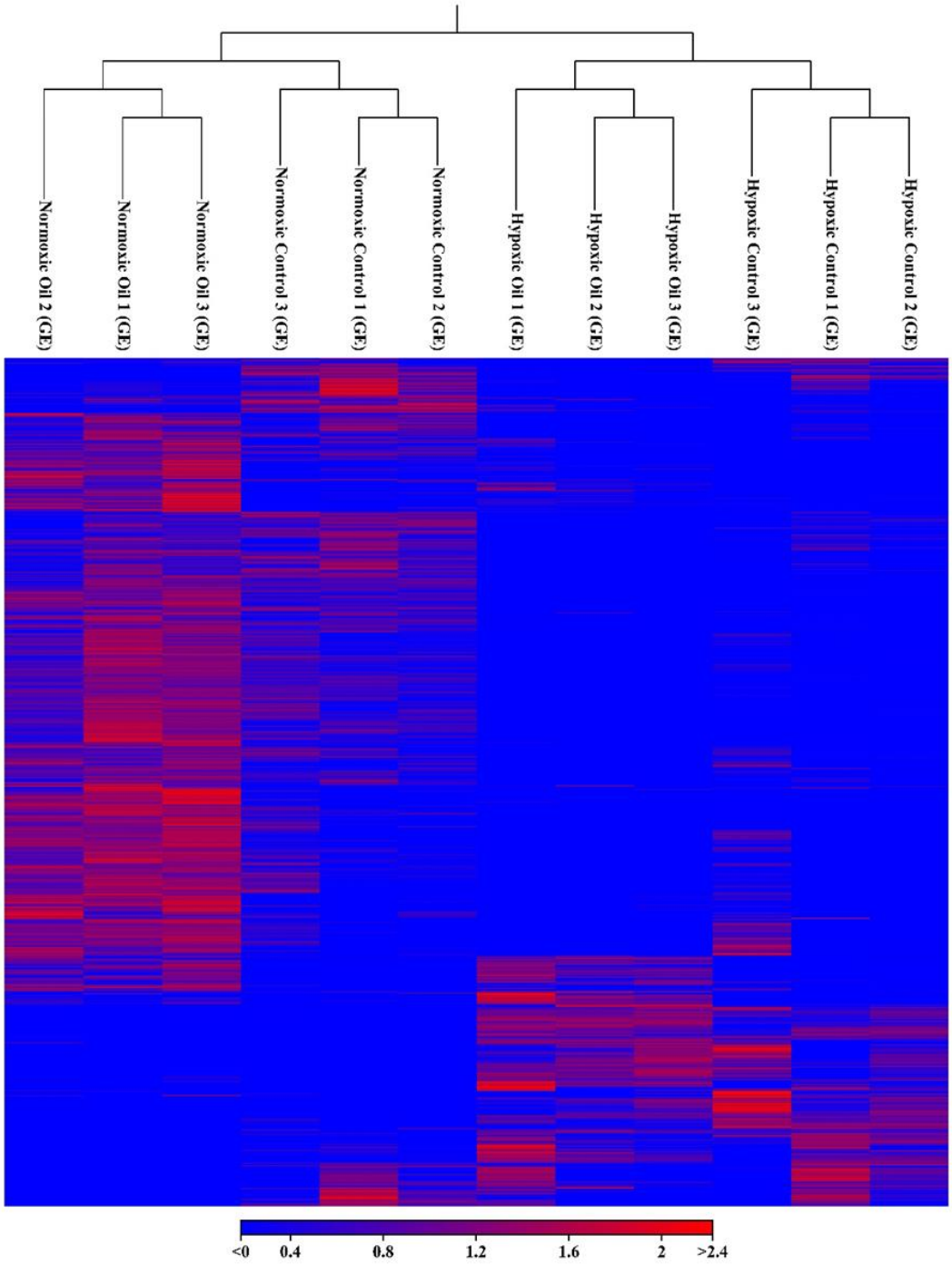

Figure 25. *Cyprinodon variegatus* significantly differentially expressed genes heat map for embryonic exposures.

The total gene counts were generated from the embryonic gene expression tracks of the sample reads. Clustering patterns reveal different molecular response used under different oxic regimes in *C. variegatus* embryos. The columns represent individual sample expressions and the rows represent individual gene expression Heatmap generated using the Euclidean distance with complete linkage clusters. Statistical comparison of all oil and oxic treatments with a minimum absolute fold change of 1.5 and FDR $\leq$ 0.05.

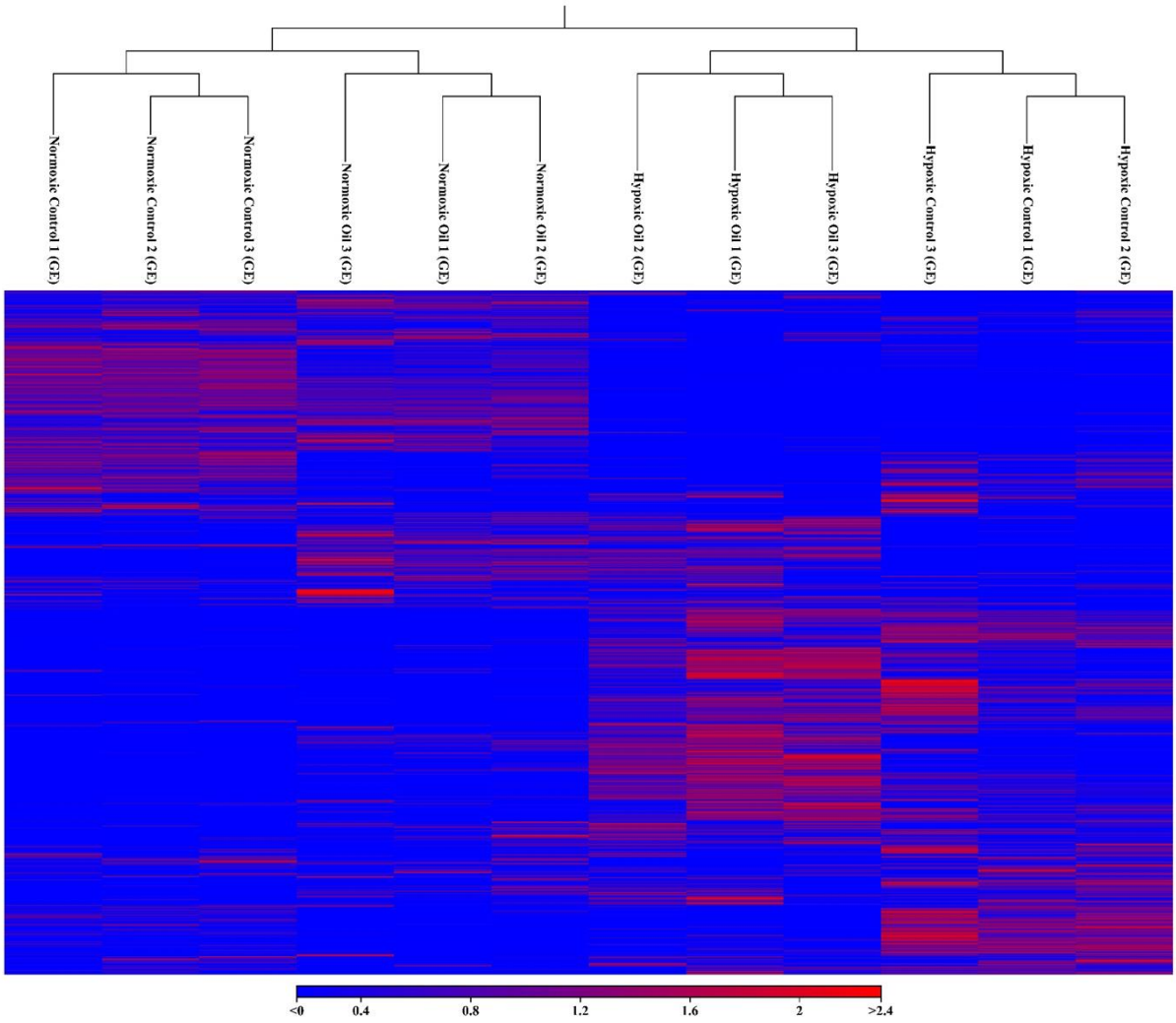

Figure 26. *Cyprinodon variegatus* significantly differentially expressed genes heat map for post-hatch exposures.

The total gene counts were generated from the embryonic gene expression tracks of the sample reads. Clustering patterns reveal different molecular response used under different oxic regimes in *C. variegatus.* The columns represent individual sample expressions and the rows represent individual gene expression Heatmap generated using the Euclidean distance with complete linkage clusters. Statistical comparison of all oil and oxic treatments with a minimum absolute fold change of 1.5 and FDR ≤ 0.05.

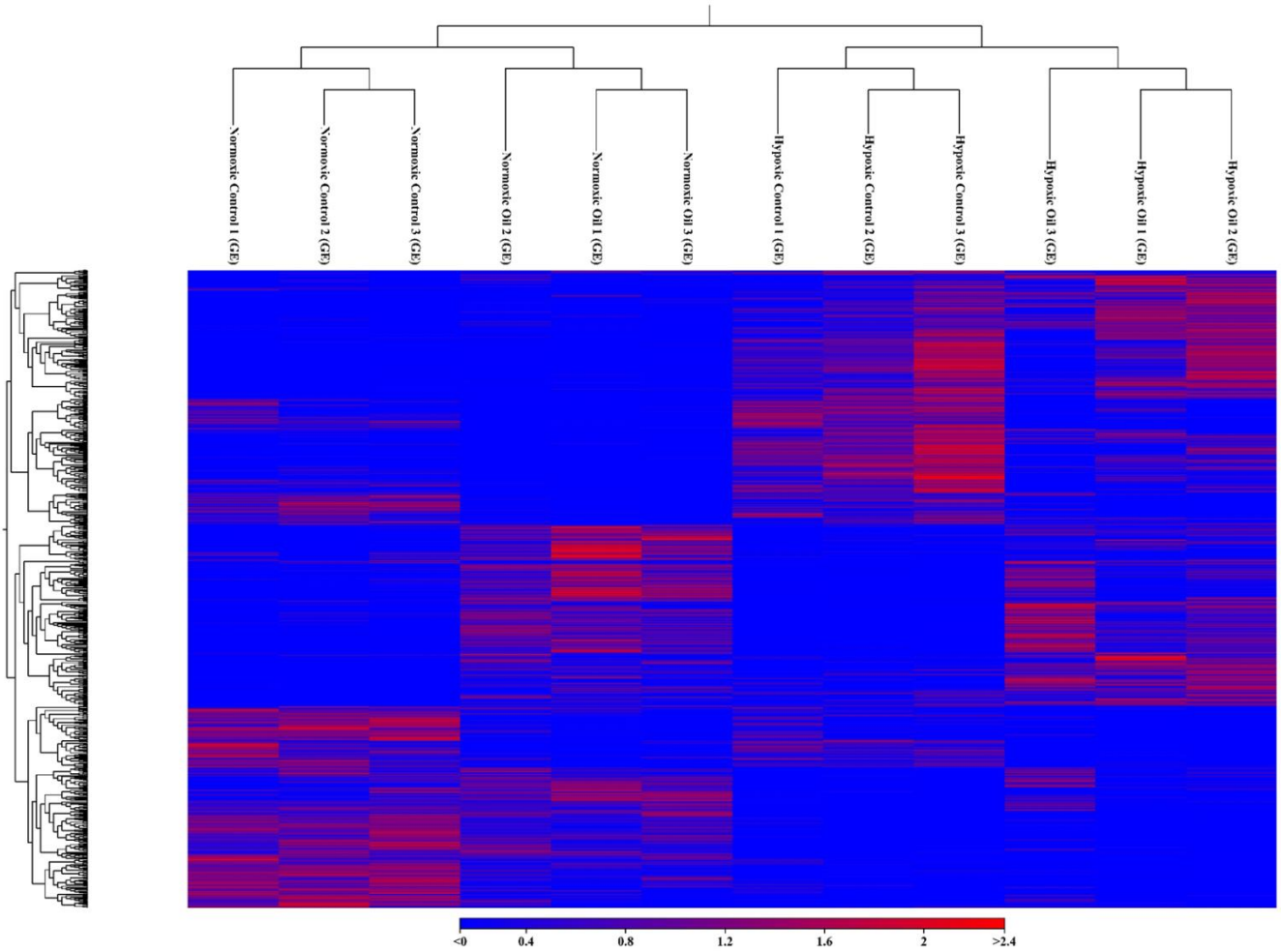

Figure 27. *Cyprinodon variegatus* significantly differentially expressed genes heat map for post-larval exposures.

The total gene counts were generated from the embryonic gene expression tracks of the sample reads. Clustering patterns reveal different molecular response used under different oxic regimes in C. variegatus. The columns represent individual sample expressions and the rows represent individual gene expression Heatmap generated using the Euclidean distance with complete linkage clusters. Statistical comparison of all oil and oxic treatments with a minimum absolute fold change of 1.5 and FDR ≤ 0.05.

Three comparisons were used to investigate the differential gene expression of the three early life stages of *C. variegatus* in response to HEWAF exposure under varying oxic regimes 1) hypoxic control vs normoxic control, 2) normoxic oil vs normoxic control, and 3) hypoxic oil vs normoxic control, with an absolute fold change > 1.5 and a false discovery rate (FDR) < 0.1. The embryonic transcriptomic response to combined HEWAF and hypoxic exposure had the lowest measurable response in gene expression with a total of 1,074 significantly differentially expressed genes, which comprised of 171 DEGs after exposure to oil alone, 105 DEGs after exposure to hypoxia alone, and 798 DEGs after combined exposure to oil and hypoxia (Figure 28B and Figure 31). The post-hatch transcriptomic response to combined HEWAF and hypoxic exposure had the greatest measurable response in gene expression with a total of 8,250 significantly differentially expressed genes, which comprised of 1039 DEGs after exposure to oil alone, 3154 DEGs after exposure to hypoxia alone, and 4057 DEGs after combined exposure to oil and hypoxia (Figure 29B and Figure 31). The post-larval transcriptomic response to combined HEWAF and hypoxic exposure had a total of 7,091 significantly differentially expressed genes, which comprised of 1516 DEGs after exposure to oil alone, 2154 DEGs after exposure to hypoxia alone, and 3421 DEGs after combined exposure to oil and hypoxia (Figure 30B and Figure 31).

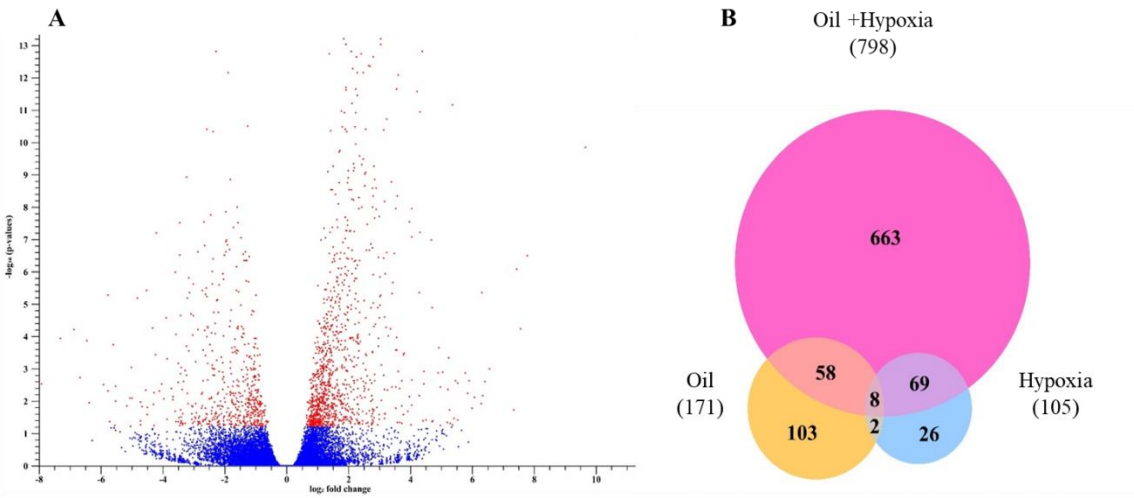

Figure 28. Embryonic Volcano plot and Venn diagram of significant DEGs.

The volcano plot (A) indicates all the genes analyzed in the embryonic RNAseq samples. The x-axis is the gene fold change (log2) and the p-values (log10) are on the y-axis. The red dotes indicate the significant differentially expressed genes with an absolute fold change of ≥1.5 and p-value ≤ 0.05. Venn diagram displays DEG in response to exposure treatments (B). All treatments normalized to the normoxic control treatments with a FDR ≤ 0.05 to identify differential transcriptome profiles.

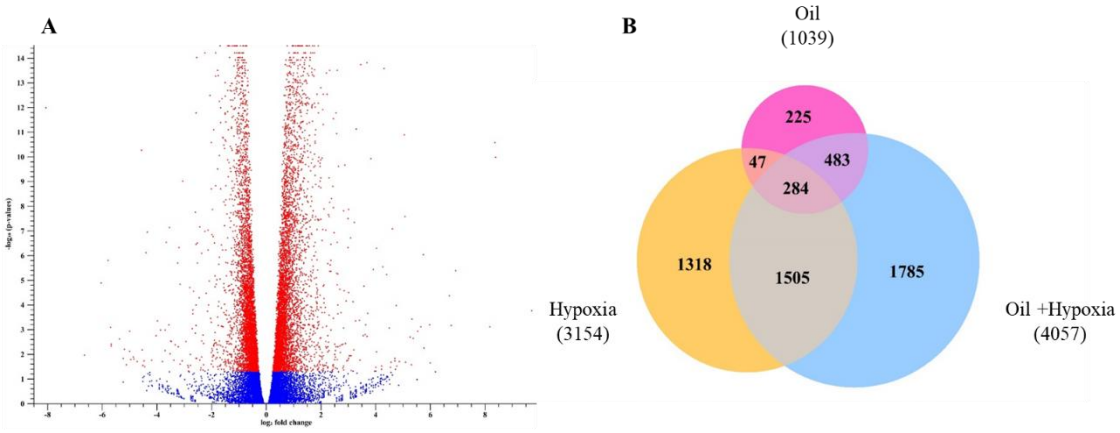

Figure 29. Post-hatch Volcano plot and Venn diagram of significant DEGs.

The volcano plot (A) indicates all the genes analyzed in the post-hatch RNAseq samples. The x-axis is the gene fold change (log2) and the p-values (log10) are on the y-axis. The red dotes indicate the significant differentially expressed genes with an absolute fold change of ≥1.5 and p-value ≤ 0.05. Venn diagram displays DEG in response to exposure treatments (B). All treatments normalized to the normoxic control treatments with a FDR ≤ 0.05 to identify differential transcriptome profiles.

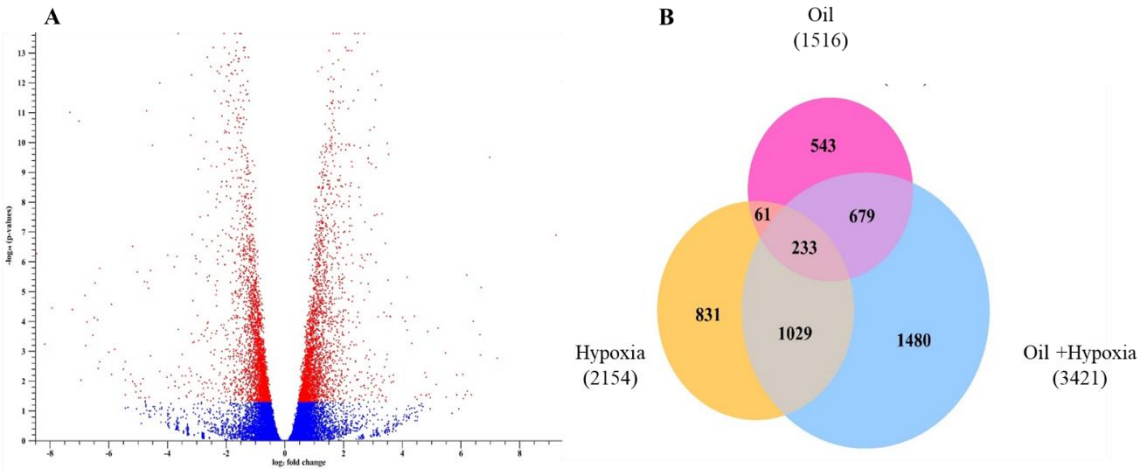

Figure 30. Post-larval Volcano plot and Venn diagram of significant DEGs

The volcano plot (A) indicates all the genes analyzed in the post-larval RNAseq samples. The x-axis is the gene fold change (log2) and the p-values (log10) are on the y-axis. The red dotes indicate the significant differentially expressed genes with an absolute fold change of ≥1.5 and p-value ≤ 0.05. Venn diagram displays DEG in response to exposure treatments (B). All treatments normalized to the normoxic control treatments with a FDR ≤ 0.05 to identify differential transcriptome profiles.

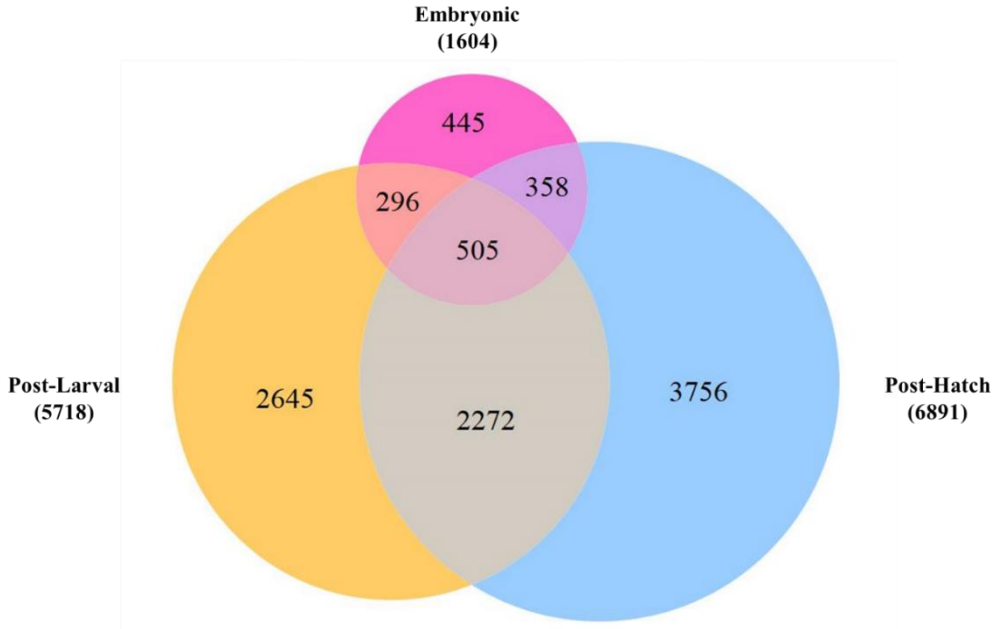

Figure 31. Venn diagram displaying all the differentially expressed genes in response to oil and oxic treatments for all three early life stages of *Cyprinodon variegatus*.

The pink circle represents the embryonic DEG (total of 1604), the Blue represents the post-hatch number of DEG (6891), and the yellow represents the post-larval DEG (5718). The size of the circles are proportionate to the number of total DEG and genes included in this graph have a FRD ≤ 0.05.

Pathway Analysis

Pathway analysis was only performed on the post-larval samples because of the increased mortality and down-regulation of target genes observed in Chapters II and III. Individual and Comparative RNAseq analysis on the human ortholog DEG lists from all four transcriptome sample comparisons were used to investigate the top canonical pathways and toxicological function affected by the different stressors during the post-larval development in *C. variegatus*. The pathways most significantly impacted by hypoxia include cell cycle control of chromatin replication, while cholesterol biosynthesis pathways were most significantly impacted after exposure to oil alone. Top toxicological functions impacted during post-larval developmental included cholesterol biosynthesis, cell cycle: G1/S checkpoint regulation, cardiac hypertrophy, and hepatic fibrosis (Table 12). The different treatment comparisons resulted in differences in significantly impacted canonical pathways, but similar toxicological outcomes.

Table 12 *The Top canonical pathways and toxicological functions impacted by exposure to oil and hypoxia.*

Treatment Comparison	HCNT vs NCNT	N.Oil vs NCNT	H.Oil vs NCNT
Top Canonical Pathways	Cell Cycle Control of Chromosomal Replication Protein Ubiquitination Pathway Superpathway Cholesterol Biosynthesis Cholesterol Biosynthesis I Cholesterol Biosynthesis II (via 24,25-dihydrolanosterol)	Superpathway of Cholesterol Biosynthesis Cholesterol Biosynthesis I Cholesterol Biosynthesis II (via 24,25-dihydrolanosterol) Cholesterol Biosynthesis III (via Desmosterol) Superpathway of Geranylgeranyldiphosphate Biosynthesis I (via Mevalonate	Cell Cycle Control of Chromosomal Replication Role of BRCA1 in DNA Damage Response Superpathway of Cholesterol Biosynthesis DNA Double-Strand Break Repair by Homologous Recombination Cholesterol Biosynthesis I
Top Tox Lists	Cholesterol Biosynthesis Cell Cycle: G1/S Checkpoint Regulation Aryl Hydrocarbon Receptor Signaling Cardiac Necrosis/Cell Death P53 Signaling	Cholesterol Biosynthesis Cardiac Hypertrophy Liver Necrosis/Cell Death Primary Glomerulonephritis Biomarker Panel Oxidative Stress	Cholesterol Biosynthesis Hepatic Fibrosis Cell Cycle: G1/S Checkpoint Regulation Cardiac Hypertrophy Aryl Hydrocarbon Receptor Signaling

Comparative analysis of canonical pathways and toxicological list in Qiagen's IPA show that cholesterol biosynthesis is a target of both hypoxic and oil toxicity during the post larval developmental stage in *C. variegatus*. The data also indicated that hypoxia toxicity also impacts pathway and functions related to DNA repair as an individual stressors response and in combination with oil, but is not observed after exposure to oil alone (Figure 32). Gene expression heat maps of genes in the superpathway of cholesterol biosynthesis, cell cycle control of chromosomal replication, and role of BRCA1 in DNA damage response pathways revealed that all three pathways were activated due to complete up-regulation of all genes measured (Figure 33A-C). The gene expression heat maps also depict a differential genomic response occurring in the presence of hypoxia. Only 21% of the genes measured in the cell cycle control of chromosomal replication pathway were significantly up-regulated after exposure to oil alone while 78.5% were up-regulated following exposure to hypoxia and 96% were up-

regulated after exposure to oil + hypoxia (Figure 33B). The same differential transcriptomic response is also observed in the gene expression heat maps of gene in the role of BRCA1 in DNA damage response pathway, were no significant gene regulation occurs in the normoxic oil samples, but is observed in both the hypoxic and hypoxic oil samples (Figure 33C). The most significantly affected toxicological functions for all three sample comparisons was the cholesterol biosynthesis (Figure 34 A-C). Oil exposure alone impacted cardiac hypertrophy, Liver necrosis, kidney function, and oxidative stress (Figure 34A). Oil exposure combined with hypoxic stress impacted hepatic fibrosis, cell cycle: G1/S Checkpoint regulation, cardiac hypertrophy, and AhR signaling (Figure 34B). Hypoxic exposure alone resulted in cell cycle: G1/S checkpoint regulation and AhR signaling (Figure 34C). The IPA tox analysis provided more evidence that oil, hypoxia, and the combination of them cause differential toxicity. The data indicates that oil toxicity targets the heart, liver, kidneys, and oxidative stress response, while hypoxic toxicity involves increased DNA damage.

Figure 32. Comparative heatmap of significant canonical pathways response to exposure regimes.

Heat maps were generated with IPA using Fisher's exact test with p-value ≤ 0.05. Data represented in inverse log form, the greater the color intensity the greater the significance.

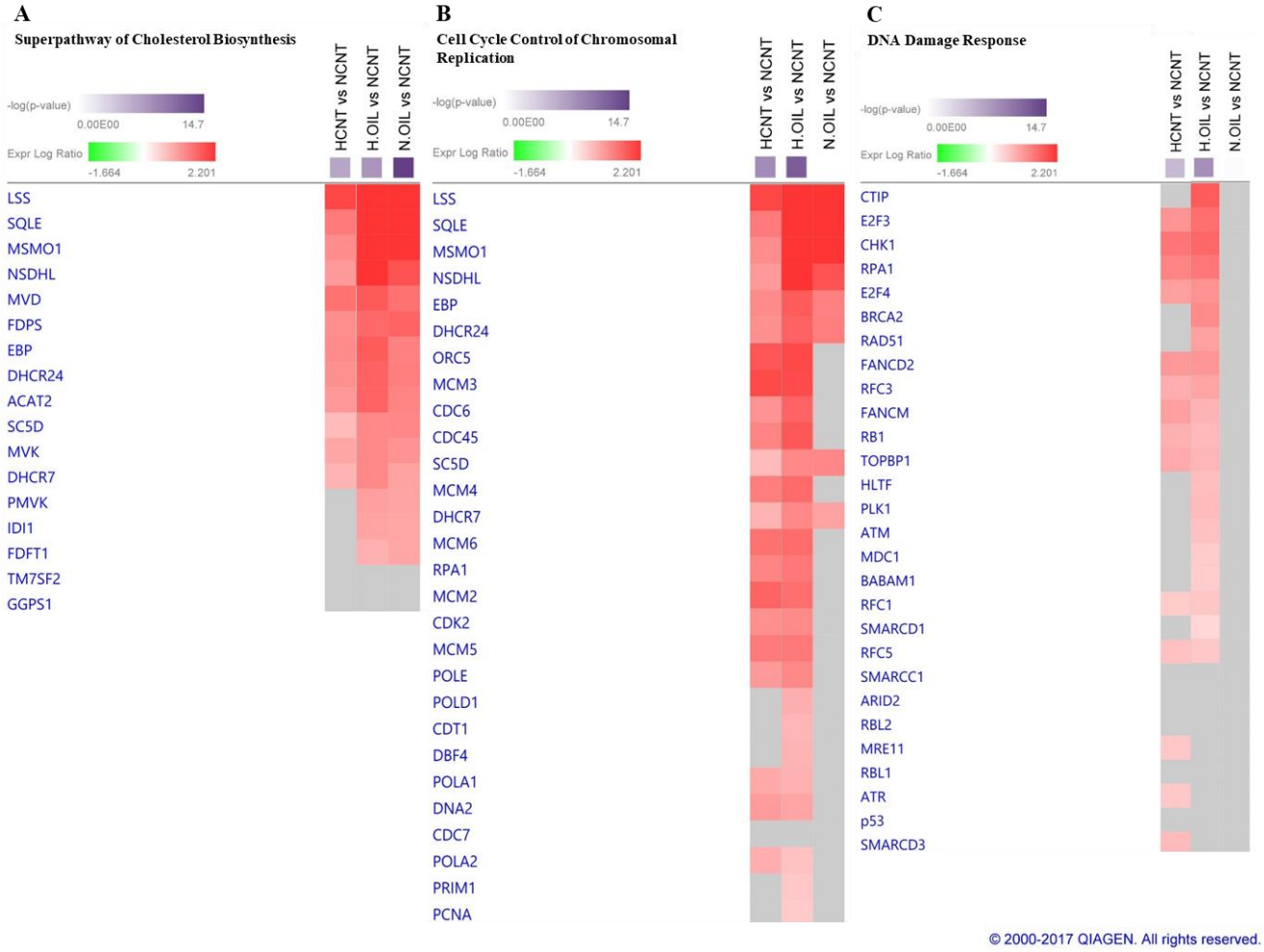

Figure 33. Comparative gene heatmaps of significantly impacted canonical pathways response to exposure regimes.

Heat maps are generated with IPA using Fisher's exact test with a p-value ≤ 0.05. Data represented in inverse log form, the greater the color intensity the greater the significance and measured fold change in log ration form. Red indicated up regulation, while green indicated down regulation.

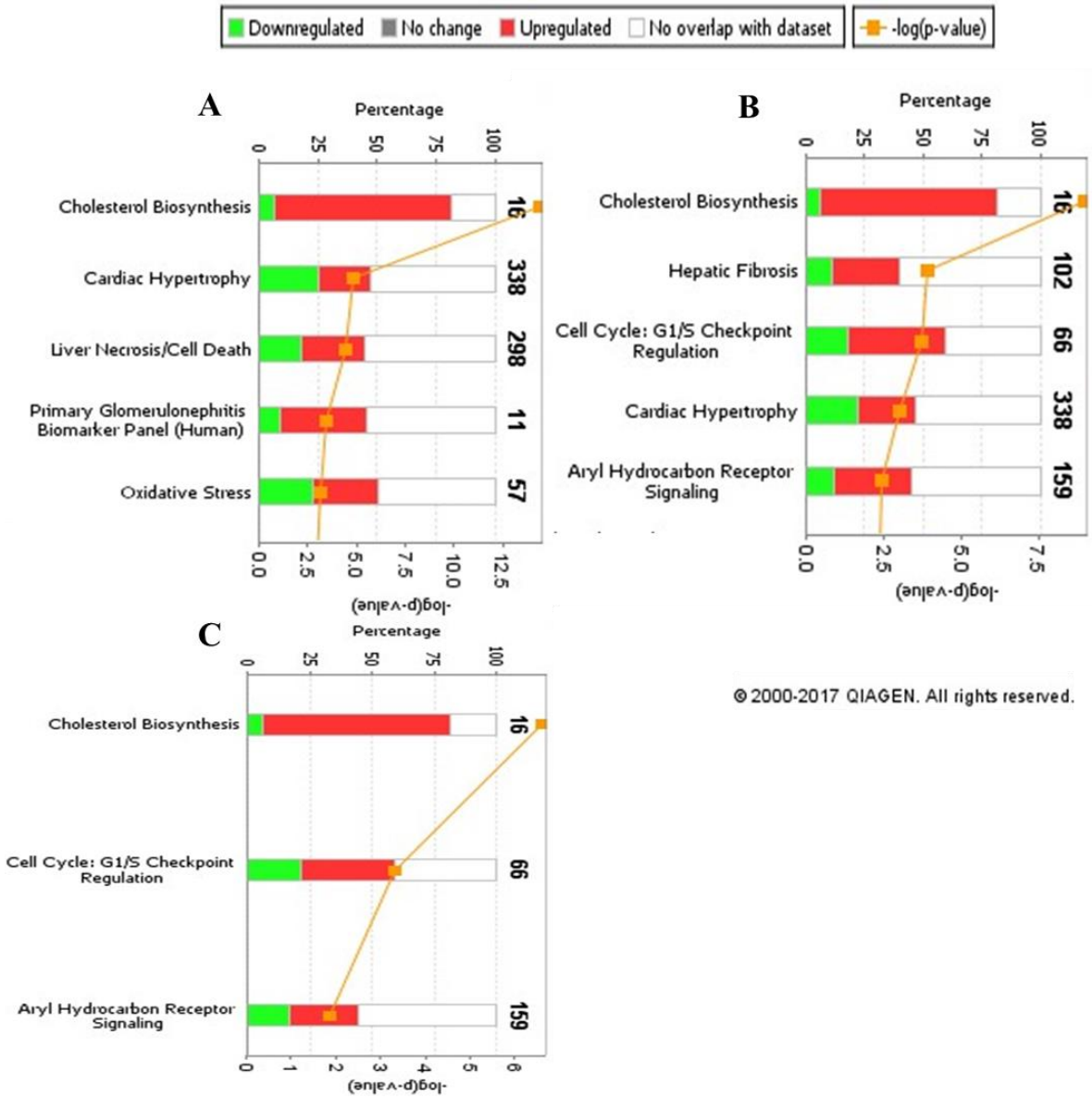

Figure 34. Stacked bar graphs of toxicological function regulation activity in response to exposure treatments.

Green indicated downregulation and red indicated upregulation. The toxicological functions are arranged in descending significance p-values (-log) on the left vertical axis. All treatments re normalized to the normoxic control samples. Response to oil (A), response to hypoxia + oil (B), and response to hypoxia (C).

Discussion

Comparison of the embryonic, post-hatch, and post-larval transcription profile response to the individual and combined stress of oil and hypoxia in *C. variegatus* resulted in separate transcriptional responses driven by age and exposure conditions. The results from the PCA plot comparing all life stages indicated that there was a distinct, age-specific clustering of gene expression tracks between all three life stages (Figure 16). The PCA clustering data indicated that the most influential factor in the organism's response to different exposure regimes is the age at which it is exposed. The oil + hypoxic exposure conditions evoked the highest differential gene response for all three life stages, embryonic (1604 genes), post-hatch (6891 genes), and post-larval (5718 genes). Though the post-hatch developmental stage had the most significantly differential expressed genes, the post-larval developmental stage was chosen for pathway analysis because this life stage had the greatest response to oil and hypoxic exposure were comparing the mortality rate and the relative gene expression of *cyp1a1*, *epo,* and *arnt1* as discussed in previous chapters.

The Ingenuity Pathway Analysis (IPA) comparative study of four post-larval exposure regimes resulted in distinct differences between larval response to hypoxic and PAH stress. Cholesterol biosynthesis pathways where the most significantly effected pathway observed in the presence of all treatment exposures, while DNA repair were significantly affected in treatments with hypoxic stress.

Cholesterol is a key component of cell membranes which is either *de novo* synthesized primarily in the liver or accumulated through diet (Siperstein, 1984; Xu et al., 2017). Many enriched canonical pathways and the most significantly affect toxicological

pathways effected by both oil and hypoxic stress were cholesterol biosynthesis. The up-regulation of cholesterol biosynthesis pathways observed in our data correspond with other transcriptomic responses to PAH stress (Regnault et al., 2014). Pathway analysis of *Xenopus tropicalis* after exposure to BaP also resulted in enrichment of cholesterol synthesis pathways (Regnault et al., 2014). The study by Olsvik et al (2013) examining the transcriptomic response of Atlantic salmon exposed to hypoxic stress indicated that cholesterol biosynthesis and protein ubiquitination pathways were significantly enriched. The up-regulation of genes in the cholesterol biosynthesis pathways observed in the transcript profiles of the *Xenopus tropicalis* was linked to hepatocyte apoptosis, depigmentation of the liver, and reactive oxygen species (ROS) production (Regnault et al., 2014). The top five enriched canonical pathways of *C. variegatus* larvae in response to oil exposure were all involved in cholesterol biosynthesis, which, interestingly, resulted in significantly enriched liver necrosis and oxidative stress toxicological pathways, further providing evidence that over regulated cholesterol pathways result in liver damage. Contradictory to our results, IPA analysis revealed the predicted inhibition of cholesterol biosynthesis pathway by decreased regulation of transport and metabolism in 96 hpf mahi-mahi larvae (Xu et al., 2017). The inhibition of cholesterol synthesis pathways in mahi-mahi larvae was speculated to be a result of AhR induction (Xu et al., 2017). Our data does not support the conclusion that the induction of the AhR pathway inhibits the synthesis of cholesterol, because the AhR pathways in the hypoxic and hypoxia + oil treatments are also significantly enriched toxicological pathways.

Cell cycle control of chromosomal replication is the most significant pathway enriched for both hypoxia and hypoxia + oil transcriptomic responses. The combined

exposure of hypoxia + oil also resulted in the significant up-regulation of two RNA repair pathways, "role of BRCA1 in DNA damage response" and "DNA double-strand break repair by homologous recombination". The significant toxicological functions associated with transcriptomic profile expression in response to hypoxia and hypoxia + oil was also related of DNA damage. Hypoxic stress alone appears to have a greater impact of DNA damage when comparing the significant toxicological functions. Three out the top five toxicological pathways enriched under hypoxic stress are related to DNA damage, cell cycle: G1/S checkpoint regulation, AhR signaling, and p53 signaling, while only two of the five toxicological pathways enriched by hypoxia + oil exposure is related to DNA damage, cell cycle: G1/S checkpoint regulation and AhR signaling. A laboratory study investigating water accommodated faction exposure on larval Atlantic cod concluded that mechanically dispersed oil affected genes responsible for DNA replication, recombination, and repair (Olsvik et al., 2012). In another study investigating the genotoxicity of WAFs on gulf killifish, the metabolism of xenobiotics was a significantly enriched KEGG pathway and comet assays showed significant DNA strand breakage in high WAF treatments relative to the controls (Pilcher et al., 2014). The cod and gulf killifish experiments provide evidence that support oil-induced DNA damage, but hypoxia induced DNA damage and AhR signaling induction is still unclear (Olsvik et al., 2012; Pilcher et al., 2014).

The objectives of this study were to investigate age-specific differences in *Cyprinodon variegatus* transcriptome response to exposure to oil, hypoxia, and the combination of both during early life stages and to compare the transcriptional response of *C. variegatus* to oil and hypoxic stress. The RNA sequencing data from all three life

stages indicated age specific responses to oil and hypoxic stress. Further analysis of the post-larval genomic responses provided evidence that oxygen concentrations primarily drove the larval genomic stress response followed by a less significant response to oil stress. Pathways analysis revealed that cholesterol biosynthesis and DNA repair pathways were primary targets of oil and hypoxic stress in post-larval *C. variegatus*. These findings provided potential molecular modes of action in response to oil and hypoxic stress in developing *C. variegatus* which can be used to investigate the effects of both stressors on targeted pathways and the implications it has on fish health.

CHAPTER V – SIGNIFICANCE OF RESEARCH

The objective of this research was to investigate the impacts of oil exposure in combination with varying environmental stressors on larval fish health at both the molecular and organismal levels. This research intended to fill gaps in knowledge in developmental toxicity response to multiple stressors using a controlled laboratory exposure setting. Most of the research investigating organismal response to crude oil exposure from the DWH oil spill have included experimental designs that only examine chemical stressors individually or in complex mixtures (WAFs). Research that included both chemical and environmental stressors usually only included a single environmental stressor (either temperature, salinity, or hypoxia), which ignores interaction effects and may lead to underestimations of oil toxicities in dynamic estuarine environments. A field study examining the resilience of salt mash ecosystems the summer following the DWH oil spill sampled fish from habitats that are prone to decreased oxygen levels, which provided some evidence of synergistic effects, but due to countless unknown variables associated with field-based studies it is difficult to link the effects back to hypoxic and oil stress alone (Garcia et al., 2012). The current research is the only controlled laboratory experiments to use a multiple toxicity approach to examine the developmental and transcriptomic response of *Cyprinodon variegatus* to crude oil simultaneously exposed to elevated temperature and varying oxygen and salinity regimes.

The data collected from this study suggest that age had the greatest effect on both phenotypic and transcriptomic response to oil and abiotic stressors. Multiple experimental endpoints including mortality, gene expression, and comparative transcriptomic responses, provided evidence that the post-larval developmental stage of

C. variegatus to be the most sensitive early life stage to oil exposure. At the organismal levels, the post-larval developmental stage had the highest observed mortality rates when compared to the embryonic and post-hatch developmental stage mortality. The post-larval *C. variegatus* was also the only developmental stage to show down-regulation of all target genes involved in the activation of the AhR and HIF-1α pathways. The observed suppression of *cyp1a1*, *epo,* and *arnt1* in larval *C. variegatus* provided evidence that an interactive effect at the cellular level between these two pathways is occurring in response to combined oil and environmental stressors. The cellular inhibition of the two defense pathways provides a possible explanation to the increased mortality rates observed in the post-larval developmental stage. Furthermore, the comparative transcriptomic response of *C. variegatus* also provides evidence indicating that free feeding *C. variegatus* larvae are most sensitive to oil exposure under adverse environmental conditions. Principal component analysis of the gene expression tracks for all three RNA sequencing libraries showed clear clustering patterns based on early life stages. Taken together, these data suggests that the most sensitive early life stage of development for the *C. variegatus* is the post-larval developmental stage, which is supported by other developmental toxicity studies that have also shown age-dependent responses to toxicants.

The research also determined that the addition of environmental stressors had a significant influence on oil toxicity, independent of age response. The lowest mortality within all developmental stages was constantly observed under normoxic – low salinity conditions. During the embryonic assays the highest cumulative mortality was observed under hypoxic-high salinity conditions. For post-hatch assays, the highest mortality was

observed under normoxic- high salinity conditions, and during the post-larval assays the highest mortality was observed under hypoxic-high salinity conditions. Synergistic toxicity effects were only observed in the embryonic assays in the presence of hypoxia, and in the post-hatch assays in the presence of high salinity. The mortality response of post-larval assays showed the greatest synergistic response to HEWAF exposure under hypoxic - high salinity conditions, but also had a similar response in the presence of hypoxia and high salinity alone.

Suppression of both AhR and HIF-1α pathways during the post-larval developmental stage of *C. variegatus*, provides evidence that cross-talk between the AhR and HIF-1α signaling pathways occurs in *C. variegatus* in a treatment-dependent manner and at the Arnt node. Decreased expression patterns of *cyp1a1*, *epo* and *arnt1* mRNA indicate that both defense pathways were inhibited under hypoxic-high salinity conditions in PAH concentrations greater than 226 µg/L, which was directly related to the decreased expression of *arnt1*. Regulation of Arnt, the shared binding partner of the AhR and HIF1-α receptors seems to be influences by hypoxia and oil contamination. These stressors caused down-regulation of the Arnt and therefore inhibited both pathways due to total saturation of available Arnt in the nucleus. Inhibition of the two defense pathways decreased the larvae's ability to combat the deleterious effects associated with PAH and hypoxic exposure. Negative effects resulting from PAH and hypoxia stress include a suite of developmental effects that result in increased mortality and lower overall fitness which have been observed in multiple fish species in current research (Incardona et al., 2004; Landry et al., 2007; Wu et al., 2003).

Global transcription analysis of oil, hypoxia, and hypoxia + oil exposures during early life stage development of *C. variegatus* resulted in treatment-specific genotoxicity. Age specific gene expression clustering was primarily influenced by oxic treatment and secondarily by oil concentration. The individual life stage heat maps also resulted in oil and oxic treatment clustering of statically significant DEGs within life stages. The embryonic life stage had a limited reaction to all exposure conditions examined, while the post-hatch life staged showed the largest response to the exposure conditions. Though the post-hatch had the greatest DEGs response to the exposure conditions, the post-larval developmental stage was chosen for pathway enrichment analysis due to the high mortality rates and suppression of target AhR and HIF-1α pathway genes observed in previous chapters.

Cholesterol biosynthesis pathways were significantly regulated in all exposure comparisons: oil (2.17e-15), hypoxia (1.31E-07), and oil + hypoxia (8.75e-09). The most significantly impacted toxicological pathways observed using IPA- Core analysis for all exposure comparisons was also cholesterol biosynthesis, oil (3.72e-15), hypoxia (2.72E-07), and oil + hypoxia (1.07e-09). Up-regulation of both canonical pathways and toxicological pathways related to cholesterol biosynthesis were observed across all three exposure conditions. Transcriptomic profile analysis of PAH and hypoxic exposure in salmon, mahi-mahi, and *X. tropicalis* have also revealed perturbation of cholesterol biosynthesis pathways (Olsvik et al., 2013; Regnault et al., 2014; Xu et al., 2017).

Differential transcriptomic effects were observed between *C. variegatus* larval response to oil and hypoxic stress. Oil exposure alone had the greatest effects on five different canonical pathways related to cholesterol which resulted in significant up-

regulation of liver necrosis (3.65E-05), acute kidney injury (3.68E-04), and oxidative stress (6.73E-04). Hypoxic stress alone and in combination with oil exposure caused increased regulation of canonical pathways involved in cell regulation and DNA damage repair. Cell cycle control of chromosomal replication was the most significantly affected canonical pathway in response to both hypoxia and oil + hypoxia (1.42E-09 and 3.33E-13 respectively) (Table 12). The oil + hypoxia exposure comparison also activated two other pathways involved in DNA damage repair, role of BRCA1 in DNA damage response and DNA double-strand break repair by homologous recombination. Even though hypoxia in combination with oil affected more canonical pathways involved in DNA damage, the same toxicological pathways were activated in response to both exposure conditions: the cell cycle: G1/S checkpoint regulation and the AhR signaling pathways.

Oil production in the Gulf of Mexico makes about a quarter of the domestically produced oil in the United States which results in increased PAH contamination in marine habitats (Incardona et al., 2005; Sammarco et al., 2013). The physical characteristics of abiotic water parameters in the Gulf of Mexico are also negatively influences due to increased nutrient loading from riverine input, which contributes to growth of hypoxic regions (Rabalais et al., 2001). The study of the interaction effect between PAHs and environmental parameters is key in developing a better understanding of oil toxicity and its implications on ecosystem health and resilience. This research has provided critical laboratory based evidence to further our understanding of the impact of oil on developing organisms in estuarine habitats in the presence of environmental stressors which is key in elevating the 2010 Deepwater

Horizon effect on the Gulf of Mexico because 30% of commercial fishes in the gulf is dependent on these estuarine habitats (Mendelssohn et al., 2012). Results from this study indicate that environmental factors influence oil toxicity to exposed organisms. The molecular mechanisms behind the synergistic toxicity observed in the presence of hypoxia and high salinity during the embryonic and post-hatch developmental stages remain unclear. Morphological and molecular observations from the current study has indicated potential mechanisms of synergistic toxicity effects between oil and environmental factors during the post-larval developmental in *C. variegatus*. Suppression of both defense pathways observed only in the post-larval developmental stage under hypoxic and high salinity condition in PAH concentrations of 220 – 350 µg/L. The suppression observed implies that the cross-talk at the *arnt1* node may be influenced by external stimuli that restrict expression of *arnt1,* rather than competitive inhibition which is a different molecular process than previously described in the literature.

REFERENCES

Adams, M., 2005. Assessing cause and effect of multiple stressors on marine systems. Mar. Pollut. Bull. 51, 649–657.

Adeyemi, J.A., Klerks, P.L., 2012. Salinity acclimation modulates copper toxicity in the sheepshead minnow, Cyprinodon variegatus. Environ. Toxicol. Chem. 31, 1573–1578. doi:10.1002/etc.1850

Allan, S.E., Smith, B.W., Anderson, K. a, 2012. Impact of the deepwater horizon oil spill on bioavailable polycyclic aromatic hydrocarbons in Gulf of Mexico coastal waters. Environ. Sci. Technol. 46, 2033–2039. doi:10.1021/es202942q

Baker, M., Steinhoff, M., Fricano, G., 2016. Integrated effects of the Deepwater Horizon oil spill on nearshore ecosystems. Mar. Ecol. Prog. Ser. View, 1–16. doi:10.3354/meps11920

Barron, M.G., Heintz, R., Rice, S.D., 2004. Relative potency of PAHs and heterocycles as aryl hydrocarbon receptor agonists in fish. Mar. Environ. Res. 58, 95–100. doi:10.1016/j.marenvres.2004.03.001

Bayha, K.M., Ortell, N., Ryan, C.N., Griffitt, K.J., Krasnec, M., Sena, J., Ramaraj, T., Takeshita, R., Mayer, G.D., Schilkey, F., Griffitt, R.J., 2017. Crude oil impairs immune function and increases susceptibility to pathogenic bacteria in southern flounder. PLoS One 12, e0176559. doi:10.1371/journal.pone.0176559

Beyer, J., Trannum, H.C., Bakke, T., Hodson, P. V., Collier, T.K., 2016. Environmental effects of the Deepwater Horizon oil spill: A review. Mar. Pollut. Bull. 110, 28–51. doi:10.1016/j.marpolbul.2016.06.027

Bianchi, T.S., DiMarco, S.F., Cowan, J.H., Hetland, R.D., Chapman, P., Day, J.W.,

Allison, M.A., 2010. The science of hypoxia in the northern Gulf of Mexico: A review. Sci. Total Environ. 408, 1471–1484. doi:10.1016/j.scitotenv.2009.11.047

Brauner, C., Ballantyne, C., Vijayan, M., 1999. Crude oil exposure affects air-breathing frequency, blood phosphate levels and ion regulation in an air-breathing teleost fish, Hoplosternum littorale. Comp. Biochem. Physiol. Part C 123, 127–134.

Brewton, R.A., Fulford, R., Griffitt, R.J., 2013. Gene Expression and Growth as Indicators of Effects of the BP Deepwater Horizon Oil Spill on Spotted Seatrout (Cynoscion nebulosus). J. Toxicol. Environ. Health. A 76, 1198–209. doi:10.1080/15287394.2013.848394

Brown-Peterson, N.J., Krasnec, M., Takeshita, R., Ryan, C.N., Griffitt, K.J., Lay, C., Mayer, G.D., Bayha, K.M., Hawkins, W.E., Lipton, I., Morris, J., Griffitt, R.J., 2015. A multiple endpoint analysis of the effects of chronic exposure to sediment contaminated with Deepwater Horizon oil on juvenile Southern flounder and their associated microbiomes. Aquat. Toxicol. 165, 197–209. doi:10.1016/j.aquatox.2015.06.001

Brown, C.A., Gothreaux, C.T., Green, C.C., 2011. Effects of temperature and salinity during incubation on hatching and yolk utilization of Gulf killifish Fundulus grandis embryos. Aquaculture 315, 335–339. doi:10.1016/j.aquaculture.2011.02.041

Chan, W.K., Yao, G., Gu, Y., Bradfield, C.A., 1999. Cross-talk between the Aryl Hydrocarbon Receptor and dioxin signal transduction pathways and identify Epo as 274, 12115–12123.

Chesney, E.J., Baltz, D.M., Thomas, R.G., 2000. LOUISIANA ESTUARINE AND COASTAL FISHERIES AND HABITATS: PERSPECTIVES FROM A FISH'S

EYE VIEW. Ecol. Appl. 10, 350–366. doi:10.1890/1051-0761(2000)010[0350:LEACFA]2.0.CO;2

Dangre, A.J., Manning, S., Brouwer, M., 2010. Effects of cadmium on hypoxia-induced expression of hemoglobin and erythropoietin in larval sheepshead minnow, Cyprinodon variegatus. Aquat. Toxicol. 99, 168–175. doi:10.1016/j.aquatox.2010.04.015

Dasgupta, S., DiGiulio, R.T., Drollette, B.D., L. Plata, D., Brownawell, B.J., McElroy, A.E., 2016. Hypoxia depresses CYP1A induction and enhances DNA damage, but has minimal effects on antioxidant responses in sheepshead minnow (Cyprinodon variegatus) larvae exposed to dispersed crude oil. Aquat. Toxicol. 177, 250–260. doi:10.1016/j.aquatox.2016.05.022

Denison, M.S., Nagy, S.R., 2003. A CTIVATION OF THE A RYL H YDROCARBON R ECEPTOR BY S TRUCTURALLY D IVERSE E XOGENOUS AND E NDOGENOUS C HEMICALS. Annu. Rev. Pharmacol. Toxicol. 43, 309–334. doi:10.1146/annurev.pharmtox.43.100901.135828

Di Giulio, R.T., Hinton, D.E., 2008. The Toxicology of Fishes.

Ekblom, R., Galindo, J., 2010. Applications of next generation sequencing in molecular ecology of non-model organisms. Heredity (Edinb). 107, 1–15. doi:10.1038/hdy.2010.152

Eldridge, P.M., Roelke, D.L., 2010. Origins and scales of hypoxia on the Louisiana shelf: Importance of seasonal plankton dynamics and river nutrients and discharge. Ecol. Modell. 221, 1028–1042. doi:10.1016/j.ecolmodel.2009.04.054

Engelhardt, F.R., Wong, M.P., Duey, M.E., 1981. Hydromineral balance and gill

morphology in rainbow trout Salmo gairdneri, acclimated to fresh and sea water. As affected by petroleum exposure. Aquat. Toxicol. doi:10.1016/0166-445X(81)90013-8

Evans, D.H., Piermarini, P.M., Choe, K.P., 2005. The Multifunctional Fish Gill: Dominant Site of Gas Exchange, Osmoregulation, Acid-Base Regulation, and Excretion of Nitrogenous Waste. Physiol. Rev. 85, 97–177. doi:10.1152/physrev.00050.2003

Finn, R.N., 2007. The physiology and toxicology of salmonid eggs and larvae in relation to water quality criteria. Aquat. Toxicol. 81, 337–354. doi:10.1016/j.aquatox.2006.12.021

Fleming, C.R., Billiard, S.M., Di Giulio, R.T., 2009. Hypoxia inhibits induction of aryl hydrocarbon receptor activity in topminnow hepatocarcinoma cells in an ARNT-dependent manner. Comp. Biochem. Physiol. - C Toxicol. Pharmacol. 150, 383–389. doi:10.1016/j.cbpc.2009.06.003

Fodrie, F.J., Able, K.W., Galvez, F., Heck, K.L., Jensen, O.P., López-duarte, P.C., Martin, C.W., Turner, R.E., Whitehead, A., 2014. Integrating Organismal and Population Responses of Estuarine Fishes in Macondo Spill Research. Bioscience 64, 778–788. doi:10.1093/biosci/biu123

Forth, H.P., Mitchelmore, C.L., Morris, J.M., Lipton, J., 2017. Characterization of oil and water accommodated fractions used to conduct aquatic toxicity testing in support of the Deepwater Horizon oil spill natural resource damage assessment. Environ. Toxicol. Chem. 36, 1450–1459. doi:10.1002/etc.3672

Fridman, S., Bron, J., Rana, K., 2012. Influence of salinity on embryogenesis, survival,

growth and oxygen consumption in embryos and yolk-sac larvae of the Nile tilapia. Aquaculture 334–337, 182–190. doi:10.1016/j.aquaculture.2011.12.034

Garcia, T.I., Shen, Y., Crawford, D., Oleksiak, M.F., Whitehead, A., Walter, R.B., 2012. RNA-Seq reveals complex genetic response to Deepwater Horizon oil release in Fundulus grandis. BMC Genomics 13, 474. doi:10.1186/1471-2164-13-474

Gassmann, M., Kvietikova, I., Rolfs, A., Wenger, R.H., 1997. Oxygen- and dioxin-regulated gene expression in mouse hepatoma cells. Kidney Int. 51, 567–74. doi:10.1038/ki.1997.81

Goanvec, C., Poirier, E., Le-Floch, S., Theron, M., 2011. Branchial structure and hydromineral equilibrium in juvenile turbot (Scophthalmus maximus) exposed to heavy fuel oil. Fish Physiol Biochem 37, 363–371. doi:10.1007/s10695-010-9435-2

Gradin, K., McGuire, J., Wenger, R.H., Kvietikova, I., fhitelaw, M.L., Toftgård, R., Tora, L., Gassmann, M., Poellinger, L., 1996. Functional interference between hypoxia and dioxin signal transduction pathways: competition for recruitment of the Arnt transcription factor. Mol. Cell. Biol. 16, 5221–31.

Greer, C.D., Hodson, P. V., Li, Z., King, T., Lee, K., 2012. Toxicity of crude oil chemically dispersed in a wave tank to embryos of Atlantic herring (Clupea harengus). Environ. Toxicol. Chem. 31, 1324–1333. doi:10.1002/etc.1828

Haney, D.C., 1999. Osmoregulafion in the Sheepshead Minnow, Cyprinodon variegatus: Influence of a Fluctuating Salinity Regime 22, 1071–1077.

Haney, D.C., Nordlie, F.G., 1997. Influence of environmental salinity on routine metabolic rate and critical oxygen tension of Cyprinodon variegatus. Physiol. Zool. 70, 511–8.

Hendon, L. a., Carlson, E. a., Manning, S., Brouwer, M., 2008. Molecular and developmental effects of exposure to pyrene in the early life-stages of Cyprinodon variegatus. Comp. Biochem. Physiol. - C Toxicol. Pharmacol. 147, 205–215. doi:10.1016/j.cbpc.2007.09.011

Incardona, J.P., Carls, M.G., Teraoka, H., Sloan, C.A., Collier, T.K., Scholz, N.L., 2005. Aryl Hydrocarbon Receptor–Independent Toxicity of Weathered Crude Oil during Fish Development. Environ. Health Perspect. 113, 1755–1762. doi:10.1289/ehp.8230

Incardona, J.P., Collier, T.K., Scholz, N.L., 2004. Defects in cardiac function precede morphological abnormalities in fish embryos exposed to polycyclic aromatic hydrocarbons. Toxicol. Appl. Pharmacol. 196, 191–205. doi:10.1016/j.taap.2003.11.026

Incardona, J.P., Day, H.L., Collier, T.K., Scholz, N.L., 2006. Developmental toxicity of 4-ring polycyclic aromatic hydrocarbons in zebrafish is differentially dependent on AH receptor isoforms and hepatic cytochrome P4501A metabolism. Toxicol. Appl. Pharmacol. 217, 308–321. doi:10.1016/j.taap.2006.09.018

Jin, Q., Pan, L., Liu, T., Hu, F., 2015. RNA-seq based on transcriptome reveals differ genetic expressing in Chlamys farreri exposed to carcinogen PAHs. Environ. Toxicol. Pharmacol. 39, 313–320. doi:10.1016/j.etap.2014.11.019

Jones, E.R., Martyniuk, C.J., Morris, J.M., Krasnec, M.O., Griffitt, R.J., 2017. Exposure to Deepwater Horizon oil and Corexit 9500 at low concentrations induces transcriptional changes and alters immune transcriptional pathways in sheepshead minnows. Comp. Biochem. Physiol. Part D Genomics Proteomics 23, 8–16.

doi:10.1016/j.cbd.2017.05.001

Jung, J.H., Hicken, C.E., Boyd, D., Anulacion, B.F., Carls, M.G., Shim, W.J., Incardona, J.P., 2013. Geologically distinct crude oils cause a common cardiotoxicity syndrome in developing zebrafish. Chemosphere 91, 1146–1155. doi:10.1016/j.chemosphere.2013.01.019

Kewley, R.J., Whitelaw, M.L., Chapman-Smith, A., 2004. The mammalian basic helix-loop-helix/PAS family of transcriptional regulators. Int. J. Biochem. Cell Biol. 36, 189–204. doi:10.1016/S1357-2725(03)00211-5

Kirman, Z.D., Sericano, J.L., Wade, T.L., Bianchi, T.S., Marcantonio, F., Kolker, A.S., 2016. Composition and depth distribution of hydrocarbons in Barataria Bay marsh sediments after the Deepwater Horizon oil spill. Environ. Pollut. 214, 101–113. doi:10.1016/j.envpol.2016.03.071

Kulkarni, R.P., Tohari, S., Ho, A., Brenner, S., Venkatesh, B., 2010. Characterization of a hypoxia-response element in the Epo locus of the pufferfish, Takifugu rubripes. Mar. Genomics 3, 63–70. doi:10.1016/j.margen.2010.05.001

Kumar, H., Choi, D.-K., 2015. Hypoxia Inducible Factor Pathway and Physiological Adaptation: A Cell Survival Pathway? Mediators Inflamm. 2015, 584758. doi:10.1155/2015/584758

Kuntz, A., 1916. Notes on the embryology and larval development of five species of teleostean fishes. Bull US Bur Fish.

Lai, J.C.C., Kakuta, I., Mok, H.O.L., Rummer, J.L., Randall, D., 2006. Effects of moderate and substantial hypoxia on erythropoietin levels in rainbow trout kidney and spleen. J. Exp. Biol. 209, 2734–2738. doi:10.1242/jeb.02279

Landry, C.A., Steele, S.L., Manning, S., Cheek, A.O., 2007. Long term hypoxia suppresses reproductive capacity in the estuarine fish, Fundulus grandis. Comp. Biochem. Physiol. - A Mol. Integr. Physiol. 148, 317–323. doi:10.1016/j.cbpa.2007.04.023

Liu, Z., Liu, J., Zhu, Q., Wu, W., 2012. The weathering of oil after the Deepwater Horizon oil spill: insights from the chemical composition of the oil from the sea surface, salt marshes and sediments. Environ. Res. Lett. 7, 35302. doi:10.1088/1748-9326/7/3/035302

Mager, E.M., Pasparakis, C., Schlenker, L.S., Yao, Z., Bodinier, C., Stieglitz, J.D., Hoenig, R., Morris, J.M., Benetti, D.D., Grosell, M., 2016. Assessment of early life stage mahi-mahi windows of sensitivity during acute exposures to Deepwater Horizon crude oil; Assessment of early life stage mahi-mahi windows of sensitivity during acute exposures to Deepwater Horizon crude oil. Environ. Toxicol. 9999, 1–9. doi:10.1002/etc.3713

McNutt, M.K., Camilli, R., Crone, T.J., Guthrie, G.D., Hsieh, P.A., Ryerson, T.B., Savas, O., Shaffer, F., 2012. Review of flow rate estimates of the Deepwater Horizon oil spill. Proc. Natl. Acad. Sci. 109, 20260–20267. doi:10.1073/pnas.1112139108

Mendelssohn, I.A., Andersen, G.L., Baltz, D.M., Caffey, R.H., Carman, K.R., Fleeger, J.W., Joye, S.B., Lin, Q., Maltby, E., Overton, E.B., 2012. Oil Impacts on Coastal Wetlands: Implications for the Mississippi River Delta Ecosystem after the *Deepwater Horizon* Oil Spill. Bioscience 62, 562–574. doi:10.1525/bio.2012.62.6.7

Michel, J., Owens, E.H., Zengel, S., Graham, A., Nixon, Z., Allard, T., Holton, W., Reimer, P.D., Lamarche, A., White, M., Rutherford, N., Childs, C., Mauseth, G.,

Challenger, G., Taylor, E., 2013. Extent and Degree of Shoreline Oiling: Deepwater Horizon Oil Spill, Gulf of Mexico, USA. doi:10.1371/journal.pone.0065087

Nebert, D.W., Dalton, T.P., 2006. The role of cytochrome P450 enzymes in endogenous signalling pathways and environmental carcinogenesis. Nat. Rev. Cancer 6, 947–960. doi:10.1038/nrc2015

Nie, M., Blankenship, A.L., Giesy, J.P., 2001. Interactions between aryl hydrocarbon receptor (AhR) and hypoxia signaling pathways. Environ. Toxicol. Pharmacol. 10, 17–27. doi:10.1016/S1382-6689(01)00065-5

Nikinmaa, M., Rees, B.B., 2005. Oxygen-dependent gene expression in fishes. Am. J. Physiol. Regul. Integr. Comp. Physiol. 288, R1079–R1090. doi:10.1152/ajpregu.00626.2004

Nixon, Z., Zengel, S., Baker, M., Steinhoff, M., Fricano, G., Rouhani, S., Michel, J., 2016. Shoreline oiling from the Deepwater Horizon oil spill. Mar. Pollut. Bull. 107, 170–178. doi:10.1016/j.marpolbul.2016.04.003

Nordlie, F.G., 1987. PLASMA OSMOTIC, Na+ AND Cl-REGULATION UNDER EURYHALINE CONDITIONS IN. Camp. Biochem. Physid 86, 57–61.

Nordlie, F.G., Walsh, S.J., Haney, D.C., Nordlie, T.F., 1991. The influence of ambient salinity on routine metabolism in the teleost Cyprinodon variegatus Lacep??de. J. Fish Biol. 38, 115–122. doi:10.1111/j.1095-8649.1991.tb03097.x

Olsvik, P.A., Lie, K.K., Nordtug, T., Hansen, B.H., 2012. Is chemically dispersed oil more toxic to Atlantic cod (Gadus morhua) larvae than mechanically dispersed oil? A transcriptional evaluation. BMC Genomics 13. doi:10.1186/1471-2164-13-702

Olsvik, P.A., Vikesa, V., Lie, K.K., Hevroy, E.M., 2013. Transcriptional responses to

temperature and low oxygen stress in Atlantic salmon studied with next-generation sequencing technology. BMC Genomics 14, 817. doi:10.1186/1471-2164-14-817

Pasparakis, C., Mager, E.M., Stieglitz, J.D., Benetti, D., Grosell, M., 2016. Effects of Deepwater Horizon crude oil exposure, temperature and developmental stage on oxygen consumption of embryonic and larval mahi-mahi (Coryphaena hippurus). Aquat. Toxicol. 181, 113–123. doi:10.1016/j.aquatox.2016.10.022

Patterson, J., Bodinier, C., Green, C., 2012. Effects of low salinity media on growth, condition, and gill ion transporter expression in juvenile Gulf killifish, Fundulus grandis. Comp. Biochem. Physiol. - A Mol. Integr. Physiol. 161, 415–421. doi:10.1016/j.cbpa.2011.12.019

Petereit, C., Hinrichsen, H.H., Voss, R., Kraus, G., Freese, M., Clemmesen, C., 2009. The influence of different salinity conditions on egg buoyancy and development and yolk sac larval survival and morphometric traits of Baltic Sea sprat (<i>Sprattus sprattus balticus</i> Schneider). Sci. Mar. 73, 59–72. doi:10.3989/scimar.2009.73s1059

Pilcher, W., Miles, S., Tang, S., Mayer, G., Whitehead, A., 2014. Genomic and Genotoxic Responses to Controlled Weathered-Oil Exposures Confirm and Extend Field Studies on Impacts of the Deepwater Horizon Oil Spill on Native Killifish. PLoS One 9, e106351. doi:10.1371/journal.pone.0106351

Pollenz, R.S., Davarinos, N. a, Shearer, T.P., 1999. Analysis of aryl hydrocarbon receptor-mediated signaling during physiological hypoxia reveals lack of competition for the aryl hydrocarbon nuclear translocator transcription factor. Mol. Pharmacol. 56, 1127–37.

Prasch, A.L., Andreasen, E.A., Peterson, R.E., Heideman, W., 2004. Interactions between 2,3,7,8-tetrachlorodibenzo-p-dioxin (TCDD) and hypoxia signaling pathways in Zebrafish: Hypoxia decreases responses to TCDD in Zebrafish embryos. Toxicol. Sci. 78, 68–77. doi:10.1093/toxsci/kfh053

Qian, X., Ba, Y., Zhuang, Q., Zhong, G., 2014. RNA-Seq technology and its application in fish transcriptomics. OMICS 18, 98–110. doi:10.1089/omi.2013.0110

Rabalais, N.N., Turner, R.E., Scavia, D., 2002. Beyond Science into Policy: Gulf of Mexico Hypoxia and the Mississippi River. Bioscience 52, 129. doi:10.1641/0006-3568(2002)052[0129:BSIPGO]2.0.CO;2

Rabalais, N.N., Turner, R.E., Wiseman, W.J.J., 2001. Hypoxia in the Gulf of Mexico. J. Environ. Qual. 30, 320–329. doi:10.2134/jeq2001.302320x

Ramachandran, S.D., Sweezey, M.J., Hodson, P. V., Boudreau, M., Courtenay, S.C., Lee, K., King, T., Dixon, J. a., 2006. Influence of salinity and fish species on PAH uptake from dispersed crude oil. Mar. Pollut. Bull. 52, 1182–1189. doi:10.1016/j.marpolbul.2006.02.009

Regnault, C., Worms, I. a M., Oger-Desfeux, C., MelodeLima, C., Veyrenc, S., Bayle, M.-L., Combourieu, B., Bonin, A., Renaud, J., Raveton, M., Reynaud, S., 2014. Impaired liver function in Xenopus tropicalis exposed to benzo[a]pyrene: transcriptomic and metabolic evidence. BMC Genomics 15, 666. doi:10.1186/1471-2164-15-666

Reynaud, S., Deschaux, P., 2006. The effects of polycyclic aromatic hydrocarbons on the immune system of fish: A review. Aquat. Toxicol. 77, 229–238. doi:10.1016/j.aquatox.2005.10.018

Sakamoto, T., Uchida, K., Yokota, S., 2001. Regulation of the Ion-Transporting Mitochondrion-Rich Cell during Adaptation of Teleost Fishes to Different Salinities. Zoolog. Sci. 18, 1163–1174. doi:10.2108/zsj.18.1163

Sammarco, P.W., Kolian, S.R., Warby, R.A.F., Bouldin, J.L., Subra, W.A., Porter, S.A., 2013. Distribution and concentrations of petroleum hydrocarbons associated with the BP/Deepwater Horizon Oil Spill, Gulf of Mexico. Mar. Pollut. Bull. 73, 129–143. doi:10.1016/j.marpolbul.2013.05.029

Sampaio, L.A., Bianchini, A., 2002. Salinity effects on osmoregulation and growth of the euryhaline flounder Paralichthys orbignyanus. J. Exp. Mar. Bio. Ecol. 269, 187–196. doi:10.1016/S0022-0981(01)00395-1

Schirmer, K., Fischer, B.B., Madureira, D.J., Pillai, S., 2010. Transcriptomics in ecotoxicology. Anal. Bioanal. Chem. 397, 917–923. doi:10.1007/s00216-010-3662-3

Schults, M.A., Timmermans, L., Godschalk, R.W., Theys, J., Wouters, B.G., Van Schooten, F.J., Chiu, R.K., 2010. Diminished carcinogen detoxification is a novel mechanism for hypoxia-inducible factor 1-mediated genetic instability. J. Biol. Chem. 285, 14558–14564. doi:10.1074/jbc.M109.076323

Semenza, G.L., 2001. Minireview HIF-1, O 2 , and the 3 PHDs: How Animal Cells Signal Hypoxia to the Nucleus. Cell 107, 1–3.

Shang, E., Wu, R., 2004. Aquatic Hypoxia Is a Teratogen and Affects Fish Embryonic Development. Environ. Sci. Technol. 4763–4767. doi:10.1021/es0496423

Siperstein, M.D., 1984. Role of cholesterogenesis and isoprenoid synthesis in DNA replication and cell growth. J. Lipid Res. 25, 1462–1468.

Sørhus, E., Incardona, J.P., Karlsen, Ø., Linbo, T., Sørensen, L., Nordtug, T., van der Meeren, T., Thorsen, A., Thorbjørnsen, M., Jentoft, S., Edvardsen, R.B., Meier, S., 2016. Crude oil exposures reveal roles for intracellular calcium cycling in haddock craniofacial and cardiac development. Sci. Rep. 6, 31058. doi:10.1038/srep31058

Spier, C., Stringfellow, W.T., Hazen, T.C., Conrad, M., 2013. Distribution of hydrocarbons released during the 2010 MC252 oil spill in deep offshore waters. Environ. Pollut. 173, 224–230. doi:10.1016/j.envpol.2012.10.019

Sumaila, U.R., Cisneros-Montemayor, A.M., Dyck, A., Huang, L., Cheung, W., Jacquet, J., Kleisner, K., Lam, V., Mccrea-Strub, A., Swartz, W., Watson, R., Zeller, D., Pauly, D., 2012. Impact of the Deepwater Horizon well blowout on the economics of US Gulf fisheries. Can. J. Fish. Aquat. Sci. 69, 499–510. doi:10.1139/F2011-171

Tanos, R., Patel, R.D., Murray, I.A., Smith, P.B., Patterson, A.D., Perdew, G.H., 2012. Aryl hydrocarbon receptor regulates the cholesterol biosynthetic pathway in a dioxin response element-independent manner. Hepatology 55, 1994–2004. doi:10.1002/hep.25571

Tomita, S., Sinal, C.J., Yim, S.H., Gonzalez, F.J., 2000. Conditional Disruption of the Aryl Hydrocarbon Receptor Nuclear Translocator (Arnt) Gene Leads to Loss of Target Gene Induction by the Aryl Hydrocarbon Receptor and Hypoxia-Inducible Factor 1␣. Mol. Endocrinol. 14, 1674–1681.

Turner, E.R., Overton, E.B., Meyer, B.M., Miles, M.S., McCLenachan, G., Hooper-Bui, L., Engel, A.S., Swenson, E.M., Lee, J.M., Milan, C.S., Gao, H., 2014. Distribution and recovery trajectory of Macondo (Mississippi Canyon 252) oil in Louisiana coastal wetlands. doi:10.1016/j.marpolbul.2014.08.011

Valentine, M.M., Benfield, M.C., 2013. Characterization of epibenthic and demersal megafauna at Mississippi Canyon 252 shortly after the Deepwater Horizon Oil Spill. Mar. Pollut. Bull. 77, 196–209. doi:10.1016/j.marpolbul.2013.10.004

Vorrink, S., Domann, F., 2014. Regulatory crosstalk and interference between the xenobiotic and hypoxia sensing pathways at the AhR-ARNT-HIF1α signaling node. Chem. Biol. Interact. 218, 82–88. doi:http://dx.doi.org/10.1016/j.cbi.2014.05.001

Vorrink, S.U., Severson, P.L., Kulak, M. V., Futscher, B.W., Domann, F.E., 2014. Hypoxia perturbs aryl hydrocarbon receptor signaling and CYP1A1 expression induced by PCB 126 in human skin and liver-derived cell lines. Toxicol. Appl. Pharmacol. 274, 408–416. doi:10.1016/j.taap.2013.12.002

Wang, Z., Gerstein, M., Snyder, M., 2009. RNA-Seq: a revolutionary tool for transcriptomics. Nat. Rev. Genet. 10, 57–63. doi:10.1038/nrg2484

Wang, Z., Liu, Z., Xu, K., Mayer, L.M., Zhang, Z., Kolker, A.S., Wu, W., 2014. Concentrations and sources of polycyclic aromatic hydrocarbons in surface coastal sediments of the northern Gulf of Mexico. Geochem. Trans. 15, 1–12. doi:10.1186/1467-4866-15-2

Whitehead, A., 2013. Interactions between oil-spill pollutants and natural stressors can compound ecotoxicological effects. Integr. Comp. Biol. 53, 635–647. doi:10.1093/icb/ict080

Whitehead, A., Dubansky, B., Bodinier, C., Garcia, T.I., Miles, S., Pilley, C., 2012. Genomic and physiological footprint of the Deepwater Horizon oil spill on resident marsh fishes. Proc. Natl. Acad. Sci. 109, 20774–20774. doi:10.1073/pnas.1118844109

Wu, R.S.S., 2002. Hypoxia: From molecular responses to ecosystem responses. Mar. Pollut. Bull. 45, 35–45. doi:10.1016/S0025-326X(02)00061-9

Wu, R.S.S., Zhou, B.S., Randall, D.J., Woo, N.Y.S., Lam, P.K.S., 2003. Aquatic Hypoxia is an Endocrine Disruptor and Impairs Fish Reproduction. Environ. Sci. Technol. 37, 1137–1141. doi:10.1021/es0258327

Xia, J.H., Liu, P., Liu, F., Lin, G., Sun, F., Tu, R., Yue, G.H., 2013. Analysis of stress-responsive transcriptome in the intestine of Asian Seabass (Lates calcarifer) using RNA-seq. DNA Res. 20, 449–460. doi:10.1093/dnares/dst022

Xu, E.G., Mager, E.M., Grosell, M., Hazard, E.S., Hardiman, G., Schlenk, D., 2017. Novel transcriptome assembly and comparative toxicity pathway analysis in mahi-mahi (Coryphaena hippurus) embryos and larvae exposed to Deepwater Horizon oil. Nat. Publ. Gr. doi:10.1038/srep44546

Xu, E.G., Mager, E.M., Grosell, M., Pasparakis, C., Schlenker, L.S., Stieglitz, J.D., Benetti, D., Hazard, E.S., Courtney, S.M., Diamante, G., Freitas, J., Hardiman, G., Schlenk, D., 2016. Time- and Oil-Dependent Transcriptomic and Physiological Responses to Deepwater Horizon Oil in Mahi-Mahi (Coryphaena hippurus) Embryos and Larvae. Environ. Sci. Technol. 50, 7842–7851. doi:10.1021/acs.est.6b02205

Yang, S.K., 1988. Stereoselectivity of cytochrome P-450 isozymes and epoxide hydrolase in the metabolism of polycyclic aromatic hydrocarbons. Biochem. Pharmacol. 37, 61–70. doi:10.1016/0006-2952(88)90755-1

Yu, R.M.K., Ng, P.K.S., Tan, T., Chu, D.L.H., Wu, R.S.S., Kong, R.Y.C., 2008. Enhancement of hypoxia-induced gene expression in fish liver by the aryl

hydrocarbon receptor (AhR) ligand, benzo[a]pyrene (BaP). Aquat. Toxicol. 90, 235–242. doi:10.1016/j.aquatox.2008.09.004